2009-01-01

Effects Of Build Orientation, Aging, And Pre-Conditioning On Mechanical Properties For Stereolithography-Manufactured Astm Type I Specimens Using A Design Of Experiments Approach

Karina Puebla
University of Texas at El Paso, kpuebla@miners.utep.edu

EFFECTS OF BUILD ORIENTATION, AGING, AND PRE-CONDITIONING ON MECHANICAL PROPERTIES FOR STEREOLITHOGRAPHY-MANUFACTURED ASTM TYPE I SPECIMENS USING A DESIGN OF EXPERIMENTS APPROACH

KARINA PUEBLA

Department of Metallurgical and Materials Engineering

APPROVED:

_____
Ryan B. Wicker, Ph.D., Co-Chair

_____
Lawrence E. Murr, Ph.D., Co-Chair

_____
Rolando Quintana, Ph.D.

_____
Patricia D. Witherspoon, Ph.D.
Dean of the Graduate School

This Thesis is dedicated to the person

who is my best friend,

who always has the right words to say,

who I admire the most,

who has been my greatest inspiration,

who has made me the person I am today,

who gave me the gift of life,

and most of all, who I love.

This is for you Mom,

Ignacia Campa Ortega

Thanks for all your love and support.

.

EFFECTS OF BUILD ORIENTATION, AGING, AND PRE-CONDITIONING ON MECHANICAL PROPERTIES FOR STEREOLITHOGRAPHY-MANUFACTURED ASTM TYPE I SPECIMENS USING A DESIGN OF EXPERIMENTS APPROACH

by

KARINA PUEBLA, B.S.M.E.

THESIS

Presented to the Faculty of the Graduate School of

The University of Texas at El Paso

in Partial Fulfillment

of the Requirements

for the Degree of

MASTER OF SCIENCE

Department of Metallurgical and Materials Engineering

THE UNIVERSITY OF TEXAS AT EL PASO

August 2009

ACKNOWLEDGMENTS

I would like to take this opportunity to thank the individuals who assisted and guided me through this thesis. I will begin by thanking Dr. Ryan B. Wicker, Director of the W.M. Keck Center for 3D Innovation (Keck Center) and co-chair of my committee, for his ongoing support, encouragement, patience and the many times he has challenged me to do better. I would also like to thank Dr. Lawrence E. Murr who is also a co-chair of my committee for his guidance and knowledgeable insight regarding the material science in this research. I would like to express my gratitude to Dr. Ronaldo Quintana for his patience and helpful contribution despite the fact that he is a professor at The University of Texas at San Antonio.

My genuine gratitude is for my colleagues who on a weekly basis were able to assist me in different aspects of this research. I would like to acknowledge the following individuals for making a difference in my research: Francisco Medina, Luis A. Ochoa, Nubia Zuverza and Marjorie Ingle. I would like to thank Daniel Aguilar for his unconditional help, support in every aspect of my research and for always being there for me.

My most sincere appreciation is for the foundation in my life, my family, who without none of this would be possible. Also for their unconditional love and support, which has given me the strength and drive to be where I am today. I would like to give special thanks to my siblings, Ivonne, Nancy, Gladys, Juan and Jasmin, who constantly push me to follow my dreams. To my parents, Lino Puebla and Ignacia Campa Ortega, who have always encouraged me by setting examples and always reminding me that life is not easy.

The research presented here was performed at UTEP in the Keck Center using equipment purchased through Grant Number 11804 from the W.M. Keck Foundation. Support for UTEP

was also provided through a research contract (Number 28643) from Sandia National Laboratories in the Laboratory Directed Research and Development (LDRD) program. Sandia National Laboratories is a multi-program laboratory operated by Sandia Corporation, a Lockheed Martin Company, for the United States Department of Energy's National Nuclear Security Administration under contract DE-AC04-94AL85000. Support was also provided through the UTEP endowed Mr. and Mrs. MacIntosh Murchison Chair I in Engineering.

This thesis was submitted to the supervising committee on May 2009.

EXECUTIVE SUMMARY

With industry's growing focus on the rapid manufacturing (RM) of end-use products, rapid prototyping (RP) or layered manufacturing (LM) machines that were originally designed to build prototypes may now be required to build functional end-use products. To successfully accomplish the transition, the available materials utilized in RP must provide the performance required for RM. The specific technology used must also be capable of producing repeatable and reproducible parts in regards to mechanical and dimensional properties.

In this work, a design of experiments (DOE) approach was performed to determine the effects of build orientation, aging, and pre-conditioning on the mechanical properties of test samples fabricated using stereolithography (SL), a RP technology. To perform the investigations, a commercial SL system (Viper Si^2, 3D Systems, Valencia, CA) equipped with a solid state laser system (355 nm wavelength) was used to manufacture ASTM D-638 Type I specimens in two different build setups. The setups were designed to build batches of 18 or 24 Type I specimens in a 25.4 cm by 25.4 cm cross-sectional area. WaterShed™ 11120 (DSM Somos®, Elgin, IL) resin was used to fabricate the specimens, according to the manufacturer's recommendations (critical exposure, E_C, of 11.5 mJ/cm^2; penetration depth, D_P, of 6.5 mJ/cm^2). Three different experimental designs were carried out to determine the effect of different factors (build orientation, aging, and pre-conditioning) in the mechanical properties of the fabricated specimens.

The first experimental design investigated if specific build orientation parameters impacted the mechanical strength of SL fabricated parts. The build setup design used in this experiment can accommodate 18 specimens in different orientations. The DOE tested three factors: axis,

layout, and position. Samples were fabricated parallel with *x*-axis or *y*-axis, or 45º to both axes (called axes 1, 2, and 3, respectively). For each axis, samples were fabricated either flat or on an edge relative to the *x*-*y* plane (called layouts 1 and 2, respectively). Three samples were manufactured for each layout and axis combination, and the samples were labeled as positions 1, 2, or 3 depending on the distance from the center of the platform with position 1 being the closest to the center. The dimensions of the 18 specimens were randomly measured by one analyst using a low-pressure caliper (Model 500-196, Mitutoyo America Co., City of Industry, CA). Each specimen was measured three times and an average was taken for the overall length, overall width, width of the narrow section, thickness, and gage length. Then, the specimens were also randomly mechanically tested in tension with a universal testing machine INSTRON® 5800 (Model 5866, INSTRON®, Norwood, MA), and the ultimate tensile strength (UTS) and modulus of elasticity (E) of the samples were determined to capture the mechanical properties of the samples. The E of the material was manually calculated in the 1-3% strain range. The results from the statistical analyses showed that axis and position had no significant effect on UTS or E. However, layout (or whether a sample was built flat or on an edge) was shown to have a statistically significant effect on UTS and E (at a 95% level of confidence). The difference between average UTS and E for each of the samples built flat and on an edge were ~3.53% (43.2 vs. 44.8 MPa) and ~4.59% (763.9 vs. 800.7 MPa), respectively. Because of the relatively small differences in means for UTS and E, the statistical differences between layouts tested most likely would not have been identified without performing the multifactor analysis of variance. Furthermore, layout was the only factor that tested different orientations of build layers (or layer-to-layer interfaces) with respect to the sample part, and thus, it appears that the orientation of the

build layer (layer-to-layer interfaces) with respect to the fabricated part has a significant effect on the resulting mechanical properties.

Using the same build setup design of the 18 Type I specimens, the second experimental design investigated the effects of aging and pre-conditioning in the mechanical properties of SL fabricated parts. To examine the effects of Aging, three different time frames were used: four days, 30 days (1 month), and 120 days (four months). Three different environmental conditions were used to test the effects of pre-conditioning the samples: ambient conditions, desiccant package, desiccant package plus 2 days at ASTM 618 preconditioning. Guidelines in Procedure A of ASTM 618 state that samples for mechanical testing should be pre-conditioned for not less than 40 hrs at 23±2ºC and 50±5% relative humidity. A total of nine batches of 18 specimens were fabricated in order to test the three types of Aging at the three different environmental conditions. The dimensions of the 18 specimens in the nine batches were randomly measured by one analyst. Each specimen was measured three times and an average was taken for the overall length, overall width, width of the narrow section, thickness, and gage length. The specimens were also randomly mechanically tested with an INSTRON® 5800 with the assistance of a static strain gauge extensometer with 2-in gauge length (Model 2630-115, INSTRON®, Norwood, MA) immediately after the corresponding aging and pre-conditioning to obtain the mechanical properties of the samples under these conditions. Results from the statistical analyses showed that both aging and pre-conditioning have statistically significant effects on the UTS and E at a 95% level of confidence. The specimens stored at ambient conditions for the different time frames (4, 30, and 120 days) had the highest values of UTS and E (UTS: 45.7±1.6, 54.2±1.8, and 52.6±2.6 MPa, E: 777.3±38.5, 873.1±36.6, and 870.8±57.3 MPa, for 4, 30, and 120 days, respectively) compared to the specimens stored in a desiccant package (UTS: 44.7±1.6,

52.1±1.5, and 51.4±2.7 MPa, E: 794.5±32.5, 839.1±39.1, and 866.1±50.0 MPa, for 4, 30, and 120 days, respectively) and stored in a desiccant plus two days ASTM pre-conditioning (UTS: 45.9±2.1, 51.3±1.8, and 48.5±2.5 MPa, E: 787.8±39.8, 857.5±32.7, and 832.6±45.9 MPa, for 4, 30, and 120 days, respectively). Thus, the % difference of the Aging and Pre-conditions for UTS and E at Ambient (UTS: 6.3, 5.2, and 8.9 %, E: 8.4, 7.4, and 11.8%, for 4, 30, and 120 days, respectively), Desiccant (UTS: 5.2, 4.0, and 9.4 %, E: 6.8, 5.2, and 10.6 %, for 4, 30, and 120 days, respectively), and Desiccant plus two days ASTM pre-conditioning (UTS: 7.8, 5.9, and 9.3 %, E: 8.7, 6.8, and 9.7 %, for 4, 30, and 120 days, respectively) at the different Aging time frames (4, 30, and 120 days) demonstrates that the samples placed in desiccant package had the lowest % difference averages of UTS and E for the specimens built flat and on an edge at 4 and 30 days of Aging this may be due to the dried environment where the samples were stored. On the other hand, the samples aged for the longest period (120 days) had the highest % difference average of UTS and E for samples built flat or on an edge. The statistical difference would not have been revealed without the performance of another DOE on the Aging and Pre-conditions of the specimens for the small difference in means for both UTS and E. Furthermore, the results showed that Aging is an important factor in the mechanical properties as it allows the material to stabilize. Pre-conditioning of the samples in Ambient had better mechanical properties compared to the other Pre-conditions. Similar to the first experiment design results also showed that build orientation (flat or on an edge) produced parts with statistically different mechanical properties.

As a result of the studies described above on the build setup design that holds 18 Type I specimens a third experimental design was carried out with a new build setup design. The build setup was designed to hold 24 specimens to test an additional build orientation parameter:

Layout 3, defined as vertical (relative to the *x-y* plane). The factors investigated were Position and Layout. On the build setup design platform there are eight Positions that hold the three different Layouts: flat, on an edge, and vertical defined as Layout 1, Layout 2, and Layout 3, respectively. The eight positions were lined-up along the *y-axis* and were numbered consecutively from 1 to 8. The 24 specimens were tested after four days on ambient conditions since the previous study showed that specimens aged under this condition had the highest mechanical properties. In addition to the four days ambient, the specimens were subject to two days ASTM D618 pre-conditioning to test effects of the different Layouts (flat, on an edge and vertical) based on their Position, in the build platform on mechanical properties. A total of three batches of 24 specimens were fabricated to replicate this experiment three times. One batch was used to perform a gauge Repeatability and Reproducibility analysis, where three analysts randomly measured the specimens. Each specimen was measured three times by each of the analysts and an average was taken for the overall length, overall width, width of the narrow section, thickness, and gage length. A total of 1,080 measurements were taken with a low-pressure caliper. The analysis was performed with a 5% level of significance using Statgraphics® software. The analysis results showed a statistically significant difference between analysts at 95% level of confidence. Also the results showed that the instrument was proficient to differentiate between the different parts of the specimens being measured with a 5% level of significance. The Type I tensile specimens were randomly mechanically tested with INSTRON® 5800 with aid of an Advanced Video Extensometer (AVE) (Model 2663-821, INSTRON®, Norwood, MA) to accurately attain the mechanical properties of the samples. The outcome of the statistical analysis revealed that Position had no significant effect on UTS and E. However, Layout (flat, on an edge, and vertical) confirmed to have a statistically significant effect on UTS

and E at a 95% level of confidence. The samples built flat (Layout 1) had a low value of UTS and E (UTS: 45.2±0.8 and E: 791.5 ±9.4 MPa) compared to the specimens fabricated on an edge (Layout 2) (UTS: 49.6±0.7 and E: 872.5±6.9 MPa) and vertical (Layout 3) (UTS: 50.3±0.6 and E: 887.1±12.5 MPa). The study results showed that Layout 3 had the highest UTS and E compared to Layouts 1 and 2. As a result, the % difference of the built orientation between the UTS and E by Layout (vertical and flat) was 10.10 and 10.80, respectively, (vertical and on an edge) was 1.40 and 1.70, respectively, and (on an edge and flat) was 8.90 and 9.30, respectively. The 24 specimen setup Layout tested different orientations of layer interfaces (flat, on an edge and vertical), which produced orthogonal layer interfaces. The orientation of the layers produced samples with statistically different mechanical properties. Therefore parts cannot be considered broadly isotropic.

Results for three experiment designs, using two different build setups, showed that Layout (flat, on an edge, or vertically) produced parts with statistically different mechanical properties as determined using measurements of UTS and E. Statistically significant differences in mechanical properties were also found as an effect of Aging (the time between sample production and mechanical testing) and Pre-conditioning (the storage conditions of the samples). The statistical analyses done can help identify and classify fabrication parameters on mechanical properties for SL fabricated parts. Knowing the effects of the mechanical properties on the commercially available resin can help improve the SL production process for end-use products.

TABLE OF CONTENTS

LIST OF TABLES

LIST OF FIGURES

CHAPTER 1 INTRODUCTION

1.1 BACKGROUND

Recent advancements in manufacturing have put a greater demand on the need for rapid prototyping (RP) technologies that can aid in the development of its progression. There is a growing desire to use RP to produce parts that can achieve the required performance and also contain the mechanical properties necessary for their application. One such RP technology that is being improved to achieve this is stereolithography (SL).

SL is an ideal RP technology that can be used to achieve the desired parts because it is capable of producing highly accurate 3D parts. The parts are created by photocrosslinking resin with an ultraviolet (UV) laser, which cures the resin in a layer-by-layer manner until the part is completed. Numerous researchers are also working on improving the resin properties that could help improve the overall properties of the part created.

The use of polymers in RP technology offers engineering advantages. Such advantages include strength, weight, and corrosion resistance among others. Current research connected with polymers involves studies of the ways in which pure polymers can be modified to make them more suitable for certain applications. One such modification would be the addition of reinforcement nanocomposites such as fibers or carbon nanotubes (Sandoval *et al*., 2005, 2006). Physically altering the crystallinity of the polymer is another modification that is utilized in the SL process. Work like this is likely to become even more important as technology continues to demand new materials with improved properties (Allcock *et al.,* 2003).

The approach taken to build the parts may play a critical role in the properties of the built part. This is due to the fact that the SL process builds the part in layers. For this reason, it is key to determine the mechanical properties of the material being used to construct the prototypes. These material properties may provide useful data for design purposes and for the control and specifications desired for the part created. It is essential to determine these properties since they can impede the performance of the part when it is used in real life applications.

Apart from specimen preparation, tensile properties may also vary with environment. Two types of conditions may affect the material. One of them is aging or the amount of time the part has existed after being built. Resins experience a variety of chemical aging that includes constant crosslinking of unreacted chemicals during a course of time. Therefore, unreacted chemicals are not appropriate because it signifies that the resin properties continually change (Scheirs, 2000). The other would be the environment that the part is exposed to. Humidity is an example of an environmental condition that may affect the mechanical properties of a part created with SL. An increase in environmental temperatures can cause a significant increase in the samples dimensions as well as accelerate the moisture absorption (Liu *et al.* 2003).

1.2 LABORATORY INVOLVED

The laboratory in which this research took place is the W.M. Keck Center for 3D Innovation (Keck Center) at the University of Texas at El Paso. The Keck Center occupies over 6,100 square feet and is home to a wide range of manufacturing, reverse-engineering, and computer-aided design technologies. The Keck Center focuses on Biomedical Engineering and Functional Manufacturing. Biomedical Engineering can be further broken down into three fields, which are Imaging, Modeling and Manufacturing; Cardiovascular Hemodynamics; and Tissue Engineering.

Likewise, Functional Manufacturing consists of 3D Electronics; Functional Rapid Prototyping; Micro Fabrication; Advanced Materials; and Rapid Tooling.

The Keck Center is an advanced engineering, rapid design and manufacturing center. Besides the RP technologies, the Keck Center also houses mechanical testing equipment, scanning systems, analytical instruments and equipment for *in vitro* experimentations. The state-of-the-art facilities hold 27 commercial rapid prototyping machines, with six of the leading technologies: Stereolithography (SL), 3D Printing (3DP), Fused Deposition Modeling (FDM), Selective Laser Sintering (SLS), Electron Beam Melting (EBM), and Multi-Jet Modeling (MJM). Recently, the facility has incorporated two of the newest technologies: Arcam A2 and Z Corp. 510. The Arcam A2, operating under vacuum and high temperature, functions with the use of an electron beam allowing high energy to be employed through a gun which melts metal powder. With the Z Corp. 510, models are created in color one layer at a time by spreading a layer of powder and inkjet, printing a binder in the cross section of the part.

Through its interdisciplinary collaborations, the Keck Center is presently focusing on tissue engineering of complex implantable hydrogel constructs for tissue regeneration with the assistance of SL and biocompatible materials. Furthermore, the creation of Multi-Material SL and Hybrid Direct Write SL that provide integrated direct write electronics and multi-material SL build capacity. The main focus is to integrate these technologies to manufacture and develop products for end-use parts.

1.3 PROJECT MOTIVATION

Recent advances in stereolithography (SL) have had a significant impact on the overall quality of parts produced using rapid prototyping (RP) processes. Several new RP technologies

have been developed and commercialized since the introduction of SL. It is only natural that these machines that were originally created to build prototypes now be required to manufacture functional end-use parts. There are factors to consider when making the transition from RP to rapid manufacturing (RM). Materials that are used in RP must be able to provide the performance that is required for RM. These parts must exhibit repeatable and reproducible performance in regards to their dimensions and properties (mechanical, thermal, electrical, etc.). SL has the potential of building highly accurate parts with a superior surface finish. For this reason, SL is a fine candidate for the advancement of the transition. The desire to take RP to RM motivated the current study on the basis to maintain the performance of these parts after transitioning. The overall goal of this research is to determine whether build orientation of parts affect their properties. The development and advancement of being able to maintain the performance of the parts can lead to the improved development of layered manufacturing (LM) testing methodology, which can be later applied to standard SL building conditions.

1.4 PROJECT OBJECTIVES

The objective of this study is to determine whether build orientation of parts affect their physical properties in order to sustain the performance of the parts which can lead to the improved development of layered manufacturing (LM). The specific project objectives for this study are as follows:

- Develop a layout for build orientation in a platform (25.4 cm by 25.4 cm cross-section) on the 3D Systems Viper Si² machine.
- Test tensile test specimens (ASTM D-638 Type I) on the developed layout based on three factors: axis, layout and position.

- Develop 3 timeframes for aging and 3 different environmental conditions to test the specimens.
- Develop a layout with different build orientations (flat, on an edge, and vertical) to test two factors: layout and position.
- Perform dimensional analysis on tensile specimens for repeatability and reproducibility.
- Perform mechanical testing on tensile specimens.

1.5 THESIS OUTLINE

The following work on this research is separated into the following chapters. Chapter 2 presents the different rapid prototyping technologies and especially focusing on the stereolithography (SL) process. It discusses the research done with this technology and the investigation performed on building parts in different orientations. Rapid manufacturing is also being discussed along with effects on the mechanical properties in regards to orientation and aging. Chapter 3 provides the experimental setups developed, procedures and design of experiments for this research on the different build setups to investigate the effects of build orientations, aging and conditioning of the specimens. A new vat design was developed for the Viper Si² to accommodate the different build layouts and the building process. Results of the mechanical testing are discussed in Chapter 4 along with the observations made on the electron microscopy characterization. Chapter 5 entails the discussion on the statistical analysis acquired from the mechanical testing results on the effects of layout, aging and conditioning of the specimens. Lastly, conclusions and recommendations on the future research work are covered in Chapter 6.

CHAPTER 2 LITERATURE REVIEW

2.1 INTRODUCTION

This chapter presents a literature review of rapid prototyping (RP) and rapid manufacturing (RM). An overview on the different types of RP technologies with a focus on stereolithography (SL) is covered. The effects of build orientation on dimensions and material properties as they pertain to RP will also be discussed as well as the effects of nanocomposites in epoxy resin on the material properties.

2.2 RAPID PROTOTYPING

Rapid prototyping (RP) is a building technique that starts with a 3D computer aided design (CAD) model of the part to build. This model is converted by software into a series of layers which are then transferred to a building machine. These layers are then printed in the material by different kinds of processes which depend on the kind of machine being used. After a layer is printed, a new layer of material is deposited on top and a new layer is printed. Depending on the process, a post-processing may be required (Rochus *et al.* 2007). The particular RP technology used to form the layer, its thickness, and how well the part is represented in the CAD model, contribute in the effectiveness to duplicate desired 3D complex parts (Wicker *et al.* 2004). The advancement to rapid manufacturing (RM) will mainly depend on cost and productivity improvements which have to include other technical progressions in material properties and most importantly accuracy and reliability (Levy *et al.* 2003, 2005, 2007).

2.2.1 3D Printing

The Eden 333™, in Figure 2.1, uses PolyJet technology to provide resolution (x axis: 600 dpi, y axis: 300 dpi, and z axis: 1600 dpi) layers of 16 µm without messy materials or post processing. Experimental results for dimensional accuracy and precision involving 3D printing indicate that they are influenced by the three factors. The first factor is the material that is used to produce the item which can significantly alter test results. The 3D printer axis that is responsible for the particular dimension is a second factor. The third factor that can influence dimensional accuracy and precision would be the magnitude of the nominal dimensions (Dimitrov *et al.,* 2006).

Figure 2.1 Objet Eden 333™.

2.2.2 Fused Deposition Modeling

Unlike other laser-based rapid prototyping (RP) technologies, fused deposition modeling (FDM) is a nonlaser-based technology. Figure 2.2 demonstrates the different FDM technologies. This method uses a heated extruding head to deposit a thin filament of molten thermoplastic. There are different types of thermoplastics used for this technology which are maintained at

several degrees Fahrenheit above the solidification temperature. The material solidifies once it is deposited onto the object. The object is created by drawing all the required cross sectional layers (Chuck *et al.,* 1998).

Figure 2.2 FDM technologies: FDM 3000, FDM Titan, FORTUS™ 400mc and FDM Maxum.

In FDM every layer is filled by roads according to a certain path, and because of this, the roads can be considered as the real building units of the process. Observations have shown that the road shape, the road-to-road interaction and the path strongly affect the properties and performance of the finished product. The mechanical properties of the final parts significantly depend on two important modeling phases. The first is the chosen building direction which has to do with the orientation of the object with respect to the substrate. The other important modeling phase is the chosen path, meaning the way every layer is filled by roads. The mechanical properties of the part depend on the orientation. Path becomes critical when FDM technology is used to produce components directly for end-use. Figure 2.3 demonstrates the path of the material as it is being deposited onto the platform. For these reasons, it is important to be

able to predict and design the object with the desired tolerances and characteristics (Bellini *et al.*, 2003, 2005).

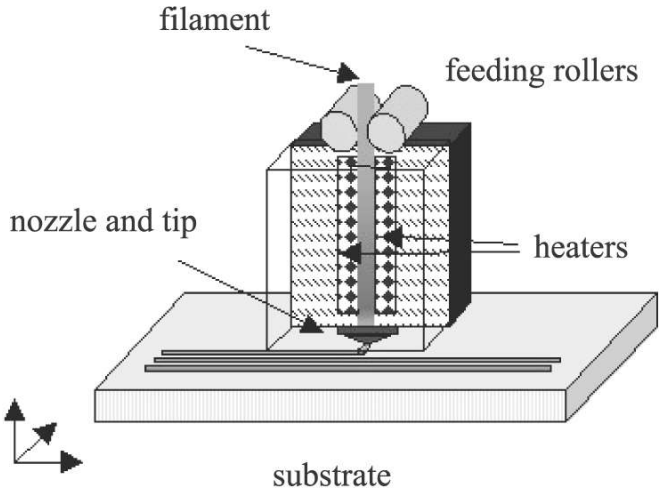

Figure 2.3 FDM schematic components (Bellini, 2003).

In a previous study by Ahn *et al.* (2002), it was found that air gap and raster orientation affect the tensile strength of an FDM part significantly as shown in Figure 2.4. In contrast, bead width, model temperature and color have little effect. Measured material properties showed that parts made by FDM have anisotropic characteristics. The compressive strength of FDM material was higher than the tensile strength and was hardly affected by build direction. The strength of a local area in the part depends on raster direction because of the anisotropic behavior of the parts created from the FDM process. Several build rules were obtained from the study. One states that parts should be built in such a manner such that tensile loads will be carried axially along the fibers. Another suggests being aware that stress concentrations occur at radiused corners because the FDM roads display discontinuities at those types of transitions. An additional rule to increase both strength and stiffness is using a negative air gap, meaning that two beads partially occupy the same space. One of the rules gives advice on bead width. It states that small bead

width increases build time and surface quality and that the wall thickness should be an integer multiple of the bead width. The effect of build orientation on part accuracy and the awareness that tensile loaded areas tend to fail easier than compression loaded areas are also among the rules obtained. Applying these rules to the FDM process can improve the strength and quality of the parts (Ahn *et al.,* 2002).

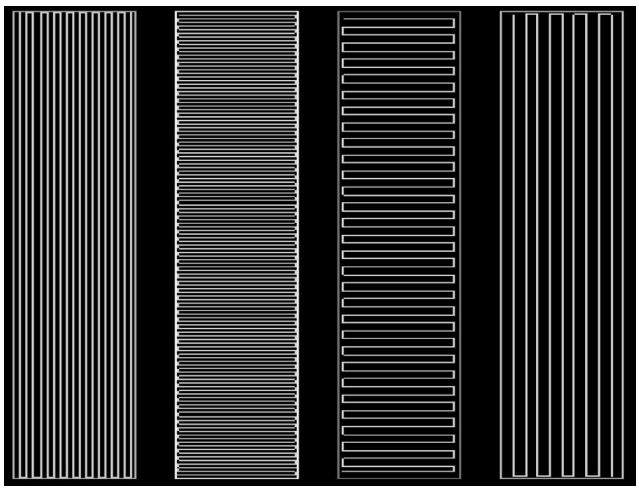

Figure 2.4 Variation on bead width, airgap, and raster orientation (Ahn *et al.* 2002).

Other studies using the FDM building process have given similar outcomes. They agree that the highest stiffness and strength values were found for loading in the fiber extrusion direction on aligned mesostructural configuration with small negative fiber-to-fiber gap settings. The conclusion that air gap and raster width are significant parameters in affecting the mechanical properties of parts is another result studies have agreed on. They also agree that the lay down pattern affected the properties of the part and that these properties can be tailored by adjusting it and thus increasing the functionality of the part (Rodriguez *et al.*, 2001; Ang *et al.*, 2006; Gray IV *et al.*, 1998).

2.2.3 Selective Laser Sintering

Selective laser sintering (SLS) is among the many rapid prototyping (RP) technologies utilized to create parts. Figure 2.5 shows the SLS machine. Heat input from a laser is applied to a polymer or metallic powder causing a solid state sintering or melting of the material. The basic process of SLS uses a pure polymeric powder, but a ceramic material can be added to improve the mechanical properties. SLS was developed to process a powder mixture containing a low melting material and a high melting material because older laser systems did not have enough power to melt high-end metal materials. There can be different versions of the SLS technique. The process can be called SLS when the low melting material is polymeric and direct metal laser sintering (DMLS) when the material is a low melting metallic powder. SLS may require a post processing but with DMLS there is none needed and the resulting part is a mixture of two alloys. When there is only one kind of metal powder that is directly melted by the laser the process is known as selective laser melting (SLM) (Rochus *et al.,* 2007).

Figure 2.5 SLS technology .

An aspect of SLS that makes it an important RP technology is the wide range of materials which can be used. The most commonly used materials in SLS are polymers which are materials made up of long-chain molecules formed mostly by carbon-to-carbon bonds. The three most commonly used polymers are thermoplastics, thermosetting plastics and elastomers. Among these the most popular are thermoplastics because they can be recycled in SLS which in turn saves material. Thermoplastic polymers can be further classified into two types, which are amorphous and crystalline. Amorphous material has chain molecules arranged in a random manner and crystalline material has chain molecules arranged in an orderly structure. Because of this, they have different thermal properties which may determine fabrication parameters in SLS. The properties of the different SLS powders can influence the fabrication parameters which can affect the mechanical properties of the resultant component (Gibson *et al.,* 1997).

The mechanical properties of SLS parts are influenced by many factors. These factors may include powders, fabrication parameters, orientation and post-processing. The powder used is the main determining factor for the mechanical properties and studies have shown that properties of SLS parts depend on the choice of powder if the fabrication parameters are to be optimal. To achieve the most favorable results, understanding of the effects of sintering and post processing must be incorporated into the design and process planning (Gibson *et al.,* 1997).

2.2.4 Stereolithography

One of the most commonly used rapid prototyping technologies is SL illustrated in Figure 2.6. The machine that is used to build the parts using the SL process is called a stereolithography apparatus (SLA®). SL is capable of creating parts with complex geometry and with a surface finish comparable to many conventionally machined components. These parts are often used as

masters to produce silicone molds for vacuum or injection molding (Upcraft *et al.*, 2003). The SL process functions with the help of a photopolymerization technique that uses a laser beam to selectively draw or print cross sections of a model on a photocurable resin surface. This action is repeated on the surface of the resin in a layer-by-layer method until a 3D part is created.

Figure 2.6 SLA technologies: Viper Si² and 250/50.

In order for the laser to know what needs to be drawn, it first needs the instructions from a computer aided design (CAD). A solid model of the desired part is first created using CAD software and is then converted to a file format known as STL (stereolithography). The file format originated from 3D Systems and is sufficient to meet the needs of rapid prototyping technology since it generally builds monomaterial parts. The STL file format has been successful because of its sufficiency and its simplicity. It is sufficient mathematically because it is able to describe a solid object using a boundary representation (B-rep) technique. An STL file format represents the CAD model of the object to be prototyped as a collection of triangular facets. When taken together, the triangular facets describe a polyhedral approximation of the object's surface. It is nothing more than a list of x, y, and z coordinate triplets that describe a connected set of triangular facets (Noorani 2006).

Once the SL machine receives the instructions from the STL file it is ready to begin building the part. Figure 2.7 demonstrates the main components of the SL machine. An ultraviolet (UV) laser beam is moved by a computer-controlled optical scanning system across the top of a vat containing liquid resin to selectively solidify the liquid photopolymer on the surface. The laser draws each layer of the part from the information provided by the CAD build data file. As the laser beam makes contact with the resin it solidifies it. After a layer is completed, the supporting platform is lowered by an amount equivalent to the thickness of one layer covering it with the resin that is contained in the vat. The surface is then recoated and leveled with resin to help establish the thickness and flatness of the liquid layer. As each layer is drawn, it adheres to the previous layer that was completed to begin forming the solid part as shown in Figure 2.8 (Renap *et al.*, 1995). After the process is repeated enough to complete the part, the platform on which it is created rises out of the liquid resin to expose the completed part that had been submerged in the resin during the building process.

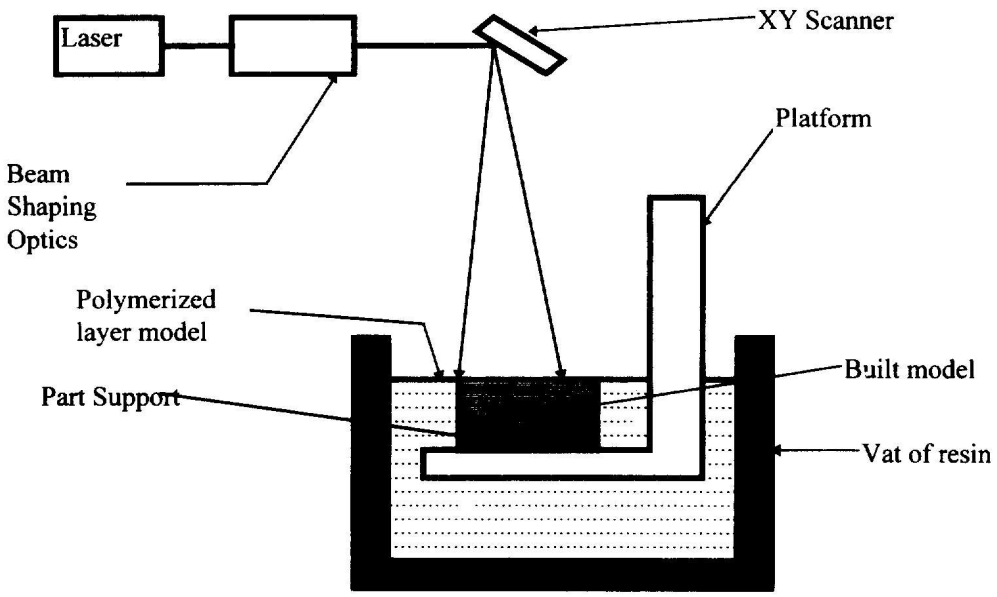

Figure 2.7 SL schematic with components (Onuh, 1997).

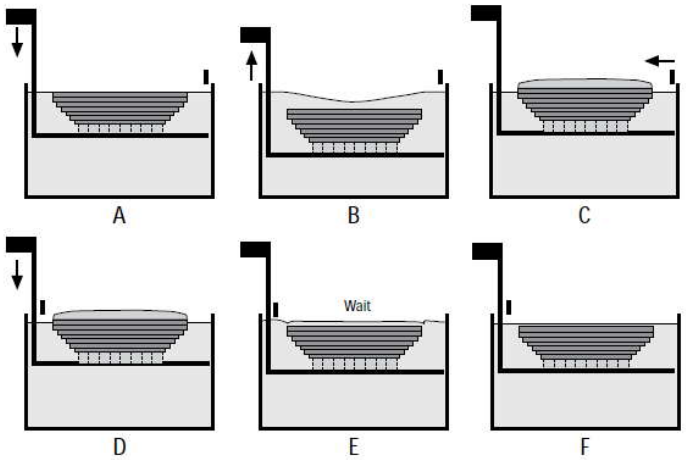

Figure 2.8 Process for recoating (Renap, 1995).

After the building process, the necessary clean up and post-curing is performed. During the photopolymerization process the resin that is solidified does not reach full solidification. For this reason, the part created from the SL process may be put into a UV oven to be cured up to 100% and to help complete the photopolymerization process (Chuk *et al.*, 1998; Campanelli *et al.*, 2006).

2.2.4.1 Thermosetting

An important factor that makes stereolithography possible is the incorporation of thermosetting polymers to the process. Also known as a thermoset, it is created when chemical linkages form a rigid, cross-linked molecular structure. A thermosetting polymer exists initially as a liquid that upon heating undergoes a reaction to form a solid, involving a highly cross-linked matrix. Thermosets are cured or hardened into a permanent shape and usually have a high elastic modulus or stiffness that makes them more brittle (Noorani 2006). An uncross-linked thermoplastic material can be re-formed into a different shape by heating but a thermosetting polymer cannot. Some types of systems remain partly polymerized and are still capable of liquid

flow. They are known as prepolymers and are often preferred as starting materials in technology (Allcock *et al.*, 2003).

Thermosets can exist either as a liquid or solid at room temperature. Once the thermoset has been reacted and cured it cannot be re-formed by any means that will not split the covalent bonds. They have covalent bonds that join the atoms together in a polymer chain and that also join the chains to one another (Arcaute 2004).

2.2.4.2 Photopolymerization

SL depends on the photopolymerization process to turn a liquid resin into a solid part. Photopolymerization is defined as the linking of small molecules (monomers) into larger molecules (polymers). Typical polymers may consist of hundreds of thousands of monomers that can have molecular weights up to thousands of grams per mole. Liquid photopolymers can be solidified by electromagnetic radiation whose wavelengths may include γ-rays, X-rays and UV. Most RP systems including SL systems are curable in the UV range (Noorani 2006). The dynamics of polymerization during the process can fundamentally influence the accuracy of the parts created. Selections of SL resins may be dependent on the evaluation of photopolymers with respect to these dynamics of polymerization (Wiedemann *et al.*, 1995).

2.2.4.3 WaterShed™ 11120

WaterShed™ 11120 (DSM Somos®, Elgin, IL) is the SL resin used in the studies on orientation, aging and pre-conditioning. This thermoset liquid photopolymer is produced by DSM Somos® and is an epoxy-based resin composed from chemical family of epoxy, oxetane, and acrylates each with its respective % by weight. Epoxy is able to form a cross linked polymer that can be known by being tough, strong and low in shrinkage. Epoxy is composed of epoxide

rings at the ends of the molecule and agent for curing. Acrylates are well-known for their transparency and resistance to breaking. WaterShed™ 11120 is a long lasting, strong, clear and water resistant photopolymer. The commercial SL resin has a viscosity of ~260 cps at 30°C and a density of ~1.12 g/cm³ at 25°C. The resin is for use with SL solid state laser systems (355 nm laser wavelength) with the manufacturers recommendations of critical exposure, $E_{C,}$ of 11.5 mJ/cm^2 and a penetration depth, D_P, of 6.5 mJ/cm^2 (Product Data Sheet, DSM Somos®).

Table 2.1 shows the mechanical properties stated by the Product Data Sheet by DSM Somos® for better understanding and usage of the commercial resin when it comes to applications. This epoxy resin material can mimic other types of polymers which can be used for many applications such as medical, automotive, aerospace and consumer product industries. Figure 2.9 show 3D parts manufacture in Viper Si^2 out of WaterShed™ 11120 demonstrating the versatility that this rapid prototyping technology has to build, from a university seal to a skull. Epoxy based resin is suitable for producing high-quality models to be used in two-dimensional photoelasticity (Karalekas *et al.*, 2004). Adjusting the build parameters will allow the creation of a well built product like those built in epoxy based resin (Onuh *et al.*, 1997). New developments in resin have allowed non toxic and flexible photopolymers like the example given in Figure 2.10 which demonstrates the flexibility of the resin material (Bens *et al.*, 2007). Meanwhile, ceramic filled and photocurable epoxy resins can be used to manufacture highly loadable parts (Augsburg *et al.*, 2004).

Table 2.1 DSM Somos® WaterShed™ 11120 Mechanical Data Sheet.

ASTM Method	Description	WaterShed™ 11120
D638	Tensile Strength	47.1-53.6 MPa
	Tensile Strain at Break	11-20 %
	Modulus of Elasticity	2650-2880 MPa

Figure 2.9 3D parts manufactured using WaterShed™ 11120 in the Viper Si².

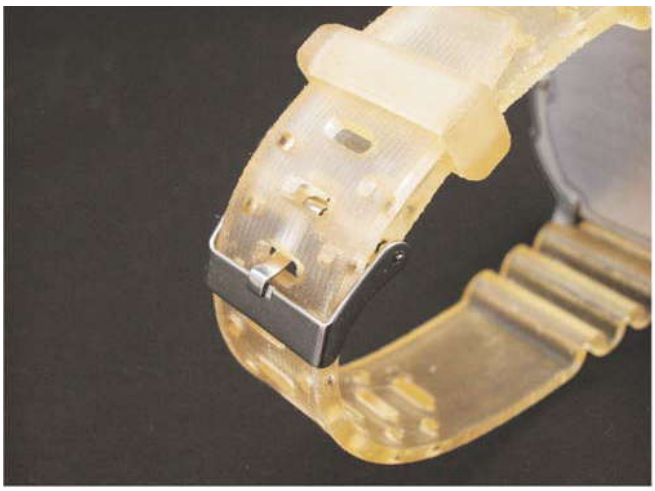

Figure 2.10 FlexSL SE-25 resin demonstrating the flexibility of the material (Bens, 2007).

2.2.4.4 SL Research

There are several important factors that can contribute to the mechanical properties exhibited in parts created using the SL process. Among these factors are the build parameters, the post curing process used when producing the parts, addition of material to the epoxy resin, and environmental effects. The prototypes fabricated with the SL process are being evaluated by the industry since the properties of the material change (Evans *et al.*, 2003).

Previous studies have illustrated the impact that SL build parameters can have on SL parts. One such study on the use of SL as it pertains to photoelastic models determined that when using standard build parameters, results show that there are effects in stereolographic specimens. One of them is a permanent effect that is associated with the manufacturing process and the other was a temporary effect caused by water absorption. The standard build parameters employed in the SL machine lead to significantly different material properties in the edge and corner specimens tested in the study (Curtis et al., 2003). Another study that looked to improve the accuracy of the SL process resulted in similar results. It showed that it was possible to increase the accuracy of parts by setting the process parameters to specific values. These parameter settings allowed the acquisition of fully cured parts during the building process without need for post-processing. These are valuable results because it allows a reduction in process time and shrinkage that is generated during the post-curing process (Campanelli *et al.*, 2006).

Other studies show the effects of post-curing on the part as in Salmoria *et al.,* (2004). In this investigation, the UV and microwave post-cured samples presented greater values for the elastic modulus, tensile strength and ultimate strength than green samples. SL samples with different degrees of cure can present different relations between the ultimate tensile strength and the critical flaw size. The degree of cure results in changes in the mechanical properties of the prototype as the post cure exhibits improved strength and toughness of the part along with the durability (Cheah *et al.*, 1997 and Karalekas *et al.*, 2002). Another component studied is the layer thickness of the build 3D part in which smaller thickness increases the strength of the part (Chockalingam *et al.*, 2006). Similar results have determined that uncured and partially cured resins trapped within the photopolymer have resulted in inhomogeneity of curing in the parts which causes shrinkage and distortion leading to undesired dimensions (Fuh *et al.*, 1999).

Meanwhile, the curing of the laser has a potential of improving the resolution of the part in the rapid prototyping process (Chua *et al.*, 1998).

Environmental conditions can also contribute the resulting properties of SL parts. The effects of humidity and temperature have been observed on the dimensional changes of photo-cured SL resin. As described in Yang *et al.*, (2003), moisture absorption by the SL resin is a slow process at ambient temperatures and varying the relative humidity (RH) between 20 and 90 percent in the environment only resulted in slight changes in the sample dimensions. An increase in environment temperature resulted in an increase (0.7% relative displacement) in the sample dimensions through thermal expansion along with accelerated moisture absorption at 50 percent or higher RH. An increase in equilibrium water content in plastics, greater water vapor pressure in the environment and higher thermal energy of water molecules are believed to be the cause for an increase in the moisture absorption rate at higher temperatures. In a separate study, SL resins were investigated to show the results due to environment and aging. The resins were studied under four different moisture environments at 30ºC over seven weeks. A drop in mechanical properties was observed whereas aging time had no significant influence on the properties. Moisture uptake was assumed to be mainly responsible for the behavior (Ottemer *et al.*, 2002). There has been an interest to remove the drop in the mechanical properties by adding of an additional material to the resin.

In order to improve the mechanical properties of the material, adjustments have been made. The addition of glass fiber increases the tensile properties of the polymer resin when being incorporated by 27% for UTS and 71% for E as shown in a study by Cheah *et al.,* 1999 and 36% UTS in a study by Karalekas *et al.,* 2004. Another main component is the electroplating of the part to improve the mechanical properties of the epoxy based resin (Saleh *et al.,* 2004).

2.3 RAPID MANUFACTURING

Rapid Manufacturing (RM) is a fabrication technique for manufacturing solid objects by the delivery of material to specified points in space in order to produce that part. RM is a set of techniques and technologies that provide rapid manufacturing applications (Munguia *et al.,* 2008). The production of a functional part needs to meet the real part production (Kruth *et al.,* 2007). The stereolithography process has evolved to better resolution for the manufacturing of small and precise prototype parts (Bertsch *et al.*, 2000) which in turn helps to know if the designs are compatible with the process (Hanumaiah *et al.*, 2007). The increasing use of Rapid Protoyping (RP) for the production of end-use parts is quickly commiting itself to the concept of RM since it provides fully developed and functional parts (Laurentis *et al.,* 2004).

Three generic methodologies exist for the production of prototypes or manufactured parts. The first is subtractive which is a process that removes material from a bulk material. This removal can include processes such as millilng, turning or electro-discharge machining among others. The second methodology is formative. This method uses a tool to produce a part such as injection molding, die casting or forging. The third is a relatively new approach which is additive. This method includes stereolithography which is commonly used in RP (Hague *et al.*, 2004).

RM will have a significant affect on the way that designers work. In conventional product design, the industrial engineer would pass the initial design ideas to a mechanical engineer who would incorporate and consider the manufacturing route. Design for RM will actually be a design for RP technologies. The conversion of industrial design sketches to a useable computer aided design (CAD) model is important as there is a difficulty in re-producing the exact design intent. With the introduction of the RM technologies, designers are able to manufacture any

freeform shape that they design and are no longer constrained by the limitations brought upon by either the conventional molding process or the tool making process. Therefore, it is likely that the initiation of RM will lead to a new breed of unique multi-skilled designers (Hague *et al.*, 2003).

A breakthrough in RM can happen on the basis of manufacturing applying the RP technologies on a large scale (Levy *et al.*, 2003). To have a successfully transition from RP to RM there are three features that have to be present. The process must demonstrate good accuracy, speed and surface finish (Hull *et al.*, 1995). SL is capable of manufactuing Meso manufacturing with high resolution with accurate mesocale parts (Palmer *et al*., 2006). Accuracy can vary considerably depending on the RP technology and also on which dimension is being measured (Upcraft *et al.*, 2003). With the trend and wish to move further towards RM, attention has to be focused on consistent results (Levy *et al.*, 2003).

2.4 ORIENTATION

Orientation is a significant factor in the manufacturing of parts. It can affect the mechanical properties and the time to manufacture the part. The orientation of the building part is an important factor in the layered manufacturing that affects the part quality of the part (Cheng *et al.*, 1995) as well as its impact on the SL build performance and process (Chockalingam *et al*., 2008 and McClurkin *et al*., 1998). Mechanical properties are affected since they are anisotropic in nature and depend strongly on the direction in which they are tested. The adhesion of the material between successive layers is weaker than the adhesion between material inside a layer. Time to manufacture a part is dependent on the orientation since the number of layers used to manufacture the part varies from orientation to orientation (Kulkarni *et al.*, 2000).

Variability can be introduced in multiple ways when building rapid prototyping (RP) parts. Research has shown varying mechanical performance as a result of different layer thickness. Many factors associated with built orientation need to be explored if layer thickness results in property anisotropy. Studies by Hague *et al.* (2004) and Dulieu-Barton *et al.* (2000) have shown that in parts built in a number of orientations and subjected to tensile testing, differences were found in the tensile strength measurements for different orientations. Their build orientations can be seen in Figures 2.11 and 2.12, respectively. These differences were less than 5% for Hague *et al.* (2004) and as much as 13% for Dulieu-Barton *et al.* (2000). Hague et al. (2004) concluded that the 5% variation showed that SL produced what could be considered essentially isotropic parts for the orientations tested by them. Layout or whether a sample was built flat or on an edge was shown to have a significant effect on the ultimate tensile strength and modulus of elasticity. The orientation of the build layer with respect to the fabricated part has a significant effect on the resulting mechanical properties (Quintana *et al.*, 2007).

2.5 AGING

Aging effects can change the mechanical properties of a sample. Epoxies may go through a form of chemical aging which involves continuous crosslinking of unreacted species over a period of time. This is not desirable because it indicates that the epoxy's material properties constantly change. Changes can be observed in the tensile modulus, elongation and impact strength (Scheirs, 2000).

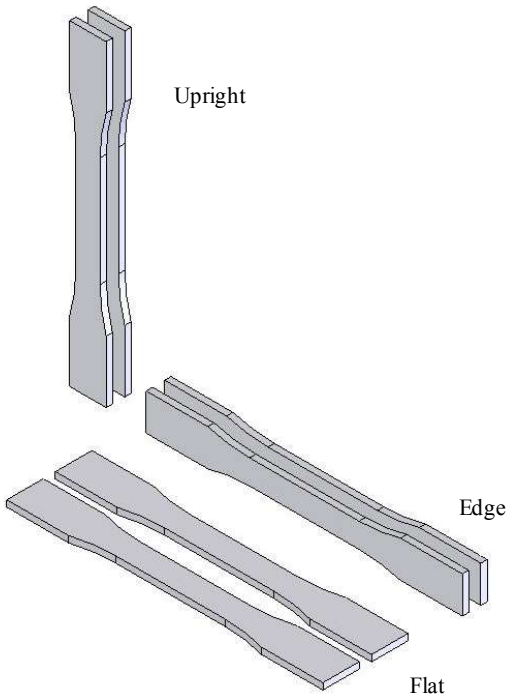

Figure 2.11 Build orientation for Hague, 2004.

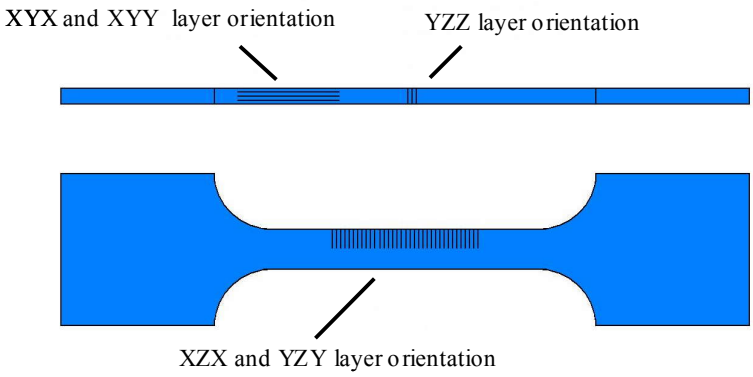

Figure 2.12 Build orientation for Dulieu-Barton, 2000.

CHAPTER 3 EXPERIMENTAL SETUP AND PROCEDURES

3.1 INTRODUCTION

The following chapter covers the experimental setup and the techniques used to fabricate ASTM D-638 samples. It describes the modification and improvements used to manufacture stereolithography (SL) fabricated parts. The following sections in this chapter provide specifications on the equipment, instruments, and material involved in the setup. It also demonstrates the procedures used to run tensile tests on the specimens to determine the specific build orientation and aging parameters that impact their mechanical properties.

3.2 EXPERIMENTAL SETUP

The next section covers a detailed description of the different build setups which are investigated in order to know how the different build orientation factors affect the mechanical properties of the commercially available epoxy resin WaterShed® 11120 (DSM Somos®, Elgin, IL). The first build setup shown in Figure 3.1 involves the study of 18 specimens, each with its respective category, which involves the study on axis, position, and layout of the Type I tensile specimen. Figure 3.2 entails the study of an additional layout component and position of the 24 specimens, which is also being investigated. Both of the build setups deal with the interaction of the layer to layer manufacture of the parts done in Viper Si^2 and how the build layers due to orientation affect the mechanical properties.

3.2.1 Two Build Setups

Two different studies were analyzed and for one, axis, position, and layout were reviewed under different conditions and time periods. Figure 3.1 shows the layout of the Viper Si^2 build platform illustrating the 18 specimens with 6 different orientations and 3 replicates for each orientation. In this study, only two different layer to layer interfaces were studied flat and

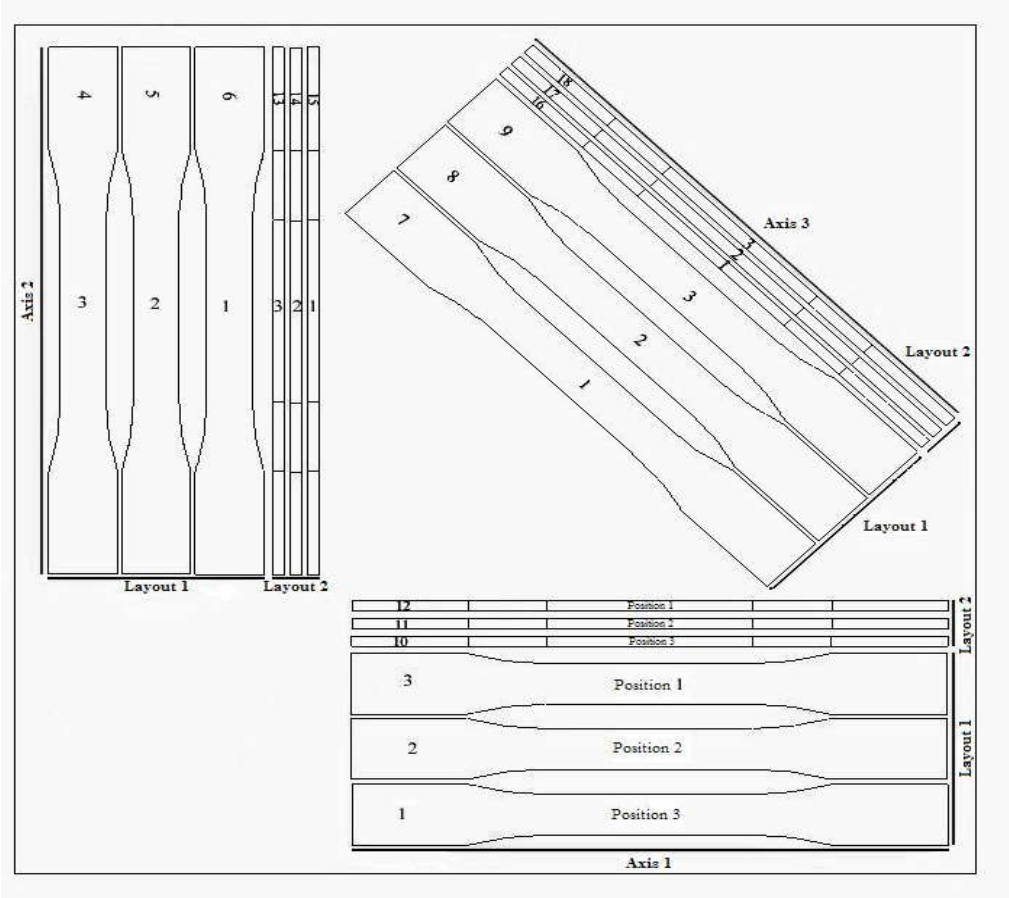

Figure 3.1 Layout of the Viper Si² build platform illustrating 18 test specimens in 6 different orientations with 3 replicates for each orientation.

on an edge as shown in Figure 3.3. Figure 3.5 shows an isotropic view of the build platform of the 18 tensile test specimens. In this study, aging and pre-conditioning were performed to understand the effects in the mechanical properties based on these changes in the environment.

For aging, the different time periods taken into consideration were four days, one month, and

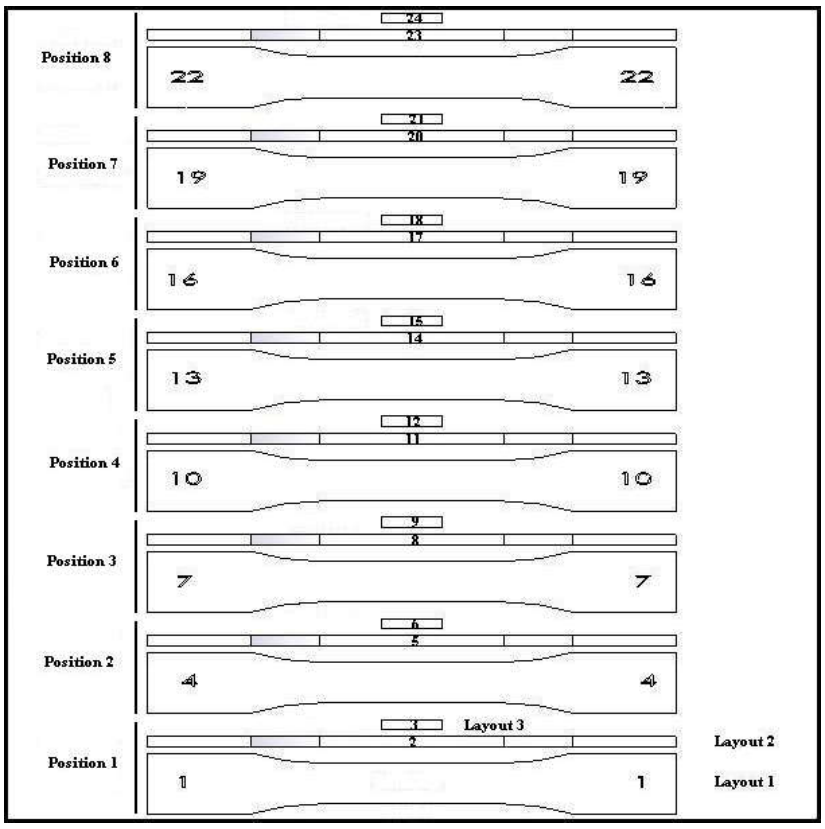

Figure 3.2 Layout of the Viper Si² build platform illustrating 24 test specimens in 3 different orientations with 8 replicates for each orientation.

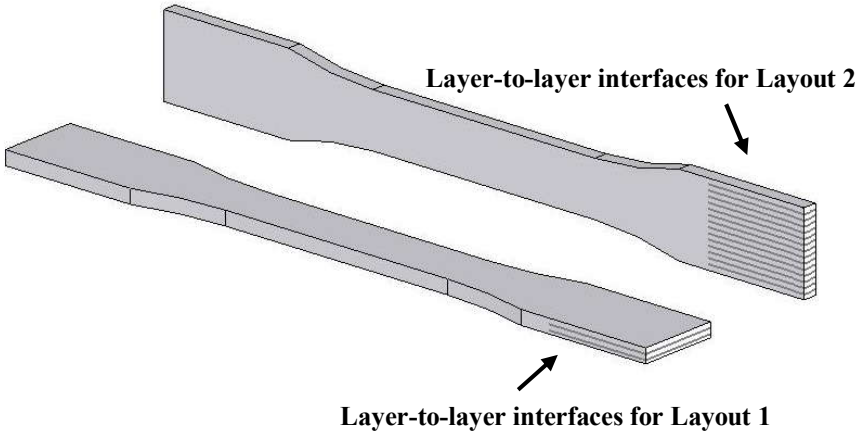

Figure 3.3 Layer to Layer interfaces of Layout 1 and Layout 2.

four months. The difference in aging times was investigated to understand the mechanical behavior of the resin after being fabricated and how time has an effect on it. Each time period involved three different conditions which were ambient, desiccant and desiccant plus two days at environmental conditioning (23±2°C and 50±5% relative humidity) as shown in Table 3.1. The environmental conditions applied in the studies are based on ASTM D638 Standard. In ambient, specimens were placed on a table top in the laboratory at room temperature for four days, one month, or four months. Figure 3.4 demonstrates that for desiccant, the test specimens were placed in a plastic bag with desiccant to prevent any moisture or humidity. The specimens

Figure 3.4 Test specimens with desiccant.

were kept in the plastic bag with desiccant for the period of time stated and then conditioned as stated in the ASTM D638, temperature of 23±2°C and humidity of 50±5% for not less than 40 hours prior to testing. This was done for each time period. In the other study, different positions and layouts were analyzed to better understand the effects of build orientation. Three different layouts were analyzed which were flat, on an edge, and vertical as shown in Figure 3.6. The

Table 3. 1 Two different setups with their respective pre-condition, aging, and test factors.

No. of specimens	Pre-condition	Aging (Days)	Factors Tested
18	Ambient	N/A	Position, Axis, and Layout
	Ambient	4	Aging and Pre-conditioning
		30	
		120	
	Desiccant	4	
		30	
		120	
	Desiccant plus two days (23±2ºC and 50±5% RH)	4	
		30	
		120	
24	Ambient plus two days (23±2ºC and 50±5% RH)	4	Position and additional Layout (vertical)

layout of the build platform for the second study of the 24 test specimens is shown in Figure 3.2. This shows the study of three different build orientations and the study of the eight different positions of the test specimens on the platform of the Viper Si^2. The addition of another orientation to the study would give a better understanding of the layer-to-layer interfaces for the build platform. For this study of 24 specimens, they were analyzed four days ambient and two days under the condition of 23°±2°C and 50±5% relative humidity. An isometric view of the layout of the specimens in the Viper Si^2 is illustrated in Figure 3.7. The conditioning is the same as previously mentioned and stated in the ASTM D638.

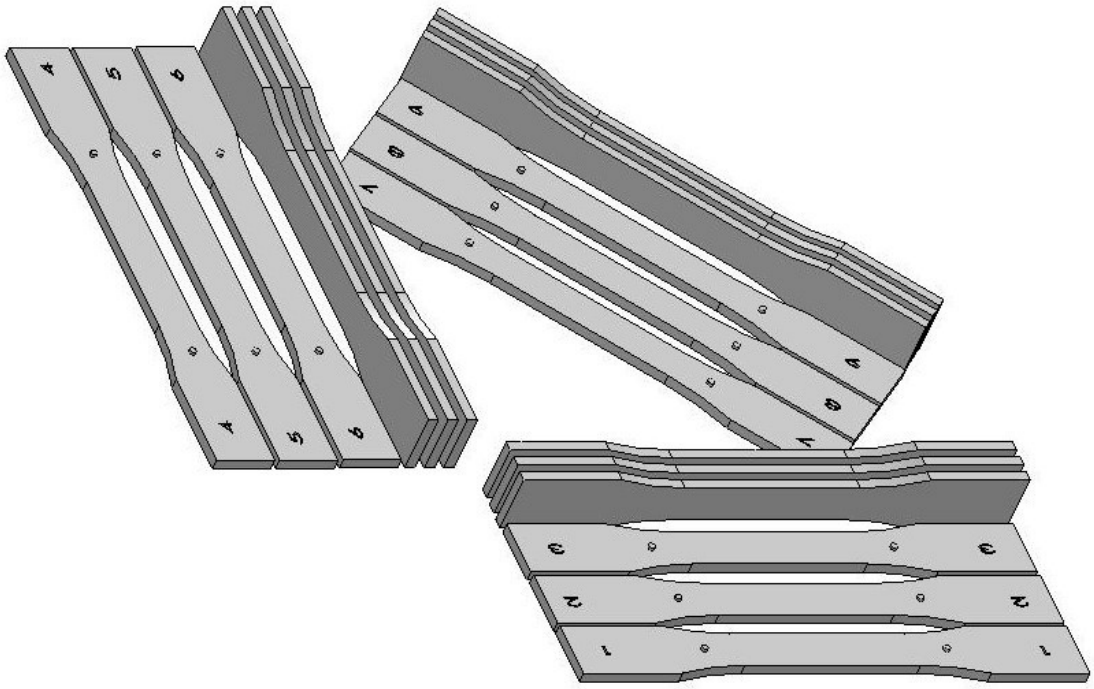

Figure 3.5 Isometric view of the study of the 18 specimens built in the Viper Si².

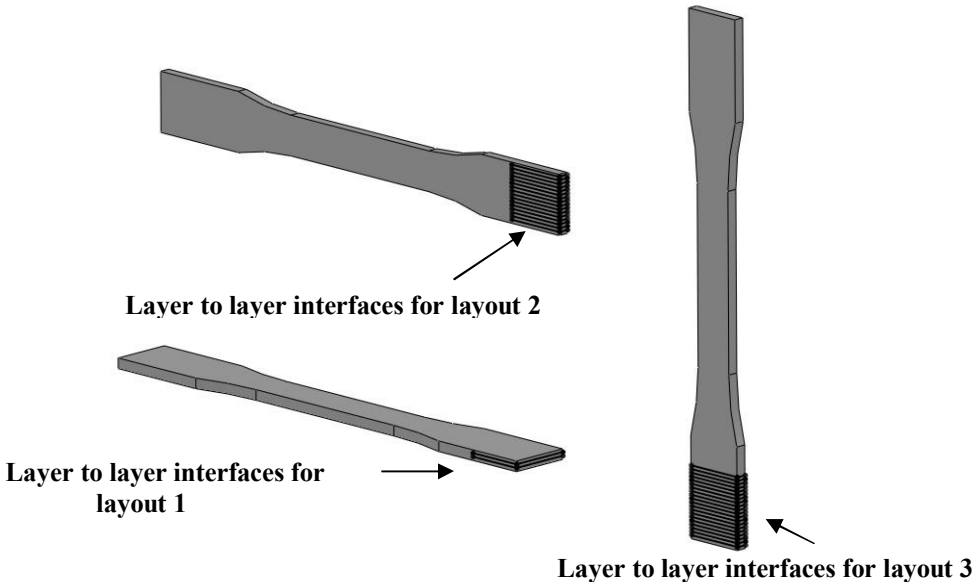

Figure 3.6 The three different layer to layer interfaces for the different layouts studied (flat, on an edge and vertical).

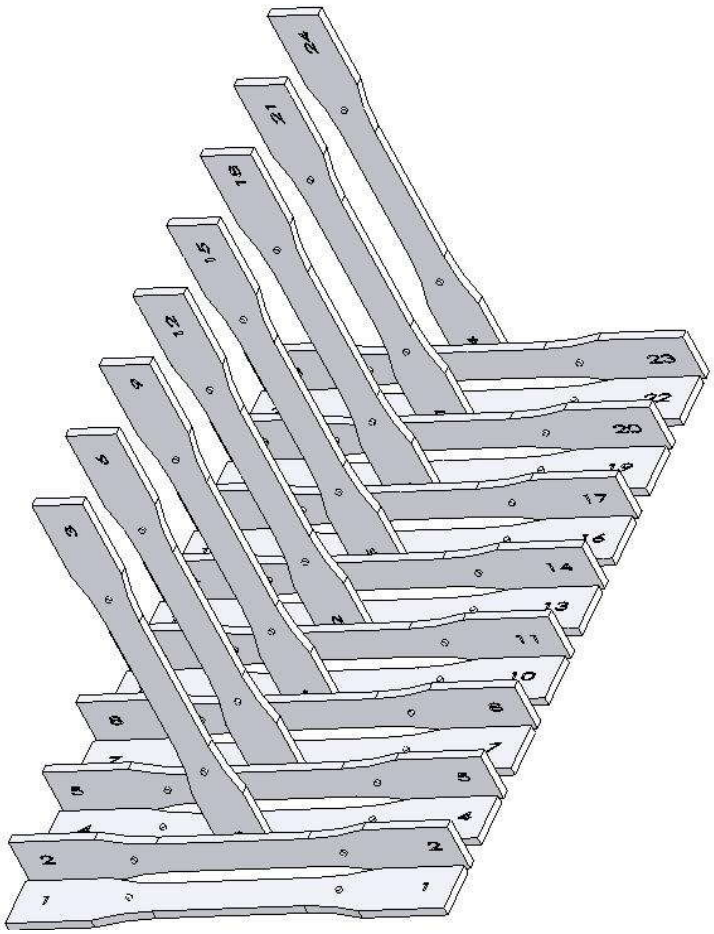

Figure 3.7 Isometric view of the study of the 24 test specimens built in the Viper Si².

3.3 ENGINEERING DESIGN

Based on the ASTM D630 standard and the requirements for the experimental investigation on composite resin, a new vat design was developed to manufacture the Type I tensile specimens in order to successfully build the specimens. The new vat design was then used to manufacture tensile specimens. For the first build setup study which only involved manufacturing two types of layouts (flat and on an edge), an insert was designed to save usage of epoxy resin. For the second build setup investigation of the three different layouts (flat, on an edge, and vertical), the

insert design component is removed for addition of commercially available WaterShed® 11120 epoxy resin. It was also designed for the build not to fail when the build platform comes into contact with the vat. This new design can be used to manufacture 3D parts of new costly epoxy resin material for which the amount can be limited due to the price.

3.3.1 Viper Si^2

Based on the experimental design setup, the manufactured Type I tensile specimens were built in a 3D Systems Viper Si^2 prototyping machine with a single platform with cross sectional area of 25.4 cm by 25.4 cm. The two different build setups were manufactured with WaterShed™ 11120 (DSM Somos®, Elgin, IL) to investigate the effects of the orientations with respect to different aging and environmental conditions. By using the recommended settings and build parameters by the Product Data Sheet from DSM Somos® shown in Table 3.2, all test specimens investigated in this research were manufactured with this technology. The layer thickness of the specimens build was 0.1 mm with a laser power of ~45 mW. During the process of building the batches, the condition in which they were being built, such as temperature, relative humidity, and duration of the build along with other specifications of the build obtained from the Viper Si^{2,} were monitored as can be seen in Appendix B.

Table 3.2 Recommended settings and build parameters from DSM Somos®.

WaterShed™ 11120 Optical Properties (355 nm wavelength)	
Viscosity	~260 cps at 30ºC
Density	~1.12 g/cm³ at 25ºC
Critical Exposure, E_C	~11.5 mJ/cm²
Penetration Depth, D_P	0.16 mm

3.3.1.1 Vat and Top

Based on the standard test method for tensile properties of plastics ASTM D68 was followed to complete the study. Some restrictions were set, however an experiment was done to have appropriate and relevant testing of the material. In the commercial SL machine in the building envelope, the vat used in this technology has the dimensions of 250 x 250 x 250 mm. Therefore, the vat was redesigned to fit the needs of the experiment as it pertains to the building of specimens vertically to test the different orientations of test specimens. Even though the vat was redesigned, another component was added to the engineering design. The followed standard states that the Type I specimen used for this study should have the correct dimensions, specified in Table 3.1, as well as it ought to have sufficient material. The vat was designed not to have to use a large amount of material however build successful parts. The original vat holds approximately 32 L of material. The vat design shown in Figure 3.8 was set to have the dimensions of approximately 367 x 299 x 195 mm which holds the capacity of approximately 20 L of resin. An insert was designed as well as the other component of the design to help reduce the amount of material used. Due to the insert, the volume of the vat was decreased by approximately three liters of resin. The dimensions of the insert are approximately 356 x 288 x 50 mm, and Figure 3.9 illustrates the design. The insert was used for the study of the 18 specimens to investigate different factors (axis, layout, and position) and the aging (4, 30, and 120 days) of the specimens with corresponding pre-conditioning (ambient, desiccant, and desiccant plus two days 23±2°C and 50±5% relative humidity). This particular design can be implemented to be used to build parts of a costly material.

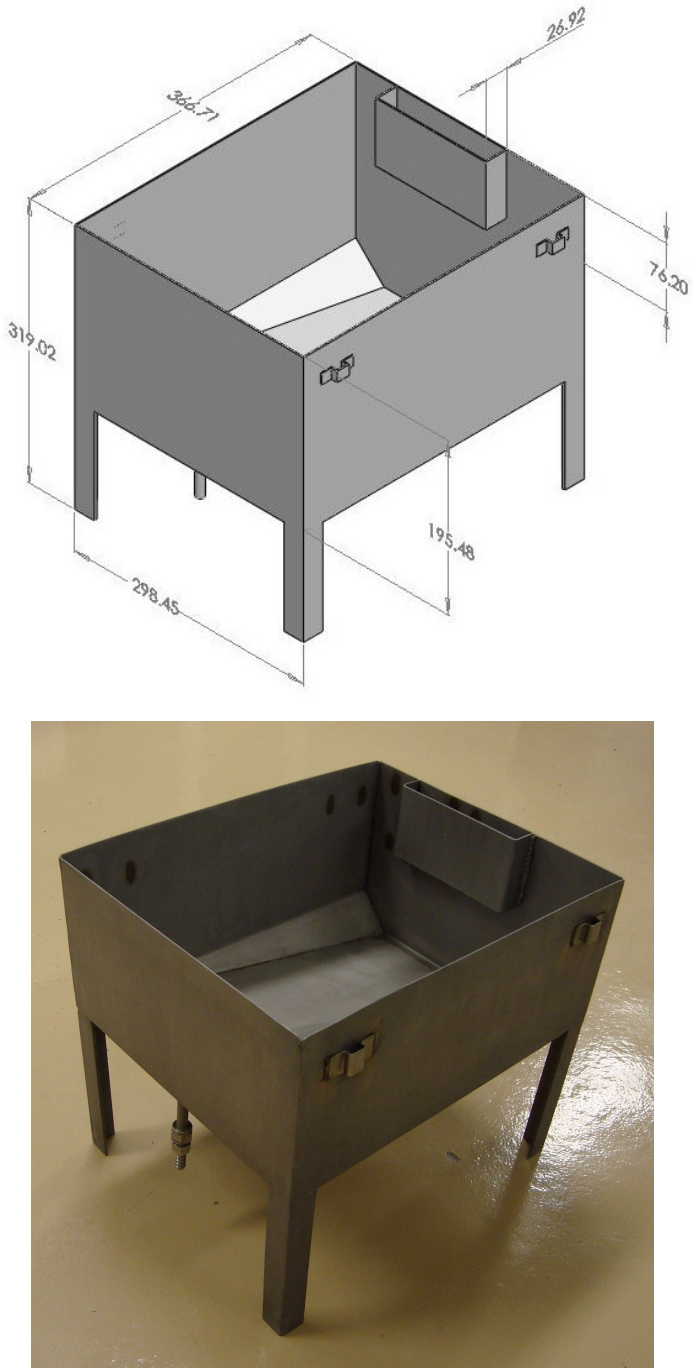

Figure 3. 8 Top: Schematic of new vat design with dimensions. Bottom: Photograph of new vat design.

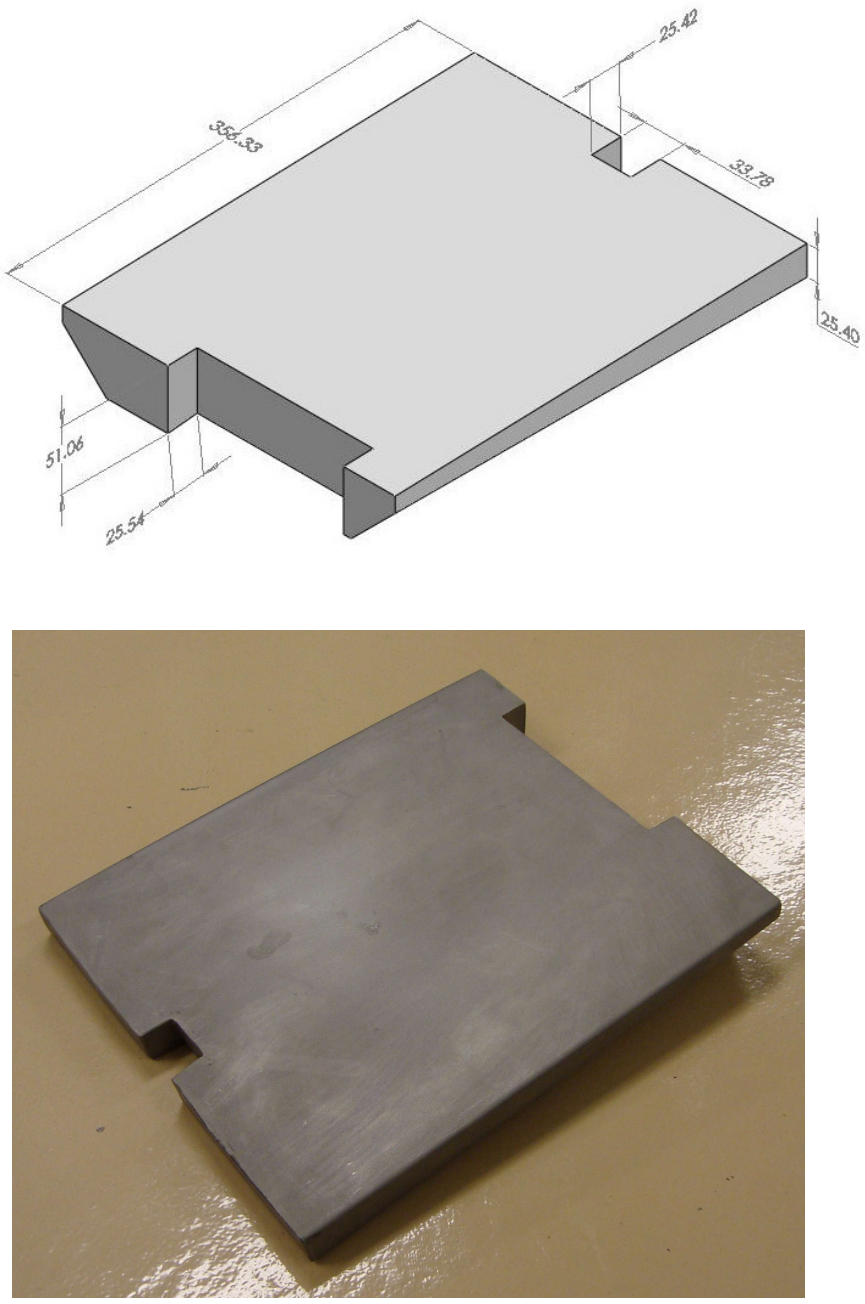

Figure 3.9 Top: Schematic of insert design with dimensions. Bottom: Photograph of vat.

For instance, Sandoval (2006) designed a vat that holds a volume of approximately 550 mL to build parts of epoxy based resin dispersed with multi-walled carbon nanotubes (MWCNTs).

This nano material is from $320 to $350 per gram and as a result there was a reduction in volume. The design implemented in this study can be used to continue a study with dispersion of MWCNTs in epoxy resin to build different types of specimens with different length dimensions as stated in ASTM D638 (165, 183, 246, 115, and 63.5 mm). The final design is shown in Figure 3.10 with vat and insert. Figure 3.11 shows the newly designed vat incorporated to Viper Si^2 used to build the different building platform design.

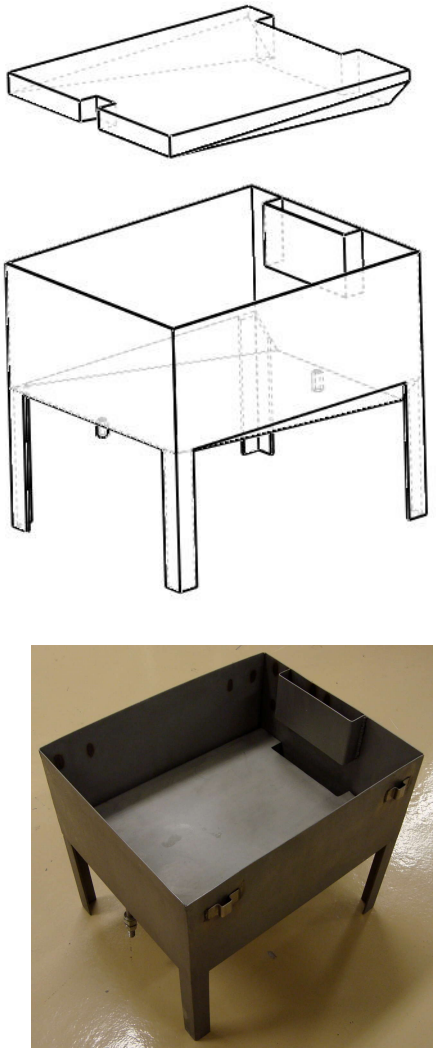

Figure 3.10 Top: Schematic showing the way the insert is introduced into the vat. Bottom: Photograph of the insert in the vat.

A) 3D Systems Viper Si^2.

B) Viper Si^2 with replaced new design vat that holds ~20 L.

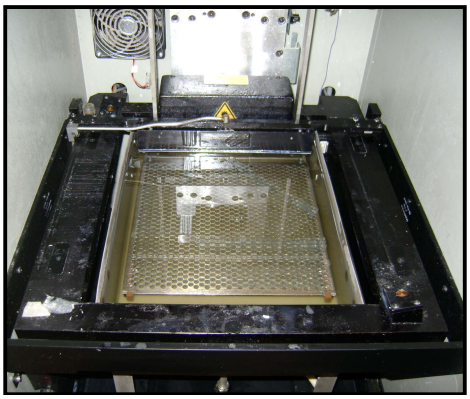

C) Viper Si^2 building envelope with a platform dimensions 25.4 cm by 25.4 cm cross-section.

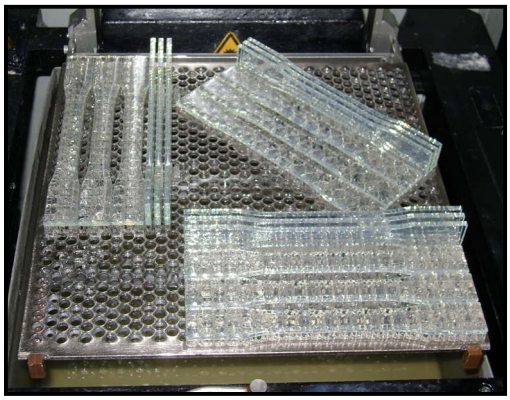

D) 1st Building platform designed to hold 18 test specimens, for test of three factors (axis, layout, position).

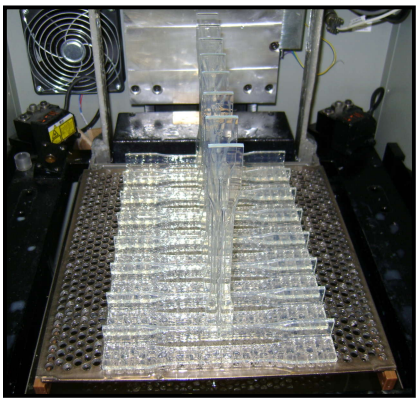

E) 2nd Building platform designed to hold 24 test specimens, for test of two factors (layout and position).

Figure 3.11 3D System Viper Si² with new designed vat able to build different layout orientations.

3.3.1.2 Building Process

Figure 3.12 shows the review of the process when the specimens were built in the Viper Si^2. For both studies, the same process was followed. Depending on the time period for aging and the pre-conditioning, the specimens were treated then mechanically tested. Figure 3.13 shows the difference in the specimens based on their built orientation of the two studies. The specimens built flat have an opaque appearance compared to the specimens build on an edge and vertical which have a clear appearance. Each study had a number of the batches that were aged and conditioned as shown in Table 3.1.

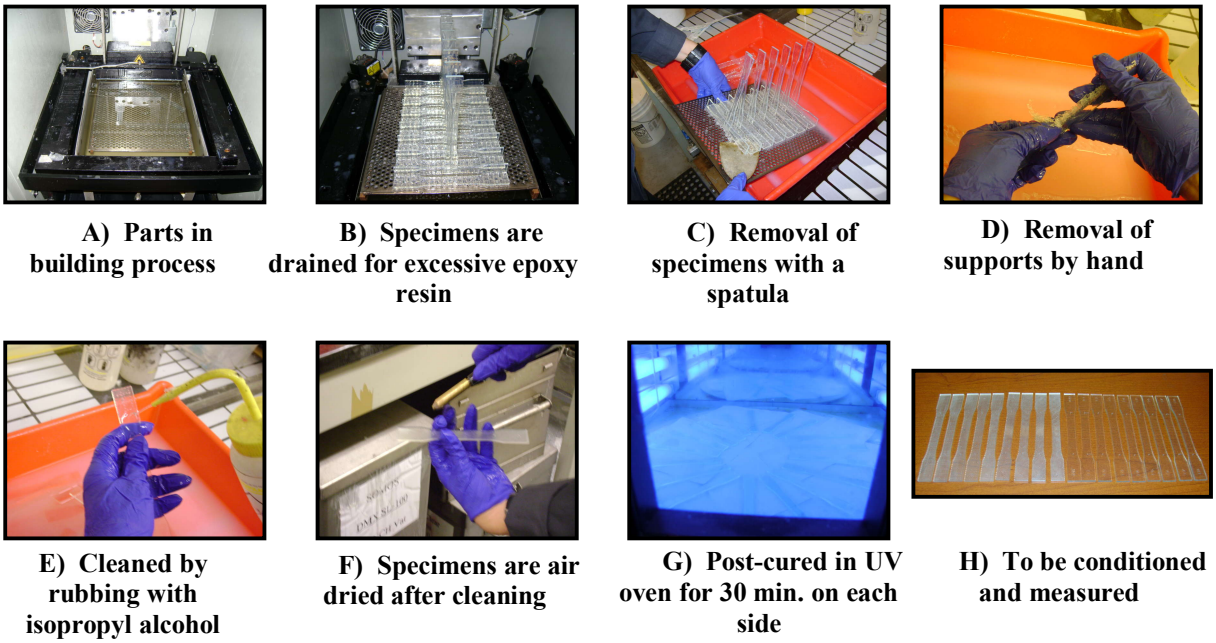

A) Parts in building process

B) Specimens are drained for excessive epoxy resin

C) Removal of specimens with a spatula

D) Removal of supports by hand

E) Cleaned by rubbing with isopropyl alcohol

F) Specimens are air dried after cleaning

G) Post-cured in UV oven for 30 min. on each side

H) To be conditioned and measured

Figure 3.12 Shows the steps taken on the building procedures of the test specimens.

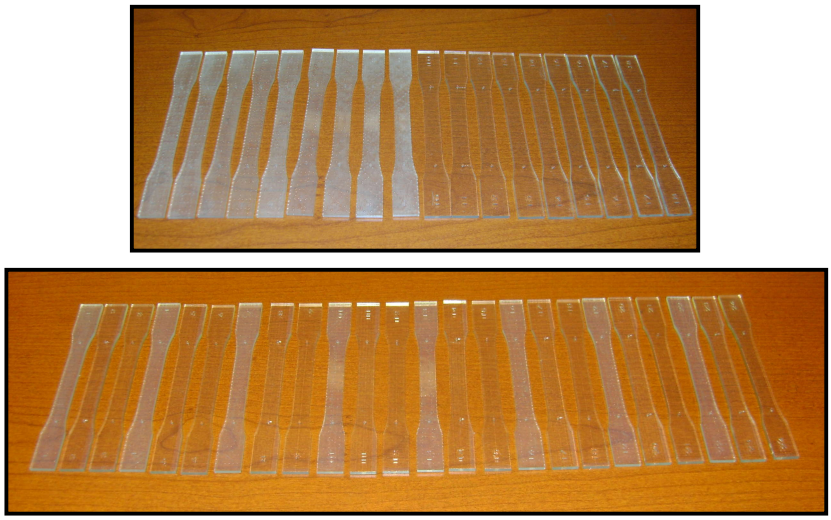

Figure 3.13 Note the difference in appearance of both studies. Top image shows the study of 18 specimens with two different layouts. Notice the opaque specimens built flat and the clear appearance of those built on an edge. The bottom image shows the study of 24 specimens of the three different layouts. Notice the differences in appearance of the specimens.

In this study, ASTM Standard D638 was followed for pre-conditioning the test specimens. The test specimens were kept in a controlled environment of 23±2°C and 50±5% relative humidity for 48 hours prior to tensile testing. Figure 3.14 shows the environmental chamber used to condition the test specimens, which has two operating systems; humidifier and dehumidifier in a portable machine. Figure 3.15 shows the operation and part identification of the DanbyPHD® (DanbyPHD® Model DHCC6020, Danby Products Inc., Findlay, OH). The conditioning of 23±2°C and 50±5% relative humidity for 48 hours as stated in the ASTM Standard D638 was controlled by the multifunctional DHCC unit of 28.38 L dehumidifier and 9.46 L humidifier and a HEPA filter for air purification. The DHCC has electronic components which control the temperature and humidity as well has the dehumidification. The humidity and temperature can be adjusted with the LED display.

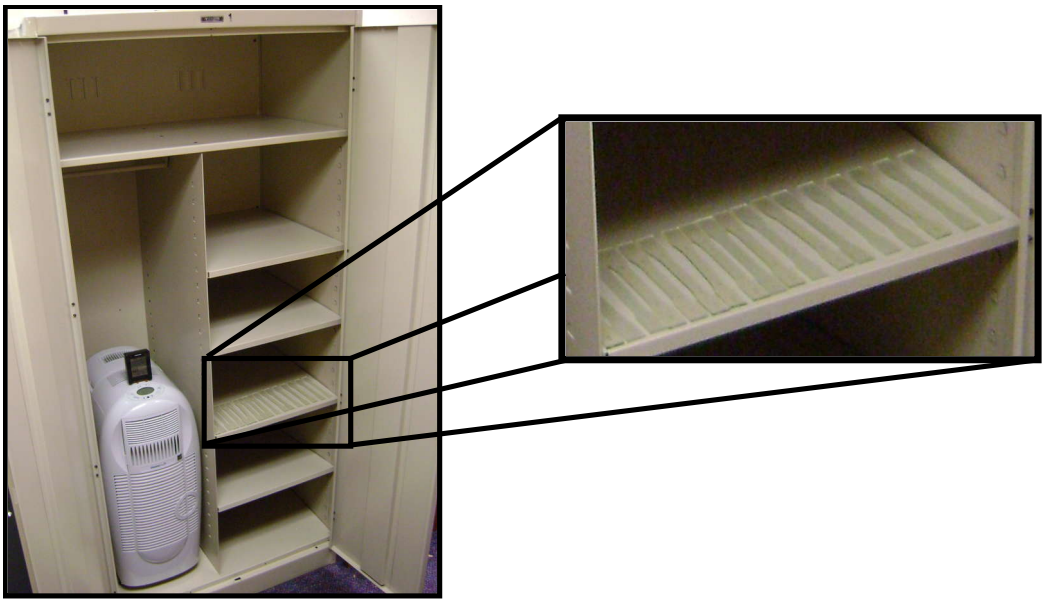

Figure 3.14 Photograph illustrating the environmental chamber where the test specimens where conditioned (23±2°C and 50±5%RH).

Figure 3.15 Demonstrate DanbyPHD® Model DHCC6020 and Upper view of DanbyPHD®.

3.4 MECHANICAL TESTING

When studying materials it is important to determine what the special properties of the material are that would favor its use in a particular application. Although advances have been made in recent years, mechanical properties cannot be predicted from basic molecular structure principles, except in a few cases. One such case being that the actual strength of the polymer may be only one tenth to one hundredth of the value calculated in regards to bond strengths and intermolecular forces. For this reason, mechanical tests provide the method of obtaining evaluations of new polymers. These types of tests are performed frequently in laboratories and most tests result in the destruction of the sample being tested. Because of this, multiple tests are needed to be performed on similar samples before valid results can be acquired. These tests strive to answer many things about the material such as the response of the sample to stress and strain, its elasticity, and how it responds to tensile forces. It is critical that answers such as these be answered before the material can be considered for any type of important or large-scale application (Allcock *et al.*, 2003).

3.4.1 Tensile Test Properties

A measure of a material's resistance to elongation or breaking when stretching forces are applied to it can be provided by its tensile strength. This is possible through the relation of stress to strain. The graphical representation of this relationship can be seen in Figure 3.16. The data are normally plotted with the strain on the x-axis and the stress on the y-axis which typifies the behavior of a plastic material. Stress ($\frac{kg}{m \cdot s^2}$) can be defined as the force ($\frac{kg \cdot m}{s^2}$) per unit cross-sectional area (m^2) applied to the sample as can be seen in Equation 3.1 where σ is the stress, F

is the force, and A is the cross-sectional area in the gage area. Strain ($\frac{m}{m}$ otherwise dimensionless) is the elongation of the sample under a given stress which is shown in Equation 3.2 where ε is the strain, l (m) is the length after fracture, and l_0 (m) is the original gage length.

$$\sigma = \frac{F}{A} \tag{3.1}$$

$$\varepsilon = \frac{l - l_o}{l_o} \tag{3.2}$$

The speed at which the stress is applied must be taken into account because the stress-strain behavior of most materials is time dependent. Stress-strain experiments are often carried out on a flat sample that resembles a dog bone shape. The sample is clamped at both ends by the jaws of a testing machine which are then separated by the application of a known mechanical force. The material being tested usually experiences elongation and breaks in the narrower central region of the sample as demonstrated in Figure 3.17. There are two ways by which the stretching ability or ductility of materials can be quantitatively expressed: percent elongation and percent reduction in cross sectional area. The percent elongation (%) may be calculated by determining the gage length l after fracture in Equation 3.3.

$$\%Elongation = \frac{l - l_o}{l_o} \times 100 \tag{3.3}$$

This elongation represents the total elongation which consists of both uniform (before necking) and nonuniform (after necking) elongations.

The stiffness of a material (E) is the measure of the ratio of stress to strain in the elastic part of the stress-strain curve or simply the slope of the straight line of the start of the graph as stated in Equation 3.4. The origin of it lies in the fact that the materials obey what is known as Hooke's

law in Equation 3.5 which states that stress is proportional to strain in this regime of the stress-strain curve.

$$E = \frac{\sigma}{\varepsilon} \tag{3.4}$$

$$\sigma \propto \varepsilon \tag{3.5}$$

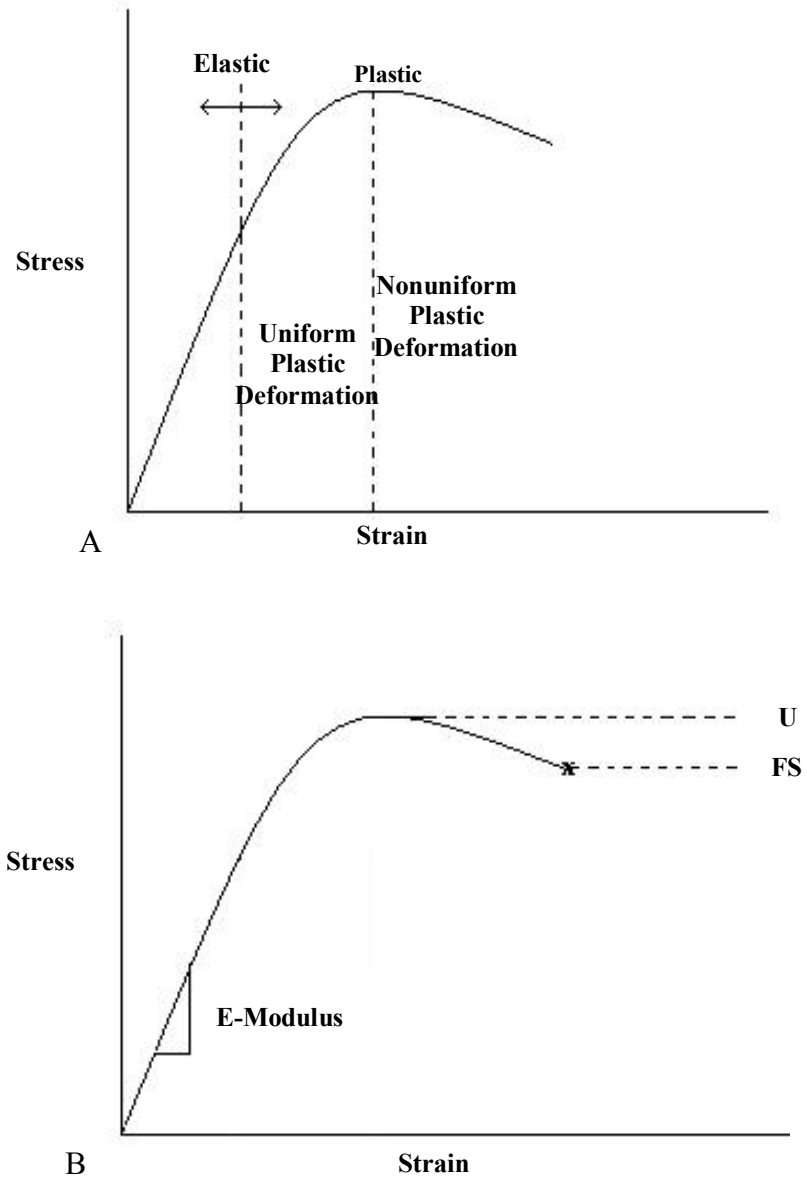

Figure 3.16 Typical stress-strain curve graph. A) Elastic and plastic deformation regions. B) UTS, FS and E-Modulus points are illustrated.

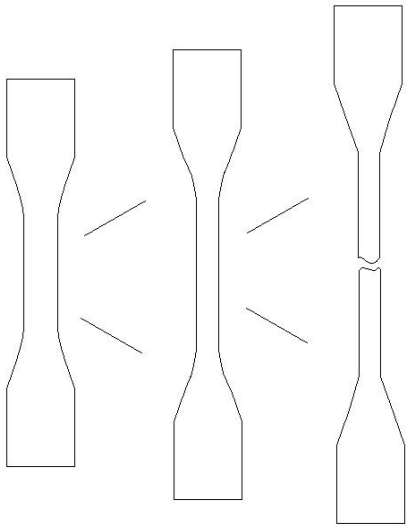

Figure 3.17 From left to right: The test specimens begins as normal, then experiences elastic deformation, and finally fractures.

The modulus of elasticity is one of the properties that were calculated by taking the data of 1-3% of the strain from the stress and strain curve. This is to exclude the initial toe of the graph in order to obtain accurate results since the correlation is ~ 1 for that portion of the graph. This represents a more accurate value for the modulus of elasticity (E-Modulus (1-3% strain)) that will distinguish this calculated value from the modulus of elasticity obtained from the equipment.

A stiff polymer will yield very little as the stress is applied, whereas a soft polymer will yield significantly under the same conditions. Another term associated with the process is toughness that is a measure of resistance to breaking and is a property that can be roughly estimated from the stress-strain curve which is a result of the plotted data. One of the most important pieces of information that is obtained from the stress-strain curve is the value of the tensile strength. It is also known as the stress at the breaking point (Allcock *et al.*, 2003).

An important characteristic that can be determined from the stress-strain curve is the modulus of elasticity. Also known as Young's modulus, it is identified as the slope of the initial

linear portion of the stress-strain curve and is defined as the measure of the stiffness of a material. The greater the modulus of elasticity, the smaller the elastic strain that results from the application of a given stress. This region of the stress-strain curve is where a material experiences elastic deformation and where stress is proportional to strain. The material can return to its original dimensions after the release of the force in the elastic deformation region. It is possible due to of the binding forces between atoms. These forces cannot be changed without altering the basic nature of the material. Modulus of elasticity is essential for computing deflections of beams and other members, which makes it an important design value (Davis 2004).

3.4.2 Equipment

To carry out the mechanical testing, an INSTRON® 5800 (Model 5866, INSTRON®, Norwood, MA), shown in Figure 3.18, tabletop machine with double column was used to perform the testing. Due to the columns, the machine provides better alignment and increased stiffness. The INSTRON® 5866 has a load capacity of 10 kN with a crosshead speed accuracy of ± 0.1% of speed. A calibrated static load cell of 10 kN (Model 2525-804, INSTRON®, Norwood, MA) with a ± 0.5% accuracy and ± 0.5% repeatability digital readout is equipped on the machine. An Advanced Video Extensometer (AVE) (Model 2663-821, INSTRON®, Norwood, MA) is operational along with the machine, with a digital camera resolution of 1µm and accuracy of ± 2.5 µm that measures the strain by tracking gauge marks placed on the test specimen. Figure 3.18 show the INSTRON® 5866 with AVE. In addition to the AVE in this research, a static strain gauge extensometer, 2 in gauge length (Model 2630-115, INSTRON®, Norwood, MA) was employed with a axial travel of +1/-0.1 in or % axial travel of 50%/-5%

maximum strain shown in Figure 3.19. To clamp the specimen, manual wedge action 30 kN capacity (Model 2716-015, INSTRON®, Norwood, MA) grips were mounted on the machine to grip the test specimens with diamond serrated faces to eliminate the slippage of the specimen when testing.

Figure 3.18 INSTRON® 5866 and AVE testing system (INSTRON, 2007).

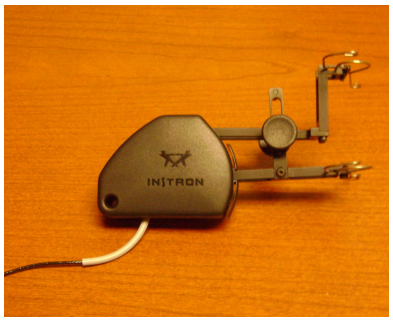

Figure 3.19 2 inch gauge length clip on extensometer.

3.4.3 Tensile Testing

The manufactured specimens were mechanically tested with the INSTRON® 5866 tabletop machine. Prior to the studies of aging, conditioning and testing, the tensile specimens were first measured with a caliper (Model 500-196, Mitutoyo America Co., City of Industry, CA). The following dimensions were measured for the tensile test specimens as stated in the ASTM D-638 (ASTM, 2005) in Table 3.3 and Figure 3.20 which show the drawing of a Type I specimen with its respective dimensions. The thickness of the specimens of 3.2 ± 0.4mm is applied to molded plastics and was followed in these studies. The dimensions were taken for the specimens with the caliper and then were marked with a specialized ruler and white marker provided from INSTRON® as shown in Figure 3.21. This was done for better reading on the Advanced Video Extensometer (AVE) in order to register the gage length of 50 mm, as shown in Figure 3.21. This study furthermore demonstrates that the Viper Si^2 is a capable process for the manufacturing of repeatable and reproducible parts by applying the tolerances of ASTM-D638 Type I test specimens. On the first study, the specimens were marked prior to the placement of the clip on extensometer, for correct placement and to achieve the respected gage length of 50

Table 3.3 ASTM D-638 Type I tensile test specimen dimensions and tolerances.

Dimensions (mm)	Type I		Tolerances
Wc - Width of narrow section	13	±	0.02
L - Length of narrow section	57	±	0.02
Wo - Width overall	19	±	0.025
Lo - Length overall	165	±	no max
G - Gage length	50	±	0.01
D - Distance between grips	115	±	0.02
R - Radius of fillet	76	±	0.04
T - Thickness	3.2	±	0.4

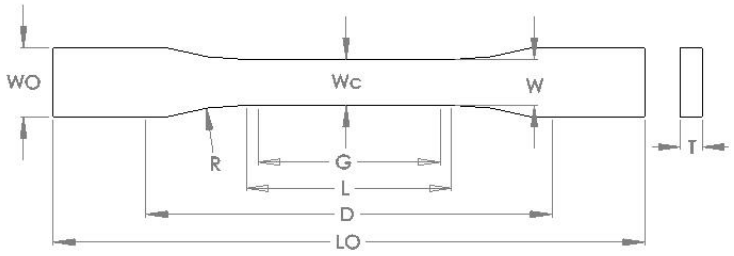

Figure 3.20 ASTM D-638 Type I tensile test specimen.

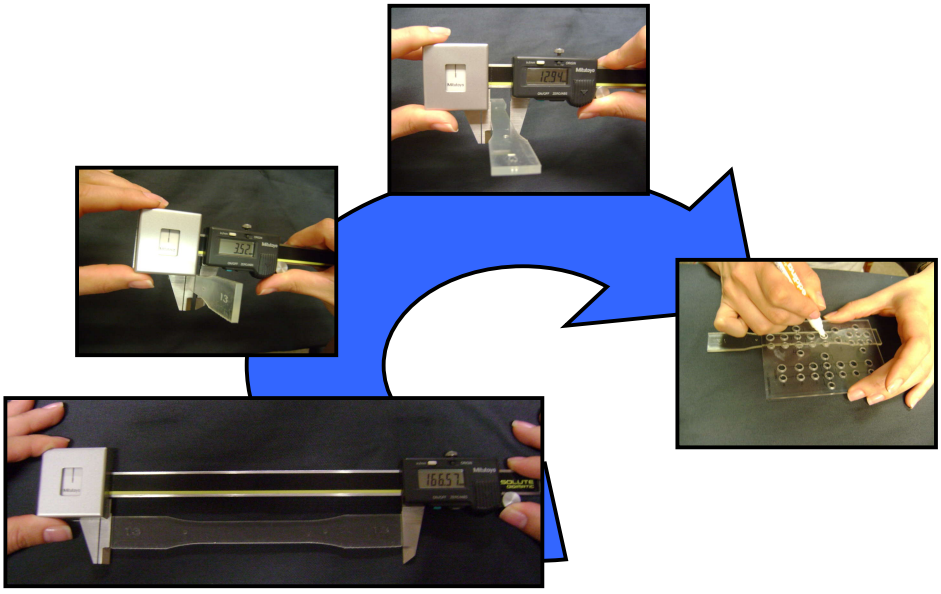

Figure 3.21 Measuring techniques with assistance of a caliper and INSTRON® ruler with specialized marker.

Figure 3. 22 Test specimen with two white dots separated by 50 mm.

mm. Following of the test specimen measurements, the specimens were conditioned correspondingly and were then mechanically tested. The specimens was first clamped in the top grip of the INSTRON® which was aligned in the center of the grip for the specimen to have an evenly distributed load on the specimen. Therefore, the specimen is suspended freely from the top grip to allow the specimen to orient itself to the lower grip. The specimen was clamped slowly closing the grips to avoid any applied load to the specimen. However, a load is applied to the specimen when clamped, this means that there is a compressive load and the crosshead of the INSTRON® needs to be moved. The applied load can be decreased by means of the thumbwheel of a control jog on the INSTRON® machine which is the fine position. The gage length is reset to zero to obtain the increment in the distance within the gage length before the test begins as shown in Figure 3.23.

The same procedure was followed when using the clip-on extensometer. However, the clip-on was clipped on after the load was removed from the specimen with the thumbwheel. Figure 3.24 demonstrates the different set-ups for the tensile test. Prior to the mechanical testing, a tensile test method was created in software Bluehill 2®, Version 2.15.615 (INSTRON®, Norwood, MA). The software allows inputting the specific information about the test specimen prior to testing, for instance the test parameters like dimensions and the speed of testing. The method provides calculations of the Ultimate Tensile Stress (UTS), Elongation at Break (%),

Fracture Stress (FS), and Modulus (E) based on the material behavior. Based on the ASTM D638 Type I specimen, the specimens were tested with a cross head speed of 5 mm/min. To measure the stiffness of the material and to accurately calculate the modulus of elasticity, an Advanced Video Extensometer (AVE) was used as well as a clip on extensometer. The AVE is a non-contact extensometer compared to the clip on extensometer. Due to the high resolution digital camera and advanced image processing, AVE obtains precise strain measurements on the test specimen. The clip on extensometer needs to be removed after the

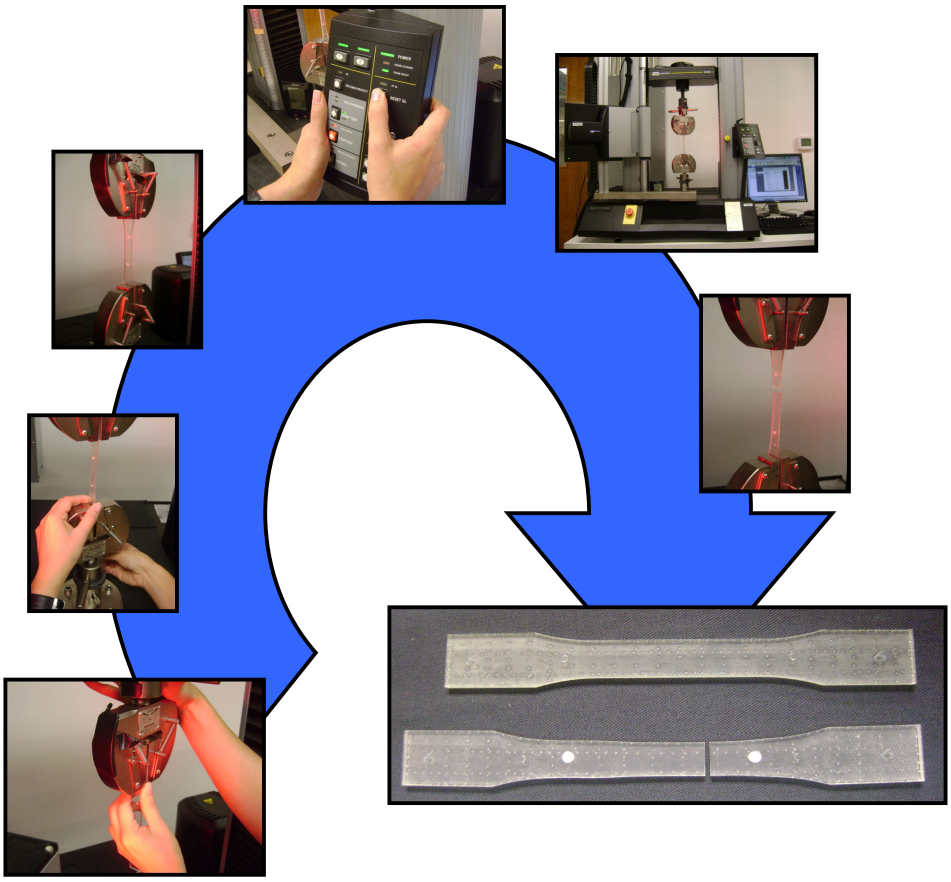

Figure 3.23 Tensile test setup with respective process.

specimen fractures. On the test method the removal of the extensometer was set to be removed at 5% strain since the extensometer can be damage. After removal of the extensometer, the

calculations of the material were transferred and calculated by the crosshead speed, the load and the time in which the test was executed, the software then correlates the load and time in which the load occurred. In following chapter, the mechanical testing results are provided.

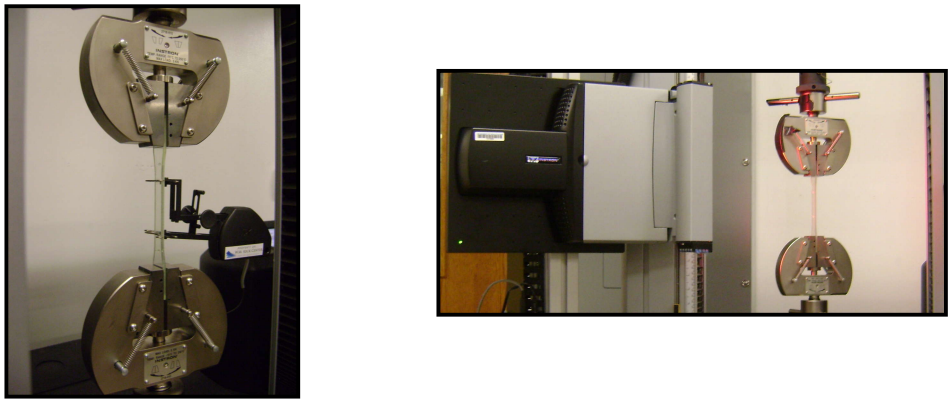

Figure 3.24 Different set-ups for tensile testing. 2 in. gage length clip-on extensometer and AVE, notice the red light from the camera which measures the distance between the two dots.

3.5 DESIGN OF EXPERIMENT

In order to determine if the SL process could produce reproducible and repeatable parts, a statistical design of experiment was performed. A study was considered on the variability of the specimen where three analysts randomly measured the specimens. Each specimen was measured three times by each of the analysts and an average was taken for the overall length, overall width, width of the narrow section, thickness, and gage length. A total of 1,080 measurements were taken with a low-pressure caliper. The analysis was performed with a 5% level of significance using Statgraphics® software.

3.5.1 Analysis of Variance

In a single factor analysis of variance design only one factor is investigated. Supposing that a treatments of a single factor are desired for comparison, then the observed response from each of the a treatments is a random variable. Generally, there would be n observations under the i^{th} treatment. A useful way to describe the observations from the experiment with a model is shown in Equation 3.6.

$$y_i = \mu + \tau_i + \in i_j \begin{cases} i = 1,2,...,a \\ j = 1,2,...,n \end{cases} \qquad 3.6$$

When testing the equality of a treatment means, the appropriate hypotheses would be Equations 3.7 and 3.8

$$H_o : \mu_1 = \mu_2 = ... = \mu_a \qquad 3.7$$

$$H_1 = \mu_i \neq \mu_j \qquad \text{for at least one pair (i, j)} \qquad 3.8$$

The treatment effects may be represented as deviations from the overall mean. A comparable way of expressing the hypothesis in terms of the treatment effects τ_i can be seen in Equations 3.9 and 3.10

$$H_o : \tau_1 = \tau_2 = ..\tau_a = 0 \qquad 3.9$$

$$H_1 = \tau_i \neq 0 \qquad \text{for at least one } i \qquad 3.10$$

CHAPTER 4 RESULTS

4.1 INTRODUCTION

This chapter summarizes results obtained from testing the WaterShed™11120 (DSM Somos®, Elgin, IL) test specimens. The sections describe the data obtained from the two build setups by testing the specimens under several aging and environmental conditions. The data are categorized into tensile testing, mechanical testing, and scanning electron microscope (SEM) results. Tensile testing results present the consequent stresses and E-modulus gathered from the testing. Mechanical testing aim to demonstrate a statistical analysis of the data while SEM results show what the effects of the testing had at a microstructural level.

4.2 TENSILE TESTING RESULTS

Type I specimens were tensile tested using both a 2 in. gage length clip on extensometer (Model 2630-115, INSTRON®, Norwood, MA) and the Advance Video Extensometer (AVE) (Model 2663-821, INSTRON®, Norwood, MA) to obtain accurate results. The two different build setups shown in Figures 3.1 and 3.2 were examined under tensile testing and different environmental and aging conditions to determine the effects of build orientation on mechanical properties. The mechanical properties that were investigated under this condition were Ultimate Tensile Stress, Tensile Strain at Break, Tensile Stress at Break, and E-Modulus. The initial testing was on the first build setup, as shown in Figure 3.1, to understand the changes of the mechanical properties with respect to different build orientation. The same build setup was analyzed to determine whether there were changes to the mechanical properties of the

WaterShed™ 11120 due to differences in environmental (ambient, desiccant, and 23±2°C and 50±5% RH) and aging (4 days, 1 month, and 4 months) conditions. The second build setup, as shown in Figure 3.2, was tested under 4 days ambient and 2 days at a temperature of 23±2°C and 50±5% RH to determine the effects due to differences in layout at the specific condition.

4.2.1 Effects of Build Orientation of the First Build Setup

Specimens for the first built setup in Figure 3.1 were randomized and kept at an ambient condition before undergoing tensile testing from an INSTRON® 5866 by utilizing the 2 in. gage length clip on extensometer. Table 4.1 shows the resulting Ultimate Tensile Stress, Tensile Strain at Break, Tensile Stress at Break, and E-Modulus (1-3% strain).

Table 4.1 Tensile testing results for 4 days ambient.

Specimen	Ultimate Tensile Stress	Tensile strain at Break	Tensile stress at Break	E-Modulus (1-3% strain)
	(MPa)	(%)	(MPa)	(MPa)
1	48.4	15.6	33.8	835.8
2	47.6	38.8	31.4	833.5
3	48.8	23.1	0.3	839.2
4	47.7	24.8	31.5	835.7
5	48.1	46.3	32.9	840.5
6	48.2	41.3	32.4	853.1
7	47.9	22.8	32.9	839.2
8	47.2	35.7	31.3	824.2
9	48.4	17.2	33.4	834.3
10	48.1	13.0	34.9	840.1
11	48.5	30.3	32.8	852.7
12	48.4	15.2	34.3	865.3
13	48.3	13.7	35.0	854.4
14	48.8	9.8	44.0	841.9
15	48.8	10.3	43.1	829.5
16	48.5	15.3	34.4	858.7
17	49.5	37.5	33.3	861.3
18	48.5	19.1	34.7	852.6
Mean	48.3	23.9	32.6	844.0
Std Deviation	0.5	11.6	8.8	11.7

4.2.2 Effects of Environmental and Aging Conditions of First Build Setup

Table 4.2 shows the resulting mechanical properties of the tensile test for the 18 specimen build setup in Figure 3.1. The test results were obtained using the 2 in. gage length clip on extensometer. The 18 specimens were randomized and were placed in an ambient condition to distinguish the differences in mechanical values as compared to the other two conditions (desiccant and 23±2°C and 50±5% RH).

Table 4.2 Conditioning tensile testing result for 4 days ambient.

Specimen	Ultimate Tensile Stress	Tensile strain at Break	Tensile stress at Break	E-Modulus (1-3% strain)	E-Modulus
	(MPa)	(%)	(MPa)	(MPa)	(MPa)
1	43.61	14.05	28.68	738.3	2475.47
2	44.65	7.98	31.73	754.89	2467.89
3	45.65	10.3	31.09	769.1	2662.68
4	44.53	15.01	29.06	749.09	2526.8
5	43.25	25.7	26.79	727.68	2438.19
6	44.39	10.02	30.72	768.52	2510.38
7	44.61	23.49	27.99	758.9	2316.89
8	44.54	27.78	27.33	777.33	2385.4
9	43.88	8.4	30.82	738.89	2486.46
10	47.84	6.74	33.3	830.88	2573.66
11	48.25	6.07	35.8	835.56	2637.6
12	47.33	5.34	38.19	842.62	2700.32
13	46.78	4.66	40.79	820.11	2775.58
15	46.95	4.11	44.25	820.71	2747.3
16	46.92	18.86	29.67	826.26	2656.42
17	46.32	13.7	31.11	801.32	2623.56
18	47.68	7.78	33.68	801.46	2549.50
Mean	45.72	12.35	32.41	785.98	2560.83
Std Deviation	1.63	7.53	4.85	38.54	127.59

For the desiccant condition, the 18 specimen build setup, as shown in Figure 3.1, was kept in a Ziploc® bag (Ziploc®, SC Johnson, Racine, WI) with desiccant for four days up until the moment of testing. For testing, the specimens were first randomized and then tensile tested

using an INSTRON® 5866 with a 2 in. gage length clip on extensometer to obtain the mechanical properties of a specimen kept under this condition. The resulting mechanical properties for this method can be seen in Table 4.3.

Table 4.3 Conditioning tensile testing results for 4 days desiccant.

Specimen	Ultimate Tensile Stress	Tensile strain at Break	Tensile stress at Break	E-Modulus (1-3% strain)	E-Modulus
	(MPa)	(%)	(MPa)	(MPa)	(MPa)
1	43.38	6.25	34.54	753.6	2533.53
2	44.26	8.26	30.84	776.13	2480.5
3	43.09	8.24	30.21	771.9	2488.25
4	42.78	21.87	27.18	738.98	2572.29
5	43.2	9.24	30.34	770.55	2574.37
6	42.35	5.58	34.52	755.85	2420.46
7	43.57	11.52	29.76	779.38	2366.15
8	45.11	5.81	37.13	801.27	2672.56
9	43.36	13.73	29.16	752.94	2544.61
10	45.88	6.81	32.16	813.61	2655.77
11	45.87	6.61	34.46	822.17	2507.5
12	48.03	6.68	35.72	842.81	2708.62
13	44.57	3.95	42.43	808.68	2491.04
14	44.54	3.78	42.95	804.59	2609.9
15	45.01	10.44	31.38	816.05	2688.47
16	46.55	4.18	44.34	831.94	2556.83
17	46.22	12.04	31.24	826.27	2409.14
18	46.48	11.44	32.1	834.7	2628.63
Mean	44.68	8.69	33.91	794.52	2550.48
Std Deviation	1.57	4.42	4.96	32.48	98.84

For the 18 specimens in Table 4.4, the test specimens were first held in desiccant within a Ziploc® bag for 4 days and where then placed in an environmental chamber at a constant temperature and relative humidity of 23±2°C and 50±5% RH respectively for two days as shown in Figure 3.14. The specimens remained randomized in the chamber up until the moment of testing which was the same tensile testing method earlier described for the previous environmental conditions.

Table 4.4 Conditioning tensile testing results for 4 days desiccant and 2 days at a temperature 23±2°C and 50±5% RH.

Specimen	Ultimate Tensile Stress	Tensile strain at Break	Tensile stress at Break	E-Modulus (1-3% strain)	E-Modulus
	(MPa)	(%)	(MPa)	(MPa)	(MPa)
1	42.62	9.21	29.73	737.27	2390.56
2	44.78	5.85	34.13	772.51	2445.8
3	45.38	13.37	30	752.87	2474.71
4	44.81	6.22	33.49	755.03	2390.75
6	43.4	5.8	33.91	707.36	2354.51
7	44.27	15.8	28.68	761.46	2366.27
8	43.98	12.08	29.87	764.64	2504.49
9	42.86	5.63	33.84	749.78	2411.46
10	47.99	5.85	36.97	823.89	2774.27
11	48.32	4.38	38.51	823.02	2763.29
12	49.46	6.2	35.22	833.93	2647.24
13	46.78	4.33	41.54	823.39	2729.77
14	46.74	4.18	41.9	796.34	2520.6
15	47.08	4.1	43.69	834.62	2843.45
16	47.18	10.04	32.81	815.28	2586.63
17	47.56	5.74	38.61	821.55	2514.57
18	47.76	6.8	34.01	819.92	2706.82
Mean	45.94	7.39	35.11	787.82	2554.42
Std Deviation	2.08	3.49	4.51	39.81	160.46

After the testing of the three environmental conditions (ambient, desiccant, and 23±2°C and 50±5% RH) for four days, the desire is to determine the behavior of the commercial resin under the same environmental conditions, but at different aging timeframes. The build setup of 18 specimens was aged for one month in an ambient condition before being randomly tested. The same testing technique mentioned above was followed for this aging. Table 4.5 shows the resulting mechanical results for this testing of one month ambient.

Table 4. 5 Conditioning tensile testing results for 1 month ambient.

Specimen	Ultimate Tensile Stress	Tensile strain at Break	Tensile stress at Break	E-Modulus (1-3% strain)	E-Modulus
	(MPa)	(%)	(MPa)	(MPa)	(MPa)
1	54.43	5.7	45.38	832.37	2873.43
2	52.55	5.89	43.45	820.56	2733.47
4	52.73	6.06	41.41	838.99	2724.53
5	53.12	6.93	35.98	844.84	2747.53
6	52.05	5.35	44.18	837.78	2597.49
7	51.96	5.4	42.4	840.72	2714.77
8	52.28	6.84	38.92	852.22	2629.79
9	52.55	5.8	43.25	833.91	2704.13
10	57.13	4.74	52.89	919.42	2893.63
11	56.67	5.48	47.67	912.78	2903.52
12	56.24	4.81	48.35	904.15	2840.81
13	53.25	3.88	52.62	874.61	2705.16
14	53.99	3.79	53.64	884.64	2795.33
15	54.95	3.73	54.49	909.28	2816.09
16	56.32	4.84	50.02	915.37	2821.51
17	55.66	3.87	54.99	907.74	2799.67
18	56.13	5.21	48.94	913.52	2782.15
Mean	54.24	5.20	46.98	873.11	2769.59
Std Deviation	1.82	0.99	5.71	36.57	86.67

In Table 4.6, the tensile testing results are given for the 18 test specimens at a desiccant condition for one month. This was achieved by placing the test specimens in a Ziploc® bag for a month with desiccant up until the moment of testing the specimens in a random order. The same procedures as previously described for tensile testing was also done for these test specimens and the resulting mechanical properties are shown.

Table 4.6 Conditioning tensile testing results for 1 month desiccant.

Specimen	Ultimate Tensile Stress	Tensile strain at Break	Tensile stress at Break	E-Modulus (1-3% strain)	E-Modulus
	(MPa)	(%)	(MPa)	(MPa)	(MPa)
1	51.69	5.85	41.5	808.88	2833.35
2	52.01	5.51	42.86	828.89	2733.97
3	51.69	5.37	44.23	832.19	2768.54
4	50.99	5.33	41.89	810.1	2757.94
5	50.21	6.37	39.07	783.68	2641.18
6	50.69	5.56	40.38	810.69	2777.02
7	50.85	5.56	40.97	830.06	2592.93
8	50.21	7.06	32.27	814.87	2537.06
9	51.06	5.52	42.6	830.77	2649.34
10	54.66	4.7	47.02	894.27	2844.3
11	54.56	4.98	44.84	898.3	2776.79
12	55.09	5.03	44.57	898.29	2792.39
13	51.78	4.21	48.83	820.65	2701.69
14	50.77	4.52	44.93	759	2525.67
15	52	4.07	50.26	875.64	2565.4
16	53.93	5.04	43.51	884.02	2774.36
17	52.55	4.79	45.92	851.04	2898.51
18	52.88	5.53	39.59	875.05	2741.69
Mean	52.09	5.28	43.07	839.24	2717.34
Std Deviation	1.55	0.73	4.05	40.67	109.00

After aging the 18 test specimens like shown in Figure 3.1 for one month in desiccant, they were then conditioned for two days at a temperature of 23±2°C and 50±5% RH. This was done to determine the effect of the environmental condition of one month compared to the other aging and environmental conditions. Table 4.7 illustrates the mechanical properties that resulted under these conditions.

Table 4.7 Conditioning tensile testing results for 1 month desiccant and 2 days at temperature 23±2°C and 50±5% RH.

Specimen	Ultimate Tensile Stress	Tensile strain at Break	Tensile stress at Break	E-Modulus (1-3% strain)	E-Modulus
	(MPa)	(%)	(MPa)	(MPa)	(MPa)
1	50.33	5.68	38.85	820.22	2486.78
2	50.42	5.33	41.02	838.28	2583.03
3	50.52	5.06	39.44	822.59	2631.48
4	50.4	6.17	38.2	851.86	2743.02
5	48.93	5.34	39.84	834.72	2533.75
6	49.83	5.3	39.38	826.92	2555.02
7	49.42	4.95	42.94	824.24	2529.02
8	49.1	4.11	40.99	815.13	2717.56
9	49.7	4	46.49	828.69	2476
11	53.71	4.92	44.21	882.38	2862.05
12	53.97	22.99	0.15	907.45	2939.69
13	53.49	3.98	51.38	896.07	2762.22
14	51.21	3.83	45.77	872.68	2778.51
15	52.81	4.32	47.13	884.25	2793.64
16	53.2	4.72	43.81	897.81	2687.15
17	52.66	5.01	40.88	885.64	2779.54
18	52.68	4.99	43.74	888.09	2784.82
Mean	51.32	5.92	40.25	857.47	2684.90
Std Deviation	1.75	4.44	10.91	32.69	138.38

Beside testing two different aging timeframes (4 days and 1 months) with different environmental conditions (ambient, desiccant and 23±2°C and 50±5% RH), there is a desire to determine how the mechanical properties of the WaterShed™ 11120 commercial resin will have an effect over a longer period of time (120 days) with respect to the different conditions the specimen is exposed to (ambient, desiccant and 23±2°C and 50±5% RH). Table 4.8 demonstrates the mechanical properties of the randomized 18 specimen test samples held at an ambient condition for four months.

Table 4.8 Conditioning tensile testing results for 4 months ambient.

Specimen	Ultimate Tensile Stress	Tensile strain at Break	Tensile stress at Break	E-Modulus (1-3% strain)	E-Modulus
	(MPa)	(%)	(MPa)	(MPa)	(MPa)
1	50.62	5.1	34.62	815.48	2766.86
2	51.42	7.05	34.17	841.45	2385.83
3	51.38	8.69	34.35	819.8	2601.71
4	49.6	7.74	32.62	794.19	2431.48
5	50.66	5.69	36.96	812.89	2435.66
6	49.82	5.84	36.51	830.44	2390.9
7	49.81	6.86	31.73	821.59	2455.59
8	50.34	14.82	32.43	829.68	2479.24
9	48.99	5.91	36.69	809.05	2645.53
10	55.9	4.12	54.27	944.68	2753.46
11	55.49	5.12	44.19	932.42	2799.09
12	55.34	5.55	43.47	921.98	2789.13
14	54.84	4.78	45.93	920.86	2709.67
15	55.27	4.25	51.81	938.89	2797.93
16	54.51	4.92	44.2	922.02	2725.91
17	55.46	4.71	48.28	926.62	2707.15
18	54.9	4.94	41.54	921.44	2761.97
Mean	52.61	6.24	40.22	870.79	2625.71
Std Deviation	2.61	2.54	7.08	57.35	158.67

A separate batch of 18 specimen test samples were maintained at a desiccant condition for a period of four months to distinguish the effect on the mechanical properties due to the difference in environmental condition. The same randomized tensile testing method which was previously described for the other conditions was utilized to obtain the mechanical property values shown in Table 4.9.

Table 4.9 Conditioning tensile testing results for 4 months desiccant.

Specimen	Ultimate Tensile Stress	Tensile strain at Break	Tensile stress at Break	E-Modulus (1-3% strain)	E-Modulus
	(MPa)	(%)	(MPa)	(MPa)	(MPa)
1	49.6	11.4	32.1	825.9	2515.4
2	49.1	6.3	36.3	802.5	2575.7
3	47.0	11.8	29.4	797.7	2482.9
4	50.3	6.5	34.3	839.8	2690.5
5	48.4	5.6	35.3	814.5	2501.6
6	49.1	5.6	36.9	822.4	2404.6
7	48.7	8.6	33.1	823.8	2449.2
8	49.1	10.3	32.6	820.1	2512.7
9	48.7	7.0	31.7	812.8	2382.5
10	54.3	6.7	37.7	914.9	2741.2
11	53.2	6.9	36.3	904.4	2665.8
12	54.4	5.4	43.8	915.9	2760.2
13	54.3	5.3	41.7	917.0	2688.7
14	54.3	4.0	53.5	923.4	2745.9
15	53.9	4.2	48.9	915.9	2758.8
16	54.8	4.4	52.1	928.7	2699.8
17	53.5	5.0	41.3	901.2	2668.9
18	53.3	8.1	36.4	909.8	2656.0
Mean	51.44	6.83	38.51	866.14	2605.57
Std Deviation	2.73	2.37	7.05	50.93	127.60

The last batch of 18 specimens from the first build setup demonstrated in Figure 3.1, was tensile tested. This batch underwent a four day desiccant condition followed by a two day controlled condition at 23±2°C and 50±5% RH before being randomly tested to acquire the mechanical properties shown in Table 4.10.

Table 4.10 Conditioning tensile testing results for 4 months desiccant and 2 days at a temperature 23±2°C and 50±5% RH.

Specimen	Ultimate Tensile Stress	Tensile strain at Break	Tensile stress at Break	E-Modulus (1-3% strain)	E-Modulus
	(MPa)	(%)	(MPa)	(MPa)	(MPa)
1	45.32	14.91	29.6	764.73	2356.24
2	45.49	16.22	31.21	777.24	2348.45
3	47.3	5.76	38.51	803.95	2379.28
5	45.88	9.87	31.44	779.09	2375.41
6	46.74	14.49	29.86	811.97	2333.97
7	46.07	12.03	30.15	784.96	2441.09
8	45.02	20.34	31.01	790.32	2392.21
9	46.54	9	31.34	790.46	2463.31
10	51.37	5.33	36.41	882.78	2703.17
11	51.96	11.62	36.09	894.57	2660.51
12	50.89	17.9	35.85	879.86	2574.72
13	49.45	5.52	39.34	849.53	2531.08
14	51.66	4.99	43.29	888.3	2776.42
15	50.46	5.33	40.42	864.46	2615.39
16	50.85	18.4	34.29	866.85	2648.99
17	50.06	7.27	33.62	865.37	2686.86
18	49.36	14.53	33.38	860.59	2696.79
Mean	48.50	11.38	34.46	832.65	2528.46
Std Deviation	2.52	5.20	4.10	45.85	150.65

4.2.3 Effects of Build Orientation of Second Build Setup

After testing the build setup illustrated in Figure 3.1 under different aging and environmental conditions, another build layout as shown in Figure 3.2 was analyzed. In this build setup, 24 specimens were randomly tested under the condition of four days ambient and two days at 23±2°C and 50±5% RH. The results of the first batch are shown in Table 4.11.

Table 4.11 Conditioning tensile testing results for 4 days ambient and 2 days at a temperature 23±2°C and 50±5% RH (1st Batch).

Specimen	Ultimate Tensile Stress	Tensile strain at Break	Tensile stress at Break	E-Modulus (1-3% strain)	E-Modulus
	(MPa)	(%)	(MPa)	(MPa)	(MPa)
1	46.25	8.53	32.56	800.09	2534.24
2	49.41	6.85	36.16	872.95	2866.41
3	50.9	5.19	42.11	897.01	2875.73
4	45.78	6.2	35.86	795.78	2507.81
5	49.91	5.45	38.59	869.05	2591.42
6	50.04	4.36	46.09	878	2652.06
7	43.99	9.5	31.07	771.5	2394.18
8	49.4	4.54	43.41	872.28	2737.24
9	49.99	4.71	42.48	890.65	2686.6
10	44.79	6.27	35.5	788.37	2418.91
11	48.05	4.76	42.25	858.89	2640
12	50.39	4.27	47.39	892.8	2682.55
13	45.27	8.82	32.06	792.36	2404.25
14	49.99	4.88	41.47	879.92	2766.45
15	50.86	4.91	41.92	891.87	2806.58
16	44.15	8.89	30.81	787.35	2529.34
17	49.86	5.67	36.76	881.42	2846.86
18	49.25	5.85	39.46	860.38	2638.32
19	45.91	5.88	38.07	795.87	2643.03
20	49.69	6.05	37.18	872.95	2670.95
21	50.48	4.37	45.83	887.98	2717.54
22	45.49	4.48	42.18	800.67	2558.64
23	50.39	5.19	41.31	872.89	2745.32
24	50.75	4.37	47.21	898.35	2824.86
Mean	48.37	5.83	39.49	850.39	2655.80
Std Deviation	2.41	1.59	4.98	43.99	142.64

These specimens were tested using INSTRON® 5866 with the AVE. Several batches were tested to assure that there would be no variation in the three different build layouts (flat, on an edge, and vertical) as well as the eight different position of the specimen built on the platform as can be seen in Figure 3.2. Table 4.12 shows the mechanical properties for the second batch tested.

Table 4.12 Conditioning tensile testing results for 4 days ambient and 2 days at a temperature 23±2°C and 50±5% RH (2nd Batch).

Specimen	Ultimate Tensile Stress	Tensile strain at Break	Tensile stress at Break	E-Modulus (1-3% strain)	E-Modulus
	(MPa)	(%)	(MPa)	(MPa)	(MPa)
1	44.68	11.49	29.92	775.42	2,305.65
2	49.27	11.22	32.12	854.28	2,606.68
3	49.41	13.19	31.55	873.52	2,555.71
4	43.96	14.63	28.66	765.82	2,284.46
5	49.01	3.7	48.36	859.51	2,625.23
6	50.05	4.53	39.34	888.77	2,542.02
7	44.11	9.54	31.06	761.25	2,191.15
8	49.32	11.36	31.89	873.27	2,516.75
9	49.67	10.64	32.83	879.92	2,587.45
10	43.76	13.07	29.04	766.31	2,253.10
11	50.05	10.83	32.74	885.29	2,684.08
12	49.7	6.3	38.28	893.09	2,589.91
13	43.94	23.92	27.61	763.82	2,239.69
14	49.46	7.29	35.44	863.7	2,590.21
15	49.73	8.44	34.6	894.97	2,643.39
16	43.82	14.22	28.58	768.49	2,250.99
17	48.92	5.32	39.93	859.33	2,509.97
18	49.98	6.58	36.77	887.64	2,660.07
19	44.96	13.21	29.56	783.46	2,362.48
20	49.46	9.46	33.13	867.14	2,614.07
21	49.57	6.76	34.96	880.91	2,617.06
22	44.92	12.25	0.05	779.48	2,303.84
23	49.63	9.65	32.98	867.83	2,605.32
24	48.96	5.1	41.94	878.62	2,581.55
Mean	47.76	10.11	32.56	840.49	2488.37
Std Deviation	2.56	4.35	8.47	51.77	162.21

The third and final batch's mechanical results are shown in Table 4.13. The 24 test specimens were tested under the same testing conditions as the previous two batches to obtain the mechanical properties shown.

Table 4.13 Conditioning tensile testing results for 4 days ambient and 2 days at a temperature 23±2°C and 50±5% RH (3rd Batch).

Specimen	Ultimate Tensile Stress	Tensile strain at Break	Tensile stress at Break	E-Modulus (1-3% strain)	E-Modulus
	(MPa)	(%)	(MPa)	(MPa)	(MPa)
1	48.71	11.97	32.1	851.21	2,383.28
2	52.41	5.93	39.54	914.84	2,557.01
3	51.11	5.06	41.24	912.62	2,548.65
4	48.33	12.72	32.21	854.48	2,219.71
5	51.52	5.9	39.44	904.82	2,744.21
6	51.33	4.64	44.69	917.14	2,442.30
7	47.03	8.14	32.01	830.5	2,286.61
8	51.51	6.87	36.12	908.81	2,670.96
9	51.32	4.65	43.64	916.37	2,508.18
10	48.71	9.64	32.52	849.76	2,376.72
11	50.52	6.1	38.35	895.63	2,556.88
12	51.66	4.5	43.25	920.26	2,520.71
13	49.09	12.12	31.89	862.03	2,405.37
14	50.7	4.63	41.48	896.78	3,213.13
15	51.09	4.33	42.57	911.37	2,619.15
16	48.7	14.07	31.2	851.64	2,370.55
17	51.1	5.26	40.49	905.21	2,492.62
18	52.05	4.99	42.83	927.45	2,550.47
19	49.05	12.27	31.59	858.86	2,412.20
20	51.29	7.57	34.04	903.09	2,580.68
21	51.81	4.6	46.43	920.86	2,552.11
22	48.6	10.51	31.92	850.74	2,375.48
23	50.28	5.26	40.29	898.66	2,470.27
24	51.89	5.62	39.71	929.08	2,590.17
Mean	50.41	7.39	37.90	891.34	2518.64
Std Deviation	1.48	3.19	5.00	30.64	190.95

4.3 MECHANICAL RESULTS

The tensile test results obtained from the different built setups with respective aging and environmental conditions were analyzed for their mechanical properties. On the first study for the build setup which included the 18 test samples, flat and on an edge, the mechanical properties changed in regards to the aging (4 days, 1 month, and 4 months) and conditioning (ambient,

desiccant, and 23±2°C and 50±5% RH) of the specimens with an ultimate tensile stress of 43.2 and 44.8 MPa, respectively and E-Modulus of 763.9 and 800.7 MPa, respectively.

Table 4.14 shows the mechanical properties for 4 days with respect to every condition. On ultimate tensile strength, specimens treated at 23±2°C and 50±5% RH had the highest strength value of 45.9 MPa and desiccant had the lowest strength value of 44.7 MPa. For the calculated E-Modulus (1-3% strain), desiccant showed the highest value of 794.5 MPa while ambient had the lowest value of 786 MPa. Elongation at break and fracture stress values are also included for every condition. Figure 4.1 illustrates the three different conditions and each condition has two build orientations which are flat and on an edge. The edge build orientation exhibited the highest ultimate tensile strength.

The analysis for the 1 month condition is shown in Table 4.15 and ambient exhibits the highest ultimate tensile strength and E-Modulus (1-3% strain) which are 54.2 MPa and 873.1 MPa respectively. Figure 4.2 illustrates a typical stress and strain curve which also supports Figure 4.1 in showing that specimens built on an edge had higher ultimate tensile strengths.

Analysis for the 4 month condition is displayed in Table 4.16. Ambient increased its Ultimate Tensile Strength value as the aging increased, resulting in a value of 57.6 MPa. The E-Modulus (1-3% strain) was the highest for the ambient condition with a value of 870.8 MPa. As previously shown, samples built on an edge had the highest ultimate tensile strength as shown in Figure 4.3.

Table 4.14 Results from mechanical testing from different conditions at 4 days. Results represent an average of 18 specimens for each condition.

4 Days		Ultimate Tensile Stress (MPa)	Elongation at Break (%)	Fracture Stress (MPa)	E-Modulus (1-3% Strain) (MPa)	E-Modulus (Mpa)
Ambient	*Mean*	45.7	12.4	32.4	786.0	2560.8
	Median	45.7	10.0	31.1	777.3	2549.5
	Std Deviation	1.6	7.5	4.9	38.5	127.6
	Std Error	0.4	1.8	1.2	9.3	30.9
	Maximum	48.3	27.8	44.3	842.6	2775.6
	Minimum	43.3	4.1	26.8	727.7	2316.9
Desiccant	*Mean*	44.7	8.7	33.9	794.5	2550.5
	Median	44.6	7.5	32.1	802.9	2550.7
	Std Deviation	1.6	4.4	5.0	32.5	98.8
	Std Error	0.37	1.04	1.17	7.66	23.30
	Maximum	48.0	21.9	44.3	842.8	2708.6
	Minimum	42.4	3.8	27.2	739.0	2366.2
Condition	*Mean*	45.9	7.39	35.1	787.8	2554.4
	Median	46.7	5.85	34.0	796.3	2514.6
	Std Deviation	2.1	3.49	4.5	39.8	160.5
	Std Error	0.5	0.8	1.1	9.7	38.9
	Maximum	49.5	15.80	43.7	834.6	2843.5
	Minimum	42.6	4.10	28.7	707.4	2354.5

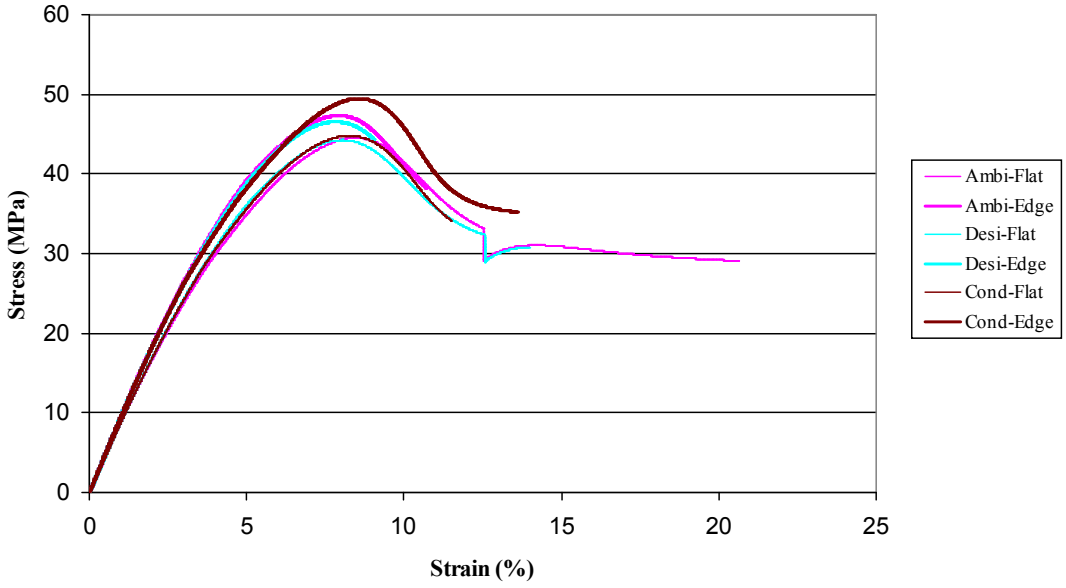

Figure 4.1 WaterShed™ 11120 4 days with respective condition and each case with two specimens: one built flat and the other on an edge. As shown by the graphs the specimens with high stress are built on an edge and are represented by the thicker lines.

Table 4.15 Results from mechanical testing for different conditions at 1 month. Results represent an average of 18 specimens for each condition.

1 Month		Ultimate Tensile Stress (MPa)	Elongation at Break (%)	Fracture Stress (MPa)	E-Modulus (1-3% Strain) (MPa)	E-Modulus (Mpa)
Ambient	*Mean*	54.2	5.2	47.0	873.1	2769.6
	Median	54.0	5.4	47.7	874.6	2782.2
	Std Deviation	1.8	1.0	5.7	36.6	86.7
	Std Error	0.4	0.2	1.4	8.9	21.0
	Maximum	57.1	6.9	55.0	919.4	2903.5
	Minimum	52.0	3.7	36.0	820.6	2597.5
Desiccant	*Mean*	52.1	5.3	43.1	839.2	2717.3
	Median	51.7	5.4	43.2	830.4	2749.8
	Std Deviation	1.5	0.7	4.2	39.1	111.3
	Std Error	0.35	0.18	0.98	9.21	26.24
	Maximum	55.1	7.1	50.3	898.3	2898.5
	Minimum	50.2	4.1	32.3	759.0	2525.7
Condition	*Mean*	51.3	5.92	40.2	857.5	2684.9
	Median	50.5	4.99	41.0	851.9	2717.6
	Std Deviation	1.8	4.44	10.9	32.7	138.4
	Std Error	0.4	1.1	2.6	7.9	33.6
	Maximum	54.0	22.99	51.4	907.5	2939.7
	Minimum	48.9	3.83	0.2	815.1	2476.0

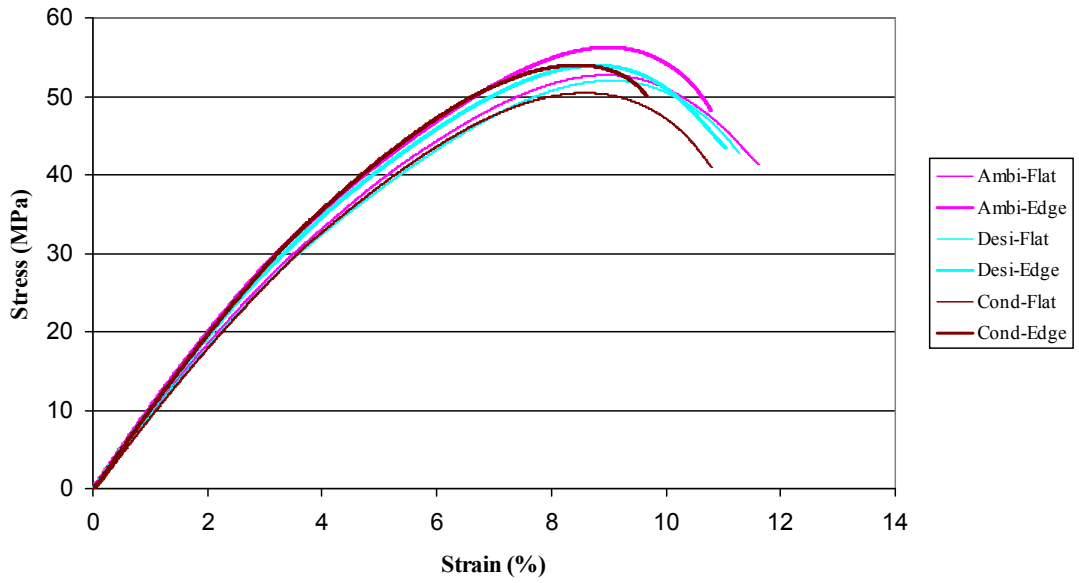

Figure 4.2 WaterShed™ 11120 1 month with respective conditions and each case with two specimens: one built flat and the other on an edge. As shown by the graphs the specimens with high stress are build on an edge and are represented by the thicker lines.

Table 4.16 Results from mechanical testing for different conditions at 4 months. Results represent an average of 18 specimens for each condition.

4 Months		Ultimate Tensile Stress (MPa)	Elongation at Break (%)	Fracture Stress (MPa)	E-Modulus (1-3% Strain) (MPa)	E-Modulus (Mpa)
Ambient	*Mean*	52.6	6.2	40.2	870.8	2625.7
	Median	51.4	5.6	37.0	841.5	2707.2
	Std Deviation	2.6	2.5	7.1	57.3	158.7
	Std Error	0.6	0.6	1.7	13.9	38.5
	Maximum	55.9	14.8	54.3	944.7	2799.1
	Minimum	49.0	4.1	31.7	794.2	2385.8
Desiccant	*Mean*	51.4	6.8	38.5	866.1	2605.6
	Median	51.7	6.4	36.4	870.5	2660.9
	Std Deviation	2.7	2.4	6.4	50.0	129.3
	Std Error	0.63	0.56	1.50	11.78	30.47
	Maximum	54.8	11.8	53.5	928.7	2760.2
	Minimum	47.0	4.0	29.4	797.7	2382.5
Condition	*Mean*	48.5	11.38	34.5	832.6	2528.5
	Median	49.4	11.62	33.6	849.5	2531.1
	Std Deviation	2.5	5.20	4.1	45.9	150.6
	Std Error	0.6	1.3	1.0	11.1	36.5
	Maximum	52.0	20.34	43.3	894.6	2776.4
	Minimum	45.0	4.99	29.6	764.7	2334.0

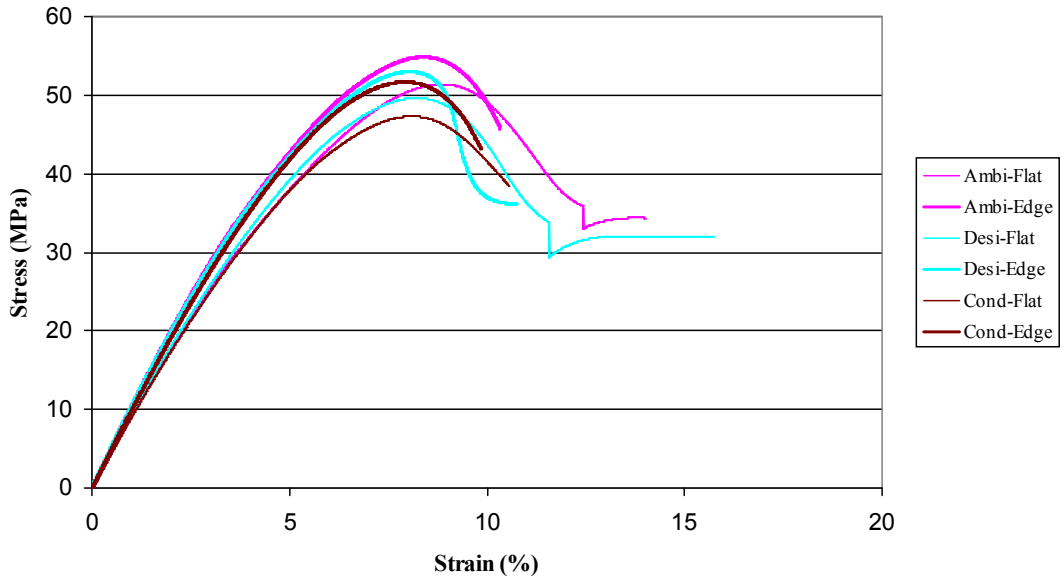

Figure 4.3 WaterShed™ 11120 4 months with respective conditions and each case with two specimens: one built flat and the other on an edge. As shown by the graphs the specimens with high stress are build on an edge and are represented by the thicker lines.

Data obtained regarding elongation at break were analyzed to determine the effects of aging on the three conditions (ambient, desiccant, and ±2°C and 50±5% RH) with respect to build orientation (flat and on an edge). The resulting data exhibited in Table 4.17 show that for an aging period of 4 days, ambient and desiccant had higher values of 15.9 and 10.1%, respectively, for samples built flat as compared to samples built on an edge. On the 23±2°C and 50±5% relative humidity condition, four months exhibited the highest elongation at break at a flat built orientation. Samples built at a flat orientation would typically exhibit a higher elongation at break because they would produce orthogonal layer interfaces with respect to the part (Quintana *et al.*, 2007).

Table 4.17 Elongation at break (%) for specimens built flat and on an edge and the different time point with their respective conditions.

Time (days)	*Ambient*							
	Flat				On an Edge			
	Mean (%)	Std Deviation		Std Error	Mean (%)	Std Deviation		Std Error
4	15.9	±	7.8	2.6	8.4	±	5.2	1.8
30	6.0	±	0.6	0.2	4.5	±	0.7	0.2
120	7.5	±	3.0	1.0	4.8	±	0.5	0.2
Time (days)	*Desiccant*							
	Flat				On an Edge			
	Mean (%)	Std Deviation		Std Error	Mean (%)	Std Deviation		Std Error
4	10.1	±	5.2	1.7	7.3	±	3.2	1.1
30	5.8	±	0.6	0.2	4.8	±	0.5	0.2
120	8.1	±	2.5	0.8	5.5	±	1.4	0.5
Time (days)	*Condition*							
	Flat				On an Edge			
	Mean (%)	Std Deviation		Std Error	Mean (%)	Std Deviation		Std Error
4	9.2	±	4.0	1.4	5.7	±	1.9	0.6
30	5.1	±	0.7	0.2	6.8	±	6.5	2.3
120	12.8	±	4.6	1.6	10.1	±	5.6	1.9

The effects of fracture stress for test specimens built flat and on an edge are analyzed under aging and environmental conditions as shown in Table 4.18. Samples built on an edge showed the highest fracture stress for one month of aging regardless of the environmental condition as compared to test samples that were built on a flat orientation.

Table 4.18 Fracture stress (MPa) for specimens built flat and on an edge and the different time points with their respective conditions.

Time (days)	*Ambient*							
	Flat				On an Edge			
	Mean (MPa)	Std Deviation		Std Error	Mean (MPa)	Std Deviation		Std Error
4	29.4	±	1.8	0.6	35.8	±	5.0	1.8
30	41.9	±	3.1	1.1	51.5	±	2.8	0.9
120	34.5	±	5.2	1.7	46.7	±	4.4	1.6
Time (days)	*Desiccant*							
	Flat				On an Edge			
	Mean (MPa)	Std Deviation		Std Error	Mean (MPa)	Std Deviation		Std Error
4	31.5	±	3.2	1.1	36.3	±	5.4	1.8
30	40.6	±	3.5	1.2	45.5	±	3.1	1.0
120	33.5	±	2.4	0.8	43.5	±	6.6	2.2
Time (days)	*Condition*							
	Flat				On an Edge			
	Mean (MPa)	Std Deviation		Std Error	Mean (MPa)	Std Deviation		Std Error
4	31.7	±	2.3	0.8	38.1	±	3.7	1.2
30	40.8	±	2.6	0.9	39.6	±	16.2	5.7
120	31.6	±	2.9	1.0	37.0	±	3.4	1.1

Table 4.19 displays the values for ultimate tensile stress for test samples subjected to aging and environmental conditions with respect to build orientation. For on an edge oriented test samples having been aged for one month, the ultimate tensile stress resulted in the highest values regardless of the environmental condition.

Table 4.19 Ultimate tensile stress (MPa) for specimens built flat and on an edge and the different time points with their respective conditions.

Time (days)	*Ambient*							
	Flat				On an Edge			
	Mean (MPa)	Std Deviation		Std Error	Mean (MPa)	Std Deviation		Std Error
4	44.3	±	0.7	0.2	47.3	±	0.6	0.2
30	52.7	±	0.8	0.3	55.6	±	1.3	0.4
120	50.3	±	0.8	0.3	55.2	±	0.4	0.1
Time (days)	*Desiccant*							
	Flat				On an Edge			
	Mean (MPa)	Std Deviation		Std Error	Mean (MPa)	Std Deviation		Std Error
4	43.5	±	0.8	0.3	45.9	±	1.1	0.4
30	51.0	±	0.6	0.2	53.1	±	1.5	0.5
120	48.9	±	0.9	0.3	54.0	±	0.6	0.2
Time (days)	*Condition*							
	Flat				On an Edge			
	Mean (MPa)	Std Deviation		Std Error	Mean (MPa)	Std Deviation		Std Error
4	44.0	±	1.0	0.4	47.7	±	0.9	0.3
30	49.9	±	0.6	0.2	53.0	±	0.9	0.3
120	46.0	±	0.8	0.3	50.7	±	0.9	0.3

Test specimens built at both flat and on an edge were analyzed under different aging and environmental conditions for values of E-modulus. The resulting data are shown in Table 4.20. Samples built on an edge have the highest E-modulus and especially for the aging condition of one month regardless of the environmental condition. Table 4.21 also coincides with the results from Table 4.20 in which the highest value of E-modulus is for the test samples that are built on an edge.

Table 4.20 E-modulus (MPa) for specimens built flat and on an edge and the different time points with their respective conditions.

Time (days)	*Ambient*							
	Flat				**On an Edge**			
	Mean (MPa)	**Std Deviation**		**Std Error**	**Mean (MPa)**	**Std Deviation**		**Std Error**
4	2474.5	±	96.0	32.0	2658.0	±	79.4	28.1
30	2715.6	±	82.6	29.2	2817.5	±	59.6	19.9
120	2510.3	±	131.3	43.8	2755.5	±	38.2	13.5
Time (days)	*Desiccant*							
	Flat				**On an Edge**			
	Mean (MPa)	**Std Deviation**		**Std Error**	**Mean (MPa)**	**Std Deviation**		**Std Error**
4	2517.0	±	90.7	30.2	2584.0	±	100.0	33.3
30	2699.0	±	98.1	32.7	2735.6	±	122.0	40.7
120	2501.7	±	92.3	30.8	2709.5	±	42.3	14.1
Time (days)	*Condition*							
	Flat				**On an Edge**			
	Mean (MPa)	**Std Deviation**		**Std Error**	**Mean (MPa)**	**Std Deviation**		**Std Error**
4	2417.3	±	53.1	17.7	2676.3	±	116.3	38.8
30	2584.0	±	95.4	31.8	2798.5	±	75.3	25.1
120	2386.2	±	45.1	15.0	2654.9	±	73.5	24.5

Table 4.21 E-modulus (1-3% Strain) (MPa) for specimens built flat and on an edge and the different time points with their respective conditions.

Time (days)	*Ambient*							
	Flat				On an Edge			
	Mean (MPa)	Std Deviation		Std Error	Mean (MPa)	Std Deviation		Std Error
4	753.6	±	16.6	5.5	822.4	±	14.9	5.3
30	837.7	±	9.3	3.3	904.6	±	15.0	5.0
120	819.4	±	13.8	4.6	928.6	±	9.1	3.2
Time (days)	*Desiccant*							
	Flat				On an Edge			
	Mean (MPa)	Std Deviation		Std Error	Mean (MPa)	Std Deviation		Std Error
4	766.7	±	18.5	6.2	822.3	±	12.7	4.2
30	816.7	±	15.8	5.3	861.8	±	46.0	15.3
120	817.7	±	12.7	4.2	914.6	±	8.6	2.9
Time (days)	*Condition*							
	Flat				On an Edge			
	Mean (MPa)	Std Deviation		Std Error	Mean (MPa)	Std Deviation		Std Error
4	750.0	±	20.2	7.1	821.3	±	11.2	3.7
30	829.2	±	11.1	3.7	889.3	±	10.8	3.8
120	787.8	±	15.1	5.3	872.5	±	14.6	4.9

The bar graphs illustrated in Figure 4.4, Figure 4.5, and Figure 4.6 allow an easier visualization of the differences on the mechanical properties (ultimate tensile strength, modulus of elasticity, and modulus of elasticity from 1 to 3% strain) with respect to the different aging time periods (4 days, 1 month and 4 months) and conditions (ambient, desiccant and 23±2°C and 50±5% RH). The error bars incorporated in the bar graphs represent 1 standard deviation. Figure 4.4 shows the average of all specimens based on their condition. Figures 4.5 and 4.6 illustrate the mechanical properties for the specimens only built flat and on an edge, respectively, for every condition.

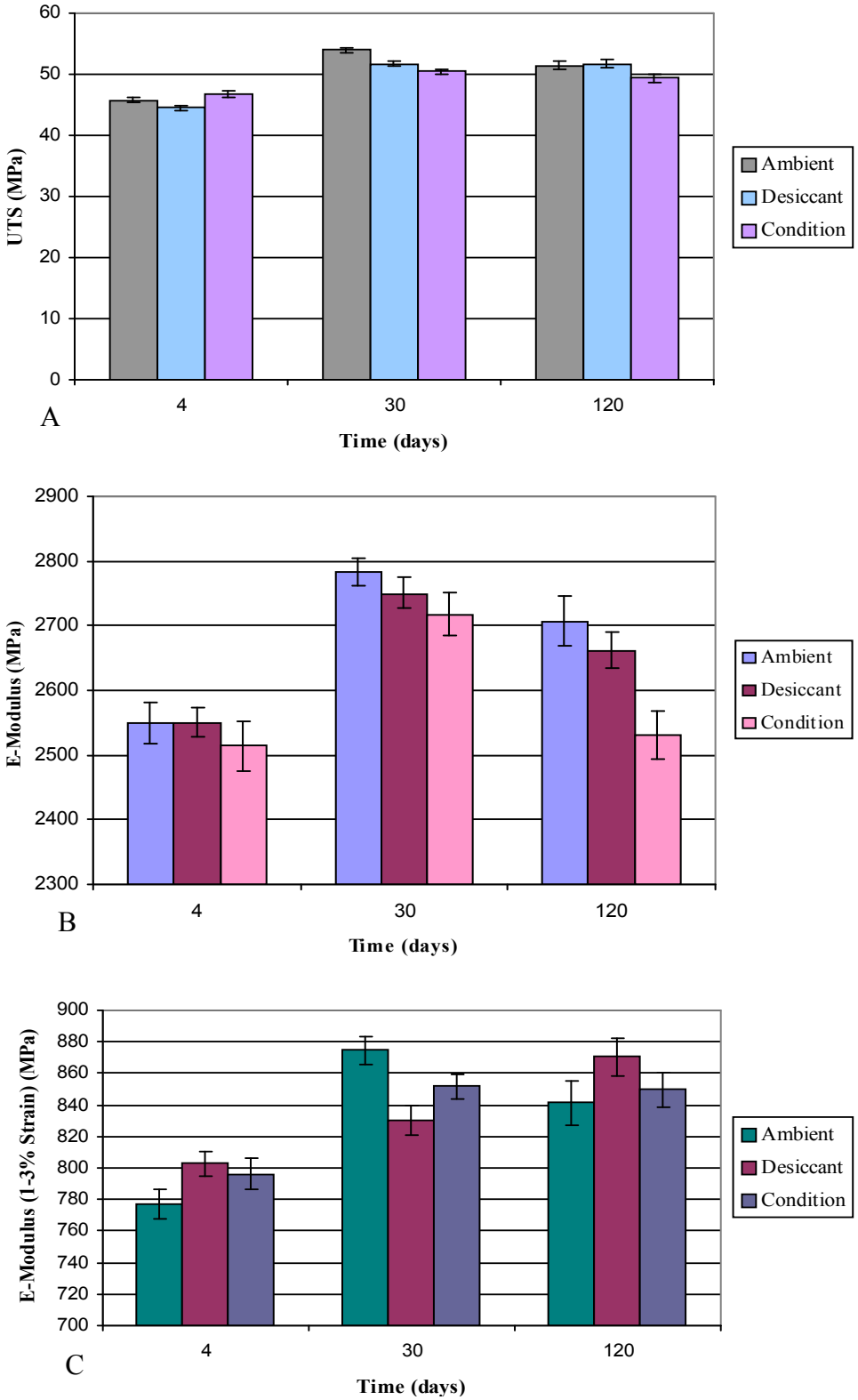

Figure 4.4 The mechanical properties of WaterShed™ 11120 at different set points with their respective environmental conditions. A) Ultimate Tensile Stress, B) E-Modulus and C) E-Modulus (1-3% strain).

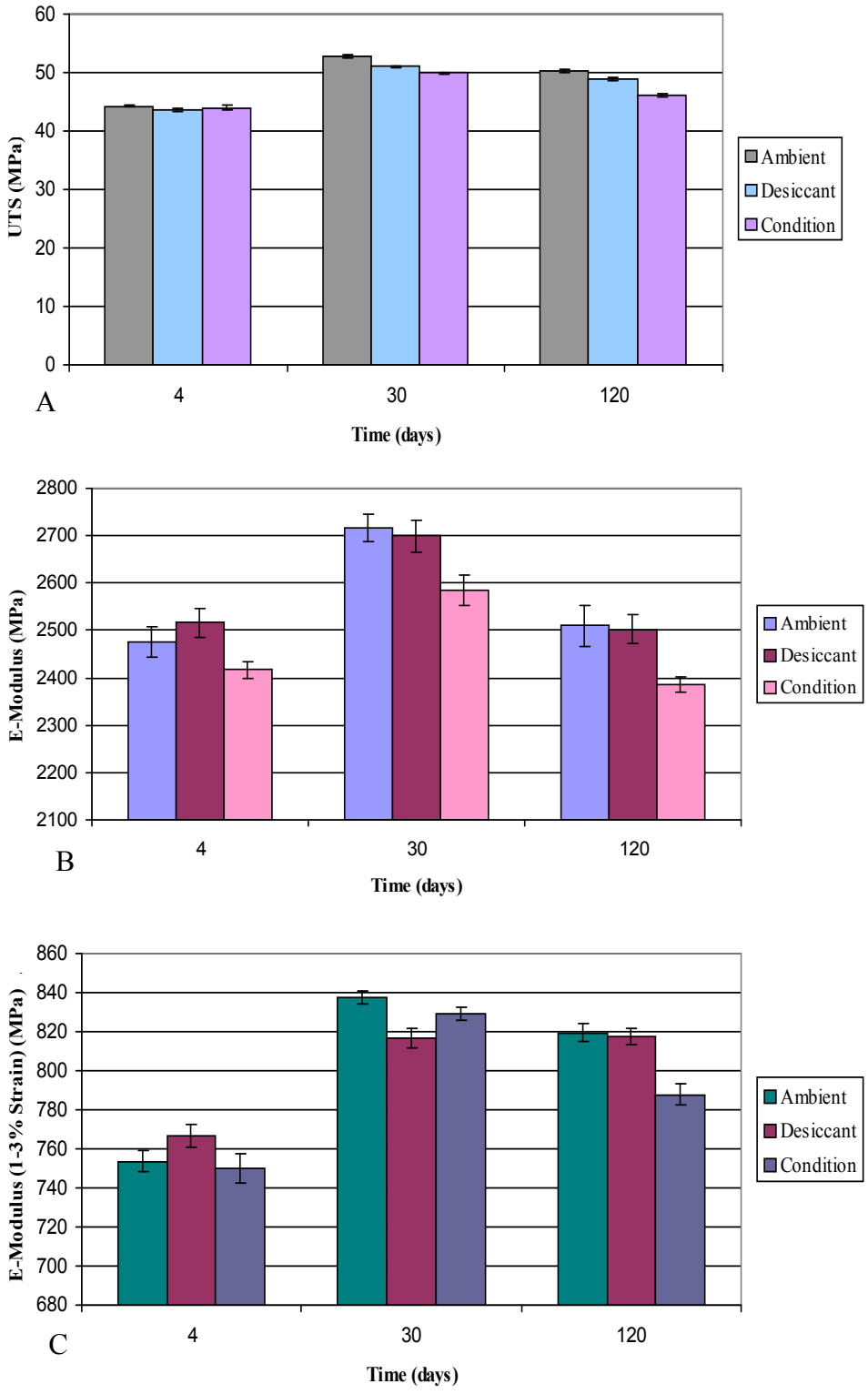

Figure 4.5 Mechanical properties of WaterShed™ 11120 built in flat orientation at different time point with their corresponding environmental conditions. A) Ultimate Tensile Stress, B) E-Modulus and C) E-Modulus (1-3% Strain).

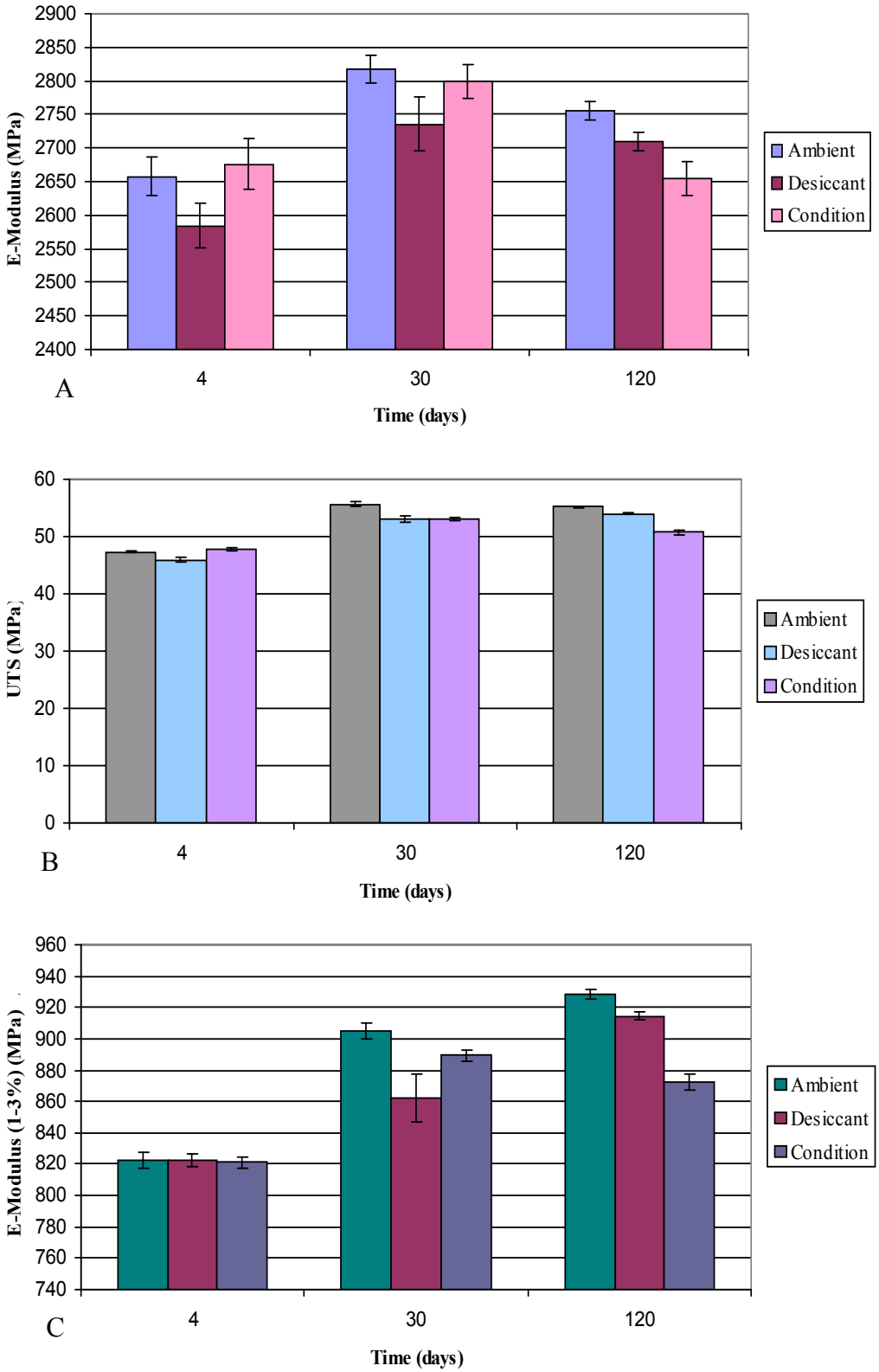

Figure 4.6 Mechanical properties of WaterShed™ 11120 built on an edge orientation at different time point with their corresponding environmental conditions. A) Ultimate Tensile Stress, B) E-Modulus and C) E-Modulus (1-3% Strain).

The build setup of the 24 test specimens with three different layout orientations was investigated in this study. Specimens were tested for four days ambient and two days 23±2°C and 50±5% relative humidity. Three batches were built under these conditions and were randomly tested as described above. Table 4.22 shows the average of the mechanical properties of these three batches and how they slightly vary on the values meaning that the behavior of the polymer is not constant. This study analyzed the mechanical properties for the three different build orientation layouts of the test specimens.

Table 4.22 Mechanical testing results for 4 days ambient and 2 days conditioned at temperature 23±2°C and 50±5% RH for three different batches. The results are averages of 24 specimens.

Batch		Ultimate Tensile Stress (MPa)	Elongation at Break (%)	Fracture Stress (MPa)	E-Modulus (1-3% Strain) (MPa)	E-Modulus (Mpa)
1	**Mean**	48.4	5.8	39.5	850.4	2655.8
	Median	49.6	5.3	40.4	872.6	2661.5
	Std Deviation	2.4	1.6	5.0	44.0	142.6
	Std Error	0.5	0.3	1.0	9.0	29.1
	Maximum	50.9	9.5	47.4	898.4	2875.7
	Minimum	44.0	4.3	30.8	771.5	2394.2
2	**Mean**	47.8	10.1	32.6	840.5	2488.4
	Median	49.3	10.1	32.8	865.4	2568.6
	Std Deviation	2.6	4.4	8.5	51.8	162.2
	Std Error	0.5	0.9	1.7	10.6	33.1
	Maximum	50.1	23.9	48.4	895.0	2684.1
	Minimum	43.8	3.7	0.1	761.3	2191.2
3	**Mean**	50.4	7.4	37.9	891.3	2518.6
	Median	51.1	5.9	39.5	904.0	2514.4
	Std Deviation	1.5	3.2	5.0	30.6	191.0
	Std Error	0.3	0.7	1.0	6.3	39.0
	Maximum	52.4	14.1	46.4	929.1	3213.1
	Minimum	47.0	4.3	31.2	830.5	2219.7

The study of the build setup for the 24 test specimens in Figure 3.2 were randomly tested under ambient conditions for four days and two days at 23±2°C and 50±5% RH. Tables 4.23, 4.24, and 4.25 show an average of eight specimens with respect to the build orientation layout (flat, on an edge, and vertical) for the first, second, and third batch, respectively. All three tables state that the vertical built orientation has the highest values for ultimate tensile stress and E-Modulus (1-3% strain). For the first batch, the ultimate tensile stress and E-Modulus values were 50.3 MPa and 872.5 MPa, respectively. The second batch had values of 49.6 MPa and 884.7 MPa while the third batch had 51.5 MPa and 919.4 MPa for ultimate tensile stress and E-Modulus. One specimen for each build layout (flat, on an edge, and vertical) were graphed in Figures 4.7, 4.8, and 4.9 which all show that vertical has the highest ultimate tensile stress followed by on an edge and then the flat build orientation in any of the three built batches. The bar graphs from Figure 4.10 demonstrate the vertical build orientation of any of the three batches has the highest mechanical value.

Table 4.23 Mechanical testing results for 4 days ambient and 2 days conditioned at temperature 23±2°C and 50±5%RH of the first batch. The results are an average of eight specimens for each orientation.

Orientation		Ultimate Tensile Stress (MPa)	Elongation at Break (%)	Fracture Stress (MPa)	E-Modulus (1-3% Strain) (MPa)	E-Modulus (MPa)
Flat	**Mean**	45.2	7.3	34.8	791.5	2498.8
	Median	45.4	7.4	34.0	794.1	2518.6
	Std Deviation	0.8	1.8	3.9	9.4	86.9
	Std Error	0.3	0.6	1.4	3.3	30.7
	Maximum	46.3	9.5	42.2	800.7	2643.0
	Minimum	44.0	4.5	30.8	771.5	2394.2
On an Edge	**Mean**	49.6	5.4	39.6	872.5	2733.1
	Median	49.8	5.3	40.0	872.9	2741.3
	Std Deviation	0.7	0.8	2.8	6.9	96.1
	Std Error	0.2	0.3	1.0	2.4	34.0
	Maximum	50.4	6.9	43.4	881.4	2866.4
	Minimum	48.1	4.5	36.2	858.9	2591.4
Vertical	**Mean**	50.3	4.8	44.1	887.1	2735.5
	Median	50.4	4.5	44.2	891.3	2702.1
	Std Deviation	0.6	0.5	2.9	12.5	88.3
	Std Error	0.2	0.2	1.0	4.4	31.2
	Maximum	50.9	5.9	47.4	898.4	2875.7
	Minimum	49.3	4.3	39.5	860.4	2638.3

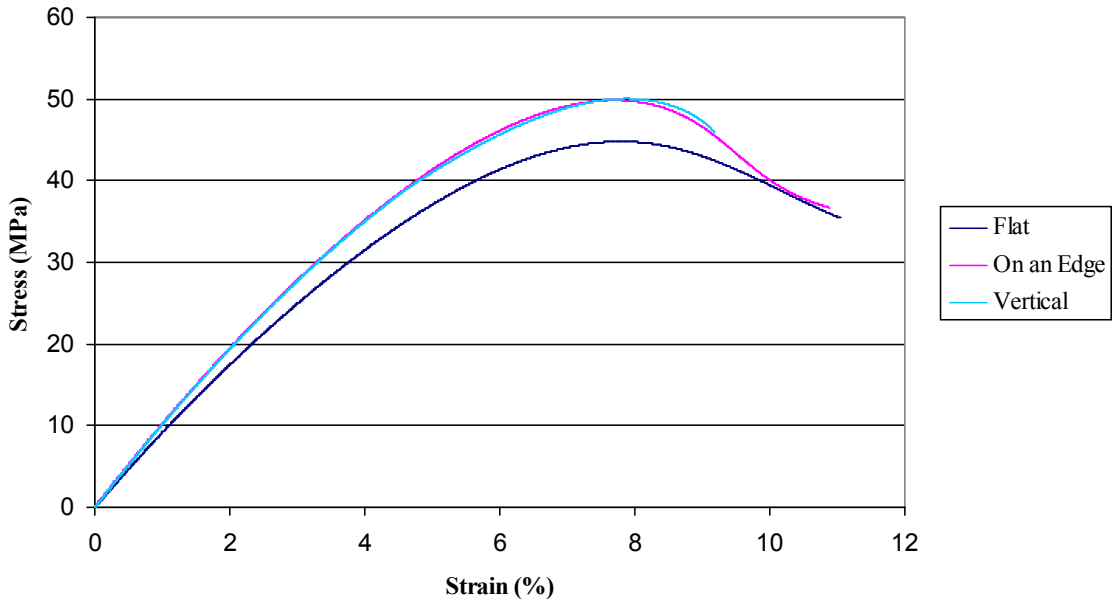

Figure 4.7 WaterShed™ 11120 specimens from the first batch built from the study of the three different layouts. Note the difference in the ultimate stress for each curve with vertical being the one with the highest stress.

Table 4.24 Mechanical testing results for 4 days ambient and 2 days conditioned at temperature 23±2°C and 50±5%RH of the second batch. The results are an average of eight specimens for each orientation.

Orientation		Ultimate Tensile Stress (MPa)	Elongation at Break (%)	Fracture Stress (MPa)	E-Modulus (1-3% Strain) (MPa)	E-Modulus (MPa)
Flat	Mean	44.3	14.0	25.6	770.5	2273.9
	Median	44.0	13.1	28.9	767.4	2268.8
	Std Deviation	0.5	4.3	10.4	8.0	51.9
	Std Error	0.2	1.5	3.7	2.8	18.3
	Maximum	45.0	23.9	31.1	783.5	2362.5
	Minimum	43.8	9.5	0.1	761.3	2191.2
On an Edge	Mean	49.4	8.6	35.8	866.3	2594.0
	Median	49.4	9.6	33.1	865.4	2606.0
	Std Deviation	0.4	2.9	5.7	9.7	57.1
	Std Error	0.1	1.0	2.0	3.4	20.2
	Maximum	50.1	11.4	48.4	885.3	2684.1
	Minimum	48.9	3.7	31.9	854.3	2510.0
Vertical	Mean	49.6	7.7	36.3	884.7	2597.1
	Median	49.7	6.7	35.9	884.3	2588.7
	Std Deviation	0.3	2.9	3.5	7.6	40.8
	Std Error	0.1	1.0	1.2	2.7	14.4
	Maximum	50.1	13.2	41.9	895.0	2660.1
	Minimum	49.0	4.5	31.6	873.5	2542.0

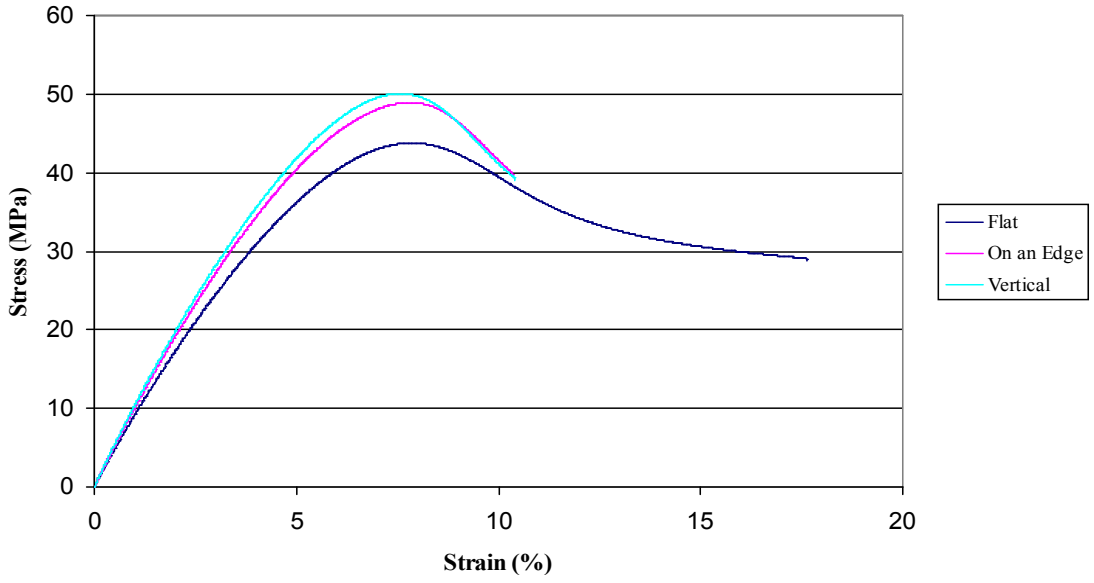

Figure 4.8 WaterShed™ 11120 specimens from the second batch built from the study of the three different layouts. Note the difference in the ultimate stress for each curve with vertical being the one with the highest stress.

Table 4.25 Mechanical testing results for 4 days ambient and 2 days conditioned at temperature 23±2°C and 50±5%RH of the third batch. The results are an average of eight specimens for each orientation.

Orientation		Ultimate Tensile Stress (MPa)	Elongation at Break (%)	Fracture Stress (MPa)	E-Modulus (1-3% Strain) (MPa)	E-Modulus (MPa)
Flat	**Mean**	48.5	11.4	31.9	851.2	2353.7
	Median	48.7	12.0	32.0	851.4	2376.1
	Std Deviation	0.7	1.9	0.4	9.4	66.2
	Std Error	0.2	0.7	0.1	3.3	23.4
	Maximum	49.1	14.1	32.5	862.0	2412.2
	Minimum	47.0	8.1	31.2	830.5	2219.7
On an Edge	**Mean**	51.2	5.9	38.7	903.5	2660.7
	Median	51.2	5.9	39.5	904.0	2568.8
	Std Deviation	0.7	0.9	2.5	6.5	240.4
	Std Error	0.2	0.3	0.9	2.3	85.0
	Maximum	52.4	7.6	41.5	914.8	3213.1
	Minimum	50.3	4.6	34.0	895.6	2470.3
Vertical	**Mean**	51.5	4.8	43.0	919.4	2541.5
	Median	51.5	4.6	43.0	918.7	2549.6
	Std Deviation	0.4	0.4	2.0	6.4	53.5
	Std Error	0.1	0.1	0.7	2.3	18.9
	Maximum	52.1	5.6	46.4	929.1	2619.2
	Minimum	51.1	4.3	39.7	911.4	2442.3

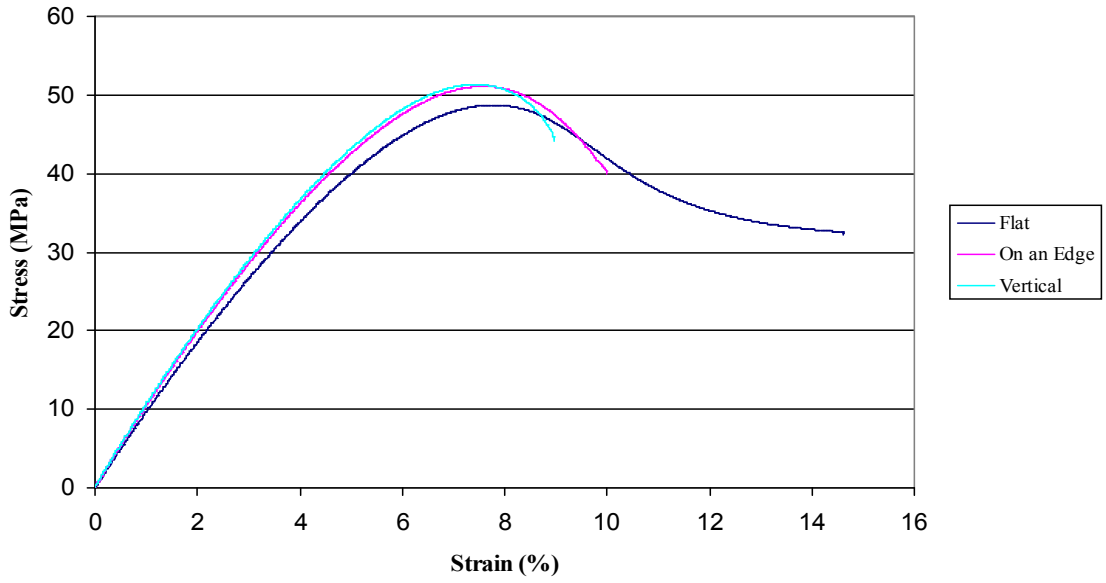

Figure 4.9 WaterShed™ 11120 specimens from the third batch built from the study of the three different layouts. Note the difference in the ultimate stress for each curve with vertical being the one with the highest stress.

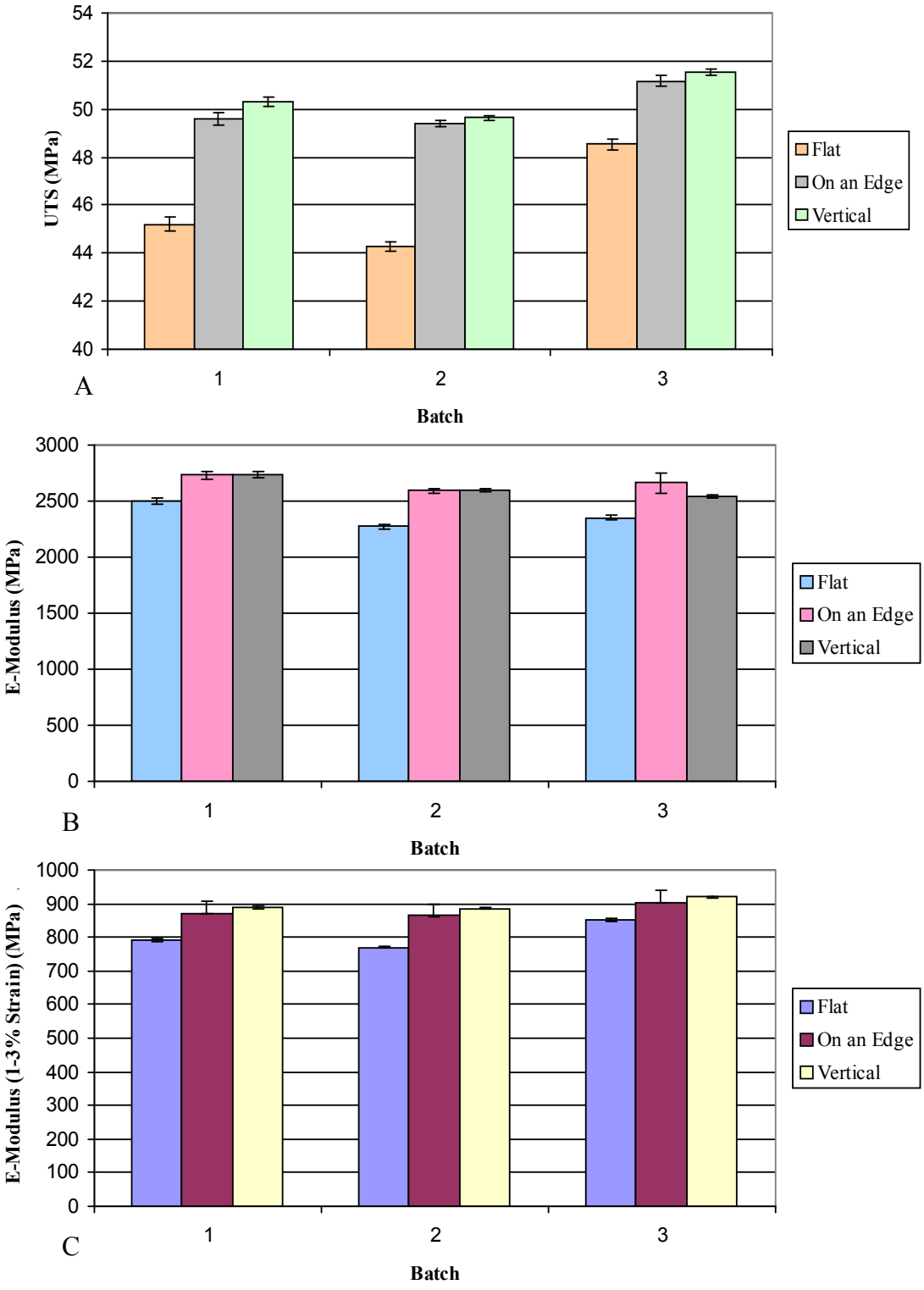

Figure 4.10 Mechanical properties of WaterShed™ 11120 in flat, on an edge and vertical build orientations based on only a set point 4 days and 2 days at a temperature 23±2°C and 50±5% RH . A) Ultimate Tensile Stress, B) E-Modulus and C) E-Modulus (1-3% Strain).

4.4 SCANNING ELECTRON MICROSCOPY RESULTS

Scanning Electron Microscopy (SEM) has the ability to study crazes and shear bands in transparent polymers which have the ability to assume the direction of applied stress for failure analysis. SEM is well suited for examining the top topography of polymer surfaces because of the large depth of field that is possible. The fracture surface of the following Figures 4.11 and 4.12 demonstrates that two different specimens of different conditions but same layout, in this case on an edge layout 2, have the same characteristics of a polymer behavior. WaterShed™ 11120 surfaces of both specimens show similar fractures surfaces of typical polymer with regions of mirror zones hounded by mist. This shows proof of craze of the polymer of early phase of crack propagation growth, and hackle regions. As the polymer continues to fracture, there is a presence change from smooth to a coarse surface. This is the presence of new fracture

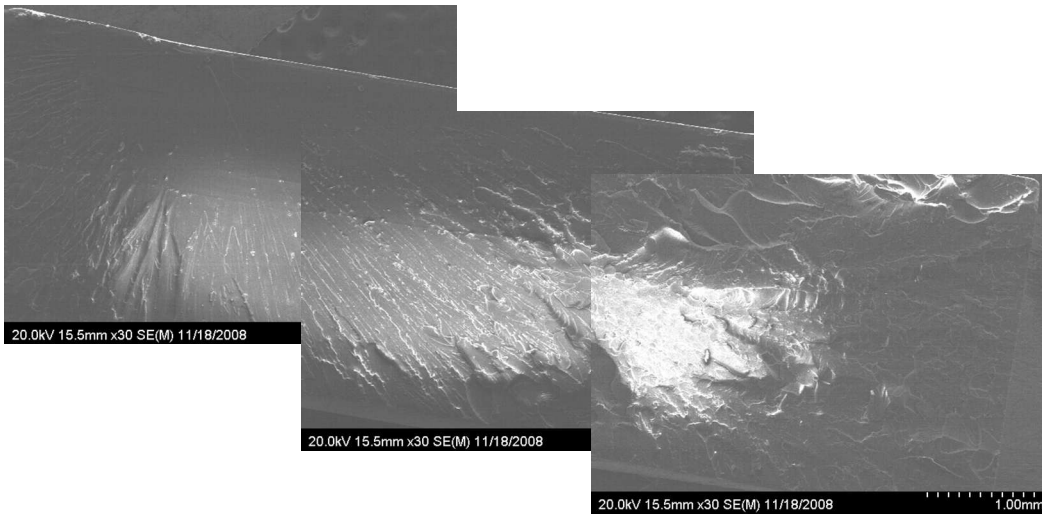

Figure 4.11 WaterShed™ 11120 on an edge specimen, SEM images showing the surface fracture indication of the mirror zone and hackle which demonstrates crack propagation path.

surface which has the crack propagation throughout the polymer. The specimens are from different conditions however are from the same time period which are 4 days, ambient and conditioned as stated in the ASTM D638. They do not demonstrate a difference in surface fracture.

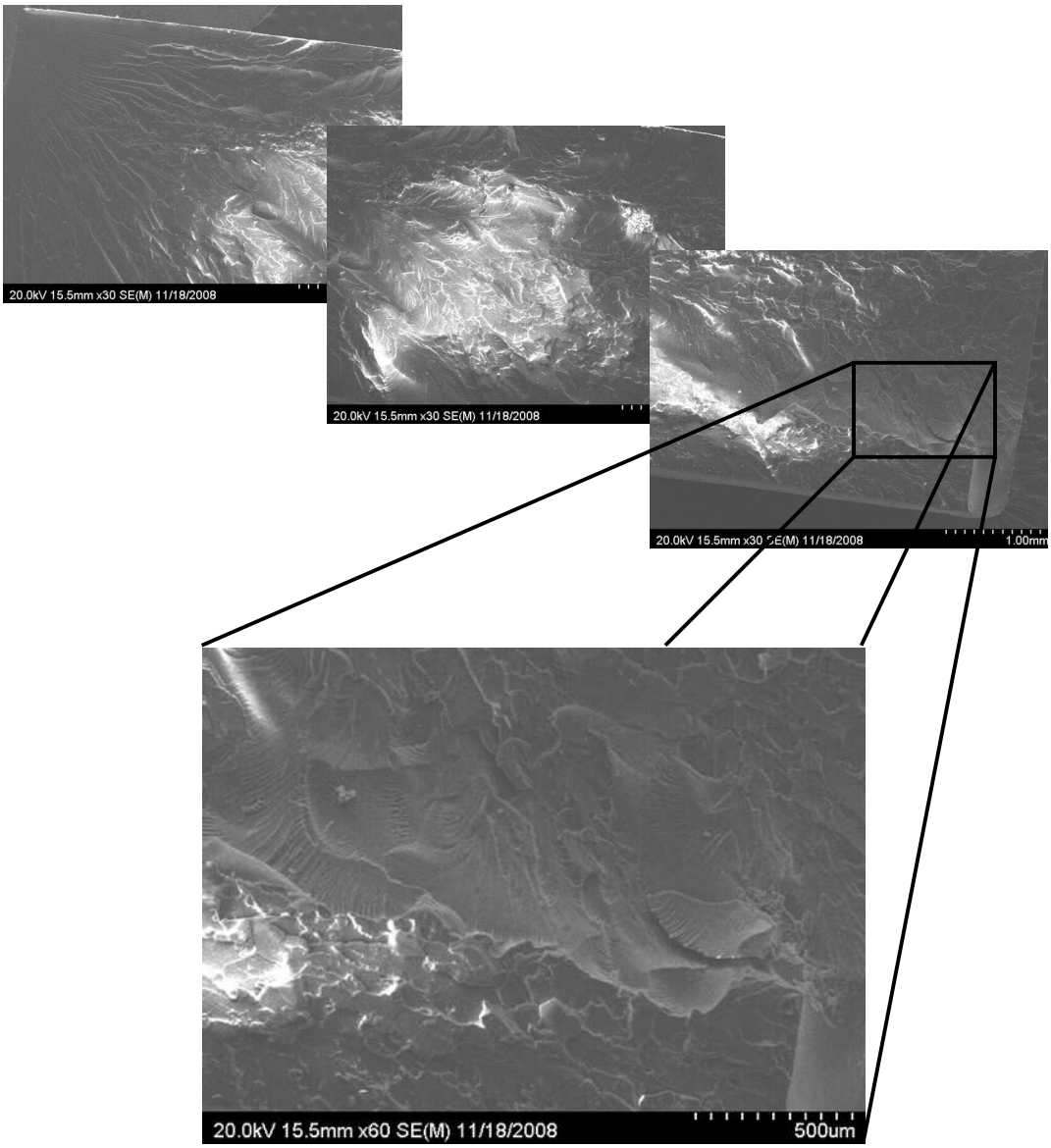

Figure 4.12 Demonstrates the many new crack fracture surfaces in the specimen of an conditioned sample in four days in ambient and two days at a temperature 23±2°C and 50±5%RH.

Apart from conditions that are one of the factors being studied, layout is another important part of the study. There are three different layouts. Figure 4.13 demonstrate the different surface fracture due to the different layout of the layers. Both specimens are from the four days and two days conditioned. The top figure of Figure 4.13 shows layout 1 being built flat which demonstrates a typical fracture surface of a polymer. On the other hand, the figure on the bottom of Figure 4.13 shows the layer to layer interaction of layout 3 being built vertically. The manner in which it is being built results in the specimen being tough and strong do to the layer interface. In this case, the picture can show the layer to layer bond which results in the polymer being stronger. Both specimens have a mirror zone section where crack propagation paths can be found in the mid sections of both specimens even though they are built differently. Figure 4.14 being only conditioned in ambient, can be compared to Figure 4.13 in both conditions (flat or on-edge, and four days ambient and two days condition). The specimen's condition has had an effect on the fracture surface built flat as shown in the figures. Furthermore, the build orientation vertical and flat has a different fracture due to the layer to layer manufacturing.

Subsequently, aging is another factor that was taken into consideration besides conditioning. Two of the aging set points were analyzed, four days and one month, in the ambient condition. Figure 4.15 shows the new fracture surfaces in the crack propagation on both aging time periods of specimens. It can also be viewed that in both specimens the aging does not have an effect on the fracture surface of the specimen. It is observed that the mirror zone also demonstrates smooth to coarse surface of the crack propagation.

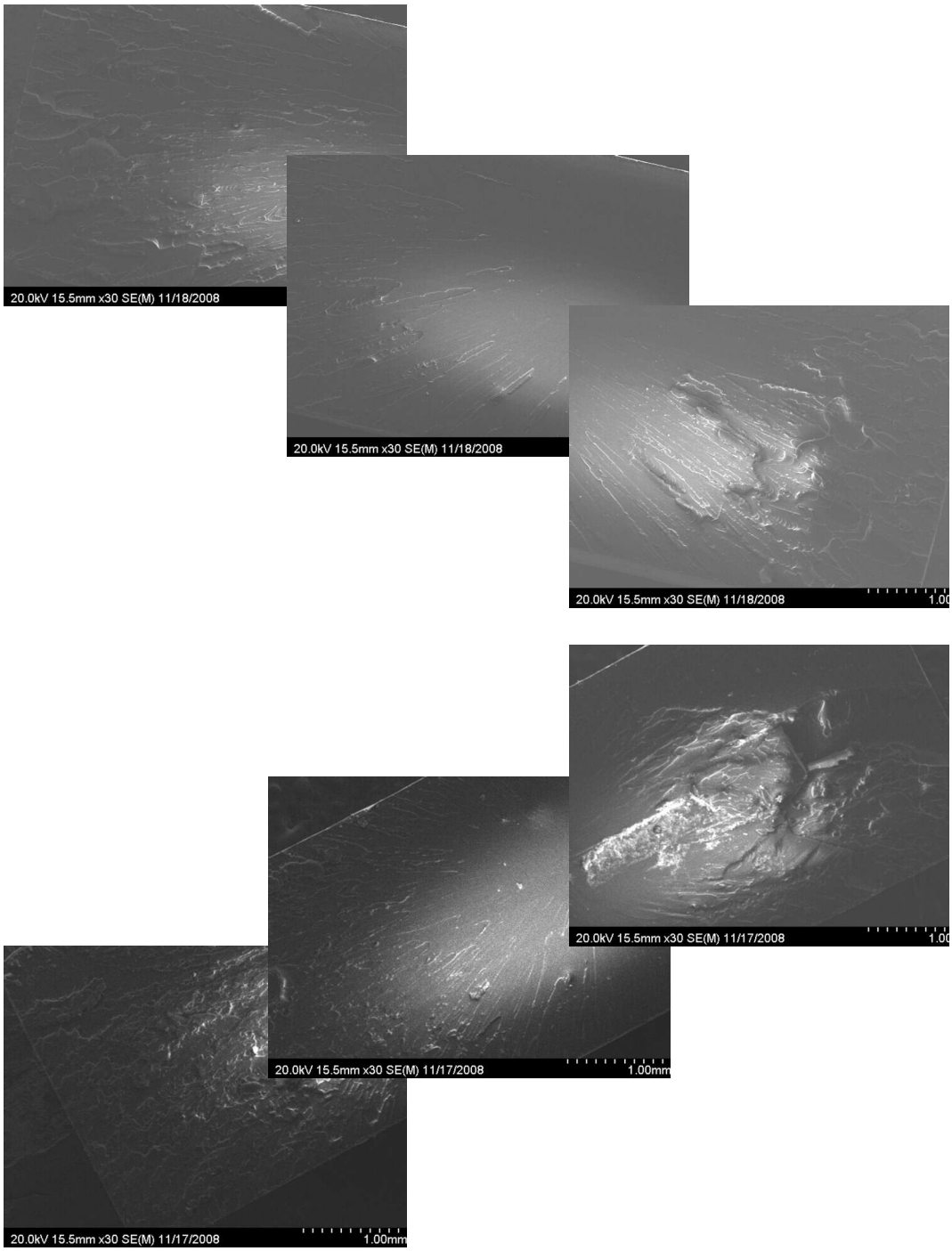

Figure 4.13 Shows two different layouts, top being flat, bottom vertical. Both layouts show different fracture surface but in both demonstrate in the mid section a mirror zone with smooth to coarse surface. Towards the end of the fracture surface of the bottom picture shows the layer to layer interface in the vertical layout.

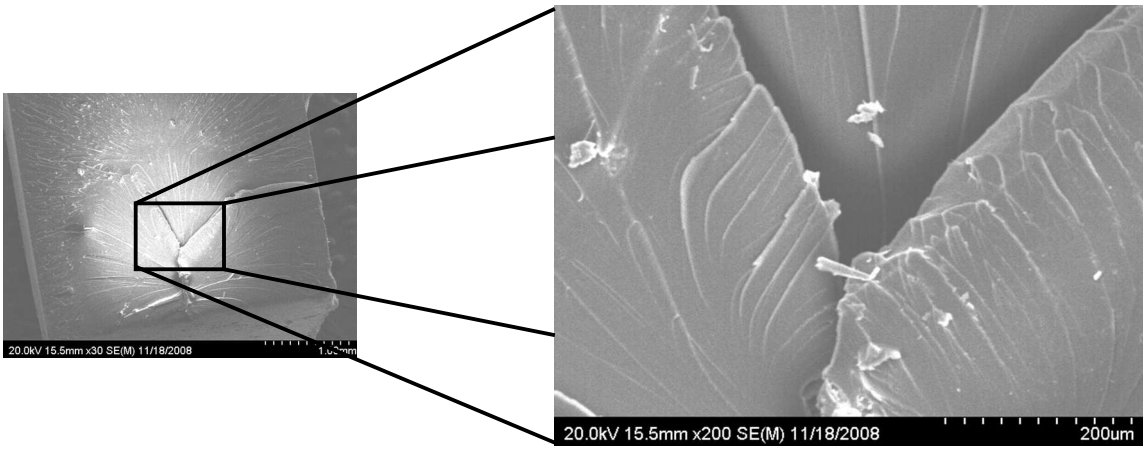

Figure 4.14 WaterShed™ 11120 specimen built in layout 2 (on an edge). The layer to layer interfaces of a specimen built on an edge ambient condition in four days ambient, shows the layers when fractured.

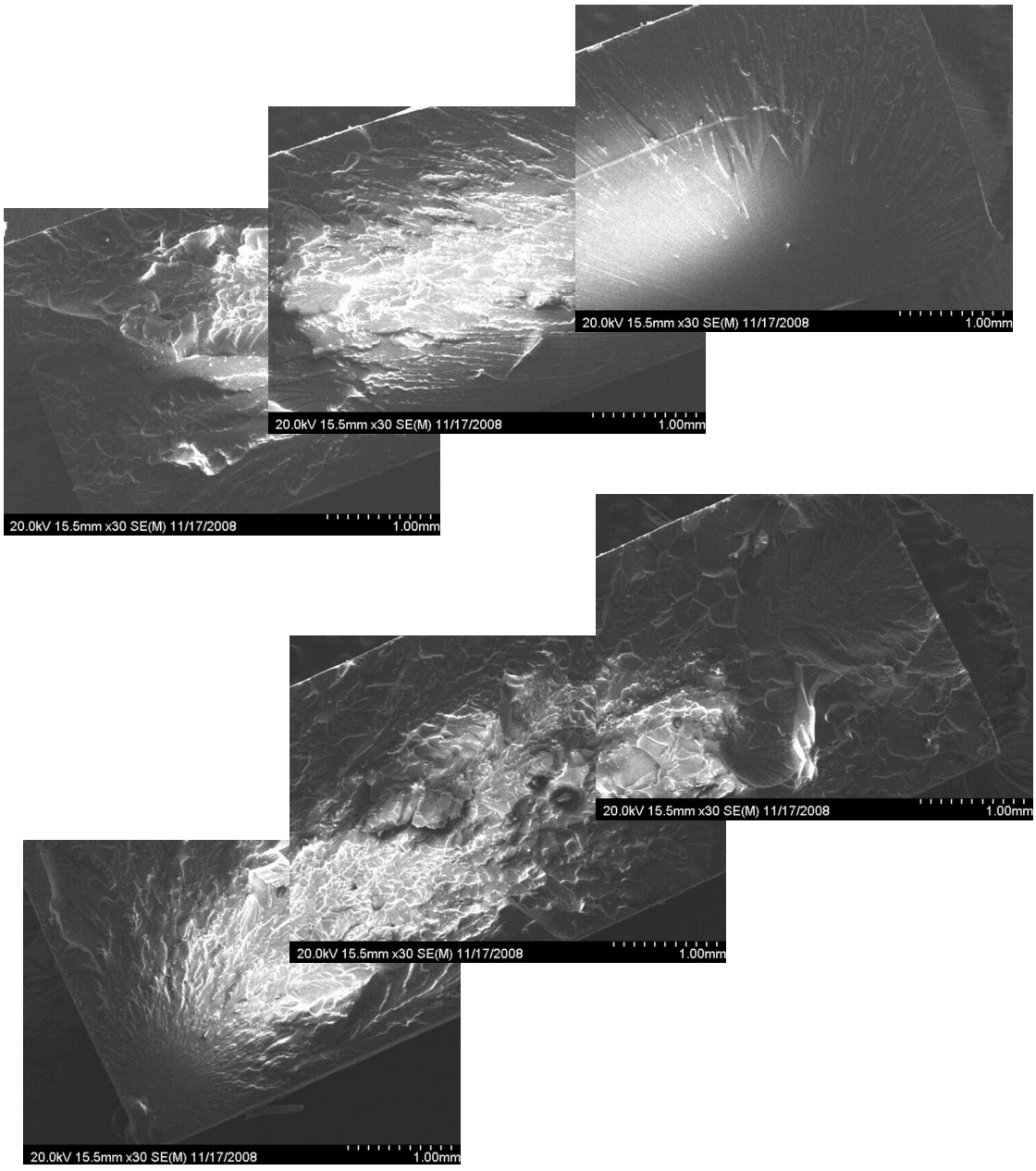

Figure 4.15 SEM pictures of different aging in ambient built on an edge: Top 4 days, Bottom 1 month. Both show the crack propagation from the mirror zone of smooth to coarse surface.

CHAPTER 5 STATISTICAL ANALYSIS RESULTS

5.1 INTRODUCTION

To investigate the effects of the two different build setups in Figure 3.1 and Figure 3.2, a statistical design of experiments was considered. The 13 batches built for both of the setups were built using the Viper Si^2 SL machine. The build setup in Figure 3.1 of 18 Type I specimens took nine hours to build a single batch and for the build setup in Figure 3.2 the 24 Type I specimens took 11 hours of build time for a single batch as can be seen in Appendix B. All of the Type I tensile specimens were measured for overall length, overall width, width of the narrow section, thickness, and gage length before being mechanically tested. The analysis done in this research was at a level of significance of 5% in Statgraphics® software.

5.2 EXPERIMENTAL DESIGN

The results obtained from the tensile testing were analyzed in order to understand the effects of the different build setups. Each setup had their own study factors. Based on Figure 3.1, the 18 Type I tensile specimens were randomized before being tested and the factors studied involved axis, layout, and position on the ultimate tensile stress and E-Modulus (1-3% Strain). On the other hand, the other build setup on Figure 3.2 that holds 24 test specimens studied the factors of layout and position. The information analyzed for the statistical analysis is covered from Tables 5.1 through 5.14. For the mechanical testing, the tensile specimens were randomly measured by one analyst. Each specimen was measured three times for its dimensions; therefore, the total measurement for each batch was 270 measurements. The specimens were mechanically

tested in the same order that they were randomly measured. Therefore, for the effect of build orientation and environmental and aging conditions, a total of 2,430 measurements were done for the build setup in Figure 3.1. Three batches were tested for the build setup of 24 Type I specimens. Two of the batches were measured by one analyst three times and each specimen randomly for a total of 720 measurements. One of the batches was measured by three analysts for each specimen three times. There were a total of 1,080 measurements of the tensile specimens. The measurements were taken at the overall length, overall width, width of the narrow section, thickness, and the gage length of the ASTM Type I specimen as shown in Figure 3.20. All the measurements were taken with a low pressure caliper (Model 500-196, Mitutoyo America Co., City of Industry, CA).

Table 5.1 4 Days ambient specimens tested in random order with testing results and measurements with respect to position, layout, and axis.

Order of Testing	Specimen	Tensile strain at Break	Tensile stress at Break	Ultimate Tensile Stress	E-Modulus (1-3% Strain)	Position	Layout	Axis	Average Measurements (mm)				
		(%)	(MPa)	(MPa)	(MPa)				L	Wo	W	T	G
1	3	23.08	0.34	48.75	839.24	1	1	1	165.97	19.33	12.99	3.62	51.35
2	17	37.51	33.35	49.52	861.27	2	2	3	166.03	19.32	12.90	3.53	51.33
3	16	15.27	34.41	48.47	858.75	1	2	3	166.04	19.33	12.91	3.51	51.30
4	6	41.31	32.37	48.21	853.14	1	1	2	166.33	19.35	12.95	3.60	51.52
5	11	30.35	32.78	48.46	852.73	2	2	1	165.93	19.32	12.94	3.49	51.26
6	8	35.72	31.30	47.17	824.15	2	1	3	166.12	19.42	13.01	3.62	51.42
7	18	19.11	34.66	48.54	852.58	3	2	3	166.01	19.31	12.89	3.52	51.28
8	13	13.72	35.03	48.30	854.36	3	2	2	166.34	19.32	12.89	3.50	51.44
9	2	38.76	31.45	47.60	833.51	2	1	1	165.94	19.32	12.92	3.61	51.35
10	4	24.82	31.50	47.74	835.75	3	1	2	166.35	19.35	12.98	3.63	51.51
11	5	46.33	32.90	48.07	840.45	2	1	2	166.33	19.35	12.98	3.62	51.53
12	9	17.15	33.38	48.41	834.32	3	1	3	166.14	19.33	12.98	3.62	51.41
13	12	15.24	34.34	48.42	865.26	1	2	1	165.95	19.30	12.91	3.48	51.22
14	7	22.76	32.94	47.95	839.17	1	1	3	166.10	19.32	12.98	3.59	51.39
15	10	12.98	34.91	48.13	840.09	3	2	1	165.95	19.31	12.95	3.48	51.24
16	1	15.60	33.84	48.37	835.80	3	1	1	166.04	19.32	12.95	3.62	51.32
17	15	10.33	43.12	48.82	829.52	1	2	2	166.31	19.33	12.93	3.48	51.40
18	14	9.84	43.97	48.79	841.85	2	2	2	166.30	19.33	12.92	3.50	51.43

Table 5.2 4 Days ambient and 2 days conditioned at 23±2°C and 50±5% RH. Specimens tested in random order with testing results and measurements with respect to position and layout. Batch 1.

Order of Testing	Specimen	Tensile strain at Break	Tensile stress at Break	Ultimate Tensile Stress	E-Modulus	E-Modulus (1-3% Strain)	Position	Layout	Average Measurements (mm)				
		(%)	(MPa)	(MPa)	(MPa)	(MPa)			L	Wo	W	T	G
1	6	4.36	46.09	50.04	2652.06	878	2	3	164.97	19.28	12.81	3.50	50.85
2	10	6.27	35.5	44.79	2418.91	788.37	4	1	165.29	19.17	12.82	3.58	51.02
3	21	4.37	45.83	50.48	2717.54	887.98	7	3	165.31	19.13	12.80	3.46	50.82
4	15	4.91	41.92	50.86	2806.58	891.87	5	3	164.96	19.18	12.91	3.46	50.86
5	3	5.19	42.11	50.9	2875.73	897.01	1	3	165.00	19.14	12.81	3.44	50.81
6	17	5.67	36.76	49.86	2846.86	881.42	6	2	165.35	19.29	12.93	3.43	50.97
7	14	4.88	41.47	49.99	2766.45	879.92	5	2	165.36	19.28	13.00	3.44	50.99
8	19	5.88	38.07	45.91	2643.03	795.87	7	1	165.26	19.19	12.82	3.61	51.03
9	4	6.2	35.86	45.78	2507.81	795.78	2	1	165.28	19.17	12.82	3.55	51.04
10	22	4.48	42.18	45.49	2558.64	800.67	8	1	165.27	19.19	12.83	3.57	51.02
11	12	4.27	47.39	50.39	2682.55	892.8	4	3	165.07	19.18	12.86	3.45	50.96
12	24	4.37	47.21	50.75	2824.86	898.35	8	3	165.11	19.12	12.79	3.48	50.88
13	5	5.45	38.59	49.91	2591.42	869.05	2	2	165.35	19.26	13.04	3.44	50.96
14	13	8.82	32.06	45.27	2404.25	792.36	5	1	165.29	19.18	12.83	3.58	51.03
15	9	4.71	42.48	49.99	2686.6	890.65	3	3	164.99	19.26	12.84	3.49	50.78
16	11	4.76	42.25	48.05	2640	858.89	4	2	165.38	19.26	12.97	3.47	50.97
17	2	6.85	36.16	49.41	2866.41	872.95	1	2	165.33	19.36	12.95	3.44	50.96
18	20	6.05	37.18	49.69	2670.95	872.95	7	2	165.32	19.32	12.93	3.46	50.96
19	16	8.89	30.81	44.15	2529.34	787.35	6	1	165.27	19.19	12.83	3.57	51.02
20	8	4.54	43.41	49.4	2737.24	872.28	3	2	165.36	19.24	12.94	3.43	50.99
21	1	8.53	32.56	46.25	2534.24	800.09	1	1	165.28	19.18	12.82	3.52	50.99
22	18	5.85	39.46	49.25	2638.32	860.38	6	3	165.04	19.14	12.81	3.56	50.81
23	23	5.19	41.31	50.39	2745.32	872.89	8	2	165.33	19.32	13.01	3.44	50.91
24	7	9.5	31.07	43.99	2394.18	771.5	3	1	165.27	19.18	12.82	3.60	51.03

Table 5.3 4 Days ambient and 2 days conditioned at 23±2°C and 50±5% RH. Specimens tested in random order with testing results and measurements with respect to position and layout. Batch 2.

Order of Testing	Specimen	Tensile strain at Break	Tensile stress at Break	Ultimate Tensile Stress	E-Modulus	E-Modulus (1-3% Strain)	Position	Layout	Average Measurements (mm)				
		(%)	(MPa)	(MPa)	(MPa)	(MPa)			L	Wo	W	T	G
1	15	8.44	34.6	49.73	2,643.39	894.97	5	3	165.13	19.17	12.85	3.44	50.92
2	13	23.92	27.61	43.94	2,239.69	763.82	5	3	165.41	19.18	12.82	3.54	51.10
3	14	7.29	35.44	49.46	2,590.21	863.7	5	3	165.48	19.30	12.92	3.45	51.01
4	20	9.46	33.13	49.46	2,614.07	867.14	7	2	165.47	19.24	12.95	3.45	50.99
5	5	3.7	48.36	49.01	2,625.23	859.51	2	2	165.48	19.25	12.93	3.45	51.02
6	6	4.53	39.34	50.05	2,542.02	888.77	2	3	165.00	19.19	12.87	3.43	50.89
7	7	9.54	31.06	44.11	2,191.15	761.25	3	1	165.43	19.17	12.82	3.50	51.10
8	3	13.19	31.55	49.41	2,555.71	873.52	1	3	164.98	19.17	12.87	3.44	50.96
9	19	13.21	29.56	44.96	2,362.48	783.46	7	1	165.46	19.21	12.82	3.50	51.11
10	16	14.22	28.58	43.82	2,250.99	768.49	6	1	165.45	19.17	12.83	3.53	51.10
11	10	13.07	29.04	43.76	2,253.10	766.31	4	1	165.41	19.16	12.86	3.53	51.09
12	23	9.65	32.98	49.63	2,605.32	867.83	8	2	165.45	19.25	12.94	3.44	50.98
13	11	10.83	32.74	50.05	2,684.08	885.29	4	2	165.47	19.25	12.91	3.42	51.01
14	2	11.22	32.12	49.27	2,606.68	854.28	1	2	165.47	19.29	12.89	3.44	51.00
15	18	6.58	36.77	49.98	2,660.07	887.64	6	3	165.12	19.18	12.85	3.43	50.88
16	9	10.64	32.83	49.67	2,587.45	879.92	3	3	165.03	19.18	12.87	3.43	50.83
17	17	5.32	39.93	48.92	2,509.97	859.33	6	2	165.49	19.28	12.91	3.47	51.00
18	4	14.63	28.66	43.96	2,284.46	765.82	2	1	165.47	19.19	12.83	3.50	51.07
19	22	12.25	0.05	44.92	2,303.84	779.48	8	1	165.39	19.20	12.83	3.49	51.07
20	24	5.1	41.94	48.96	2,581.55	878.62	8	3	165.09	19.14	12.85	3.51	50.93
21	8	11.36	31.89	49.32	2,516.75	873.27	3	2	165.49	19.26	12.88	3.44	51.01
22	12	6.3	38.28	49.7	2,589.91	893.09	4	3	165.10	19.18	12.84	3.41	50.87
23	21	6.76	34.96	49.57	2,617.06	880.91	7	3	165.02	19.23	12.84	3.44	50.92
24	1	11.49	29.92	44.68	2,305.65	775.42	1	1	165.37	19.18	12.85	3.49	51.07

Table 5.4 4 Days ambient and 2 days conditioned at 23±2°C and 50±5% RH. Specimens tested in random order with testing results and measurements with respect to position and layout. Batch 3.

Order of Testing	Specimen	Tensile strain at Break	Tensile stress at Break	Ultimate Tensile Stress	E-Modulus	E-Modulus (1-3% Strain)	Position	Layout	Average Measurements (mm)				
		(%)	(MPa)	(MPa)	(MPa)	(MPa)			L	Wo	W	T	G
1	6	4.64	44.69	51.33	2,442.30	917.14	2	3	165.18	19.15	12.85	3.54	50.96
2	10	9.64	32.52	48.71	2,376.72	849.76	4	1	165.50	19.30	12.97	3.73	51.19
3	21	4.6	46.43	51.81	2,552.11	920.86	7	3	165.28	19.15	12.85	3.54	50.97
4	15	4.33	42.57	51.09	2,619.15	911.37	5	3	165.27	19.15	12.91	3.53	51.12
5	3	5.06	41.24	51.11	2,548.65	912.62	1	3	165.13	19.19	12.84	3.55	51.04
6	17	5.26	40.49	51.1	2,492.62	905.21	6	2	165.51	19.38	13.02	3.56	51.04
7	14	4.63	41.48	50.7	3,213.13	896.78	5	2	165.52	19.37	13.05	3.56	51.02
8	19	12.27	31.59	49.05	2,412.20	858.86	7	1	165.56	19.31	12.99	3.71	51.17
9	4	12.72	32.21	48.33	2,219.71	854.48	2	1	165.56	19.37	12.96	3.68	51.13
10	22	10.51	31.92	48.6	2,375.48	850.74	8	1	165.50	19.37	13.00	3.73	51.16
11	12	4.5	43.25	51.66	2,520.71	920.26	4	3	165.31	19.15	12.85	3.54	51.07
12	24	5.62	39.71	51.89	2,590.17	929.08	8	3	165.25	19.14	12.86	3.60	51.07
13	5	5.9	39.44	51.52	2,744.21	904.82	2	2	165.49	19.35	13.02	3.56	51.01
14	13	12.12	31.89	49.09	2,405.37	862.03	5	1	165.50	19.32	12.98	3.71	51.17
15	9	4.65	43.64	51.32	2,508.18	916.37	3	3	165.19	19.15	12.85	3.55	51.02
16	11	6.1	38.35	50.52	2,556.88	895.63	4	2	165.53	19.37	13.02	3.55	51.02
17	2	5.93	39.54	52.41	2,557.01	914.84	1	2	165.47	19.37	13.06	3.44	51.02
18	20	7.57	34.04	51.29	2,580.68	903.09	7	2	165.52	19.39	13.05	3.58	51.03
19	16	14.07	31.2	48.7	2,370.55	851.64	6	1	165.53	19.32	12.98	3.74	51.15
20	8	6.87	36.12	51.51	2,670.96	908.81	3	2	165.53	19.36	13.01	3.55	51.03
21	1	11.97	32.1	48.71	2,383.28	851.21	1	1	165.44	19.37	12.99	3.70	51.10
22	18	4.99	42.83	52.05	2,550.47	927.45	6	3	165.28	19.15	12.85	3.55	51.07
23	23	5.26	40.29	50.28	2,470.27	898.66	8	2	165.51	19.41	13.18	3.58	51.04
24	7	8.14	32.01	47.03	2,286.61	830.5	3	1	165.51	19.33	12.97	3.77	51.15

Table 5.5 4 Days ambient specimens tested in random order with testing results and measurements with respect to position, layout, and axis.

Order of Testing	Specimen	Tensile strain at Break	Tensile stress at Break	Ultimate Tensile Stress	E-Modulus	E-Modulus (1-3% Strain)	Position	Layout	Axis	Average Measurements (mm)				
		(%)	(MPa)	(MPa)	(MPa)	(MPa)				L	Wo	W	T	G
1	4	15.01	29.06	44.53	2526.8	749.09	3	1	2	165.01	19.22	12.87	3.69	50.86
2	12	5.34	38.19	47.33	2700.32	842.62	1	2	1	165.12	19.39	12.95	3.42	50.82
3	6	10.02	30.72	44.39	2510.38	768.52	1	1	2	165.05	19.22	12.95	3.73	50.83
4	10	6.74	33.3	47.84	2573.66	830.88	3	2	1	165.17	19.39	12.97	3.45	50.86
5	8	27.78	27.33	44.54	2385.4	777.33	2	1	3	165.02	19.23	12.89	3.68	50.86
6	16	18.86	29.67	46.92	2656.42	826.26	1	2	3	165.28	19.37	12.99	3.49	50.78
7	11	6.07	35.8	48.25	2637.6	835.56	2	2	1	165.18	19.36	12.99	3.43	50.86
8	3	10.3	31.09	45.65	2662.68	769.1	1	1	1	165.22	19.12	12.80	3.68	50.94
9	13	4.66	40.79	46.78	2775.58	820.11	3	2	2	165.01	17.03	12.99	3.50	50.80
10	1	14.05	28.68	43.61	2475.47	738.3	3	1	1	165.13	19.26	12.79	3.68	50.87
11	9	8.4	30.82	43.88	2486.46	738.89	3	1	3	164.97	19.24	12.90	3.74	50.81
12	7	23.49	27.99	44.61	2316.89	758.9	1	1	3	165.01	19.20	12.88	3.68	50.87
13	5	25.7	26.79	43.25	2438.19	727.68	2	1	2	165.01	19.22	12.87	3.69	50.86
14	17	13.7	31.11	46.32	2623.56	801.32	2	2	3	164.94	19.38	13.01	3.51	50.75
15	2	7.98	31.73	44.65	2467.89	754.89	2	1	1	165.16	19.20	12.78	3.64	50.94
16	18	7.78	33.68	47.68	2549.5	801.46	3	2	3	164.97	19.39	12.99	3.51	50.76
17	15	4.11	44.25	46.95	2747.3	820.71	1	2	2	164.99	19.37	12.95	3.50	50.72

Table 5.6 4 Days desiccant specimens tested in random order with testing results and measurements with respect to position, layout, and axis.

Order of Testing	Specimen	Tensile strain at Break	Tensile stress at Break	Ultimate Tensile Stress	E-Modulus	E-Modulus (1-3% Strain)	Position	Layout	Axis	Average Measurements (mm)				
		(%)	(MPa)	(MPa)	(MPa)	(MPa)				L	Wo	W	T	G
1	2	8.26	30.84	44.26	2480.5	776.13	2	1	1	165.16	19.15	12.81	3.66	50.92
2	7	11.52	29.76	43.57	2366.15	779.38	1	1	3	165.02	19.22	12.92	3.69	50.86
3	16	4.18	44.34	46.55	2556.83	831.94	1	2	3	165.24	19.39	12.99	3.51	50.77
4	3	8.24	30.21	43.09	2488.25	771.9	1	1	1	165.21	19.12	12.79	3.73	50.91
5	18	11.44	32.1	46.48	2628.63	834.7	3	2	3	164.98	19.39	12.99	3.52	50.74
6	5	9.24	30.34	43.2	2574.37	770.55	2	1	2	165.00	19.23	12.88	3.69	50.83
7	14	3.78	42.95	44.54	2609.9	804.59	2	2	2	165.01	19.40	13.04	3.66	50.74
8	17	12.04	31.24	46.22	2409.14	826.27	2	2	3	164.91	19.38	12.99	3.52	50.77
9	6	5.58	34.52	42.35	2420.46	755.85	1	1	2	164.99	19.21	13.01	3.69	50.81
10	12	6.68	35.72	48.03	2708.62	842.81	1	2	1	165.12	19.38	12.98	3.43	50.85
11	9	13.73	29.16	43.36	2544.61	752.94	3	1	3	165.01	19.23	12.93	3.74	50.84
12	1	6.25	34.54	43.38	2533.53	753.6	3	1	1	165.15	19.18	12.81	3.69	50.88
13	13	3.95	42.43	44.57	2491.04	808.68	3	2	2	164.97	19.41	13.00	3.62	50.83
14	8	5.81	37.13	45.11	2672.56	801.27	2	1	3	165.04	19.24	12.92	3.58	50.88
15	10	6.81	32.16	45.88	2655.77	813.61	3	2	1	165.23	19.42	13.01	3.48	50.88
16	15	10.44	31.38	45.01	2688.47	816.05	1	2	2	164.96	19.40	12.97	3.55	50.72
17	4	21.87	27.18	42.78	2572.29	738.98	3	1	2	165.00	19.23	12.88	3.71	50.84
18	11	6.61	34.46	45.87	2507.5	822.17	2	2	1	165.14	19.41	13.01	3.45	50.87

Table 5.7 4 Days desiccant and 2 days conditioned at 23° and 50% RH. Specimens tested in random order with testing results and measurements with respect to position, layout, and axis.

Order of Testing	Specimen	Tensile strain at Break	Tensile stress at Break	Ultimate Tensile Stress	E-Modulus	E-Modulus (1-3% Strain)	Position	Layout	Axis	Average Measurements (mm)				
		(%)	(MPa)	(MPa)	(MPa)	(MPa)				L	Wo	W	T	G
1	2	5.85	34.13	44.78	2445.8	772.51	2	1	1	165.16	19.17	12.82	3.65	50.93
2	12	6.2	35.22	49.46	2647.24	833.93	1	2	1	165.13	19.38	12.92	3.42	50.83
3	4	6.22	33.49	44.81	2390.75	755.03	3	1	2	165.04	19.18	12.88	3.68	50.83
4	16	10.04	32.81	47.18	2586.63	815.28	1	2	3	164.94	19.36	12.96	3.50	50.74
5	17	5.74	38.61	47.56	2514.57	821.55	2	2	3	164.92	19.43	12.97	3.51	50.76
6	14	4.18	41.9	46.74	2520.6	796.34	2	2	2	164.71	19.38	12.99	3.62	50.76
7	8	6.8	34.01	47.76	2706.82	819.92	3	2	3	164.94	19.36	12.93	3.51	50.74
8	7	15.8	28.68	44.27	2366.27	761.46	1	1	3	165.04	19.27	12.90	3.69	50.86
9	11	4.38	38.51	48.32	2763.29	823.02	2	2	1	165.16	19.40	12.97	3.43	50.86
10	13	4.33	41.54	46.78	2729.77	823.39	3	2	2	165.01	19.43	12.91	3.57	50.85
11	15	4.1	43.69	47.08	2843.45	834.62	1	2	2	164.97	19.38	12.93	3.52	50.71
12	6	5.8	33.91	43.4	2354.51	707.36	1	1	2	165.02	19.22	13.01	3.69	50.82
13	3	13.37	30	45.38	2474.71	752.87	1	1	1	165.22	19.13	12.78	3.70	50.93
14	8	12.08	29.87	43.98	2504.49	764.64	2	1	3	164.98	19.22	12.91	3.64	50.87
15	1	9.21	29.73	42.62	2390.56	737.27	3	1	1	165.11	19.12	12.78	3.64	50.89
16	10	5.85	36.97	47.99	2774.27	823.89	3	2	1	165.19	19.40	12.92	3.45	50.87
17	9	5.63	33.84	42.86	2411.46	749.78	3	1	3	164.98	19.29	12.90	3.70	50.84

Table 5.8 1 month ambient specimens tested in random order with testing results and measurements with respect to position, layout, and axis.

Order of Testing	Specimen	Tensile strain at Break	Tensile stress at Break	Ultimate Tensile Stress	E-Modulus	E-Modulus (1-3% Strain)	Position	Layout	Axis	Average Measurements (mm)				
		(%)	(MPa)	(MPa)	(MPa)	(MPa)				L	Wo	W	T	G
1	4	6.06	41.41	52.73	2724.53	838.99	3	1	2	165.02	19.16	12.86	3.68	50.85
2	12	4.81	48.35	56.24	2840.81	904.15	1	2	1	165.17	19.36	12.91	3.46	50.84
3	6	5.35	44.18	52.05	2597.49	837.78	1	1	2	165.00	19.20	12.91	3.72	50.84
4	10	4.74	52.89	57.13	2893.63	919.42	3	2	1	165.17	19.44	12.97	3.47	50.88
5	8	6.84	38.92	52.28	2629.79	852.22	2	1	3	164.96	19.22	12.88	3.72	50.88
6	16	4.84	50.02	56.32	2821.51	915.37	1	2	3	164.93	19.40	12.89	3.52	50.77
7	14	3.79	53.64	53.99	2795.33	884.64	2	2	2	165.04	19.38	12.94	3.65	50.74
8	11	5.48	47.67	56.67	2903.52	912.78	2	2	1	165.13	19.37	12.97	3.44	50.85
9	13	3.88	52.62	53.25	2705.16	874.61	3	2	2	165.01	19.34	12.93	3.71	50.86
10	1	5.7	45.38	54.43	2873.43	832.37	3	1	1	165.13	19.11	12.79	3.64	50.88
11	9	5.8	43.25	52.55	2704.13	833.91	3	1	3	165.00	19.24	12.89	3.69	50.86
12	7	5.4	42.4	51.96	2714.77	840.72	1	1	3	165.01	19.22	12.89	3.70	50.88
13	5	6.93	35.98	53.12	2747.53	844.84	2	1	2	165.07	19.20	12.89	3.65	50.85
14	17	3.87	54.99	55.66	2799.67	907.74	2	2	3	164.95	19.38	12.91	3.53	50.78
15	2	5.89	43.45	52.55	2733.47	820.56	2	1	1	165.12	19.13	12.79	3.73	50.94
16	18	5.21	48.94	56.13	2782.15	913.52	3	2	3	164.97	19.37	12.91	3.53	50.76
17	15	3.73	54.49	54.95	2816.09	909.28	1	2	2	164.99	19.40	12.92	3.55	50.74

Table 5.9 1 month desiccant specimens tested in random order with testing results and measurements with respect to position, layout, and axis.

Order of Testing	Specimen	Tensile strain at Break	Tensile stress at Break	Ultimate Tensile Stress	E-Modulus	E-Modulus (1-3% Strain)	Position	Layout	Axis	Average Measurements (mm)				
		(%)	(MPa)	(MPa)	(MPa)	(MPa)				L	Wo	W	T	G
1	2	5.51	42.86	52.01	2733.97	828.89	2	1	1	165.18	19.15	12.80	3.72	50.96
2	7	5.56	40.97	50.85	2592.93	830.06	1	1	3	165.08	19.24	12.93	3.73	50.90
3	16	5.04	43.51	53.93	2774.36	884.02	1	2	3	164.98	19.41	13.03	3.53	50.80
4	3	5.37	44.23	51.69	2768.54	832.19	1	1	1	165.19	19.12	12.80	3.71	50.95
5	18	5.53	39.59	52.88	2741.69	875.05	3	2	3	165.06	19.45	13.06	3.61	50.82
6	5	6.37	39.07	50.21	2641.18	783.68	2	1	2	165.02	19.27	12.99	3.75	50.88
7	14	4.52	44.93	50.77	2525.67	759	2	2	2	165.10	19.41	12.99	3.71	50.75
8	17	4.79	45.92	52.55	2898.51	851.04	2	2	3	164.97	19.43	13.07	3.59	50.82
9	6	5.56	40.38	50.69	2777.02	810.69	1	1	2	165.03	19.33	12.93	3.70	50.86
10	12	5.03	44.57	55.09	2792.39	898.29	1	2	1	165.16	19.41	13.00	3.46	50.84
11	9	5.52	42.6	51.06	2649.34	830.77	3	1	3	165.05	19.31	12.94	3.73	50.89
12	1	5.85	41.5	51.69	2833.35	808.88	3	1	1	165.12	19.13	12.80	3.69	50.92
13	13	4.21	48.83	51.78	2701.69	820.65	3	2	2	165.07	19.35	13.06	3.65	50.84
14	8	7.06	32.27	50.21	2537.06	814.87	2	1	3	165.03	19.29	12.94	3.73	50.93
15	10	4.7	47.02	54.66	2844.3	894.27	3	2	1	165.22	19.41	13.03	3.46	50.90
16	15	4.07	50.26	52	2565.4	875.64	1	2	2	165.15	19.47	13.05	3.63	50.82
17	4	5.33	41.89	50.99	2757.94	810.1	3	1	2	165.04	19.22	12.98	3.70	50.85
18	11	4.98	44.84	54.56	2776.79	898.3	2	2	1	165.15	19.42	13.05	3.48	50.96

Table 5.10 1 month desiccant and 2 days conditioned at 23° and 50% RH. Specimens tested in random order with testing results and measurements with respect to position, layout, and axis.

Order of Testing	Specimen	Tensile strain at Break	Tensile stress at Break	Ultimate Tensile Stress	E-Modulus	E-Modulus (1-3% Strain)	Position	Layout	Axis	Average Measurements (mm)				
		(%)	(MPa)	(MPa)	(MPa)	(MPa)				L	Wo	W	T	G
1	2	5.33	41.02	50.42	2583.03	838.28	2	1	1	165.11	19.14	12.80	3.67	50.93
2	12	22.99	0.15	53.97	2939.69	907.45	1	2	1	165.17	19.40	12.98	3.44	50.83
3	4	6.17	38.2	50.4	2743.02	851.86	3	1	2	165.04	19.17	12.86	3.68	50.85
4	16	4.72	43.81	53.2	2687.15	897.81	1	2	3	164.99	19.43	12.99	3.51	50.77
5	17	5.01	40.88	52.66	2779.54	885.64	2	2	3	165.25	19.43	13.12	3.52	50.77
6	5	5.34	39.84	48.93	2533.75	834.72	2	1	2	164.99	19.19	12.88	3.69	50.86
7	14	3.83	45.77	51.21	2778.51	872.68	2	2	2	165.05	19.38	12.96	3.61	50.75
8	18	4.99	43.74	52.68	2784.82	888.09	3	2	3	164.99	19.37	13.00	3.51	50.77
9	7	4.95	42.94	49.42	2529.02	824.24	1	1	3	165.03	19.21	12.91	3.70	50.88
10	11	4.92	44.21	53.71	2862.05	882.38	2	2	1	165.25	19.51	12.99	3.44	50.87
11	13	3.98	51.38	53.49	2762.22	896.07	3	2	2	165.01	19.48	12.97	3.51	51.10
12	15	4.32	47.13	52.81	2793.64	884.25	1	2	2	165.00	19.39	12.98	3.52	50.75
13	6	5.3	39.38	49.83	2555.02	826.92	1	1	2	165.04	19.21	12.98	3.69	50.85
14	3	5.06	39.44	50.52	2631.48	822.59	1	1	1	165.27	19.11	12.79	3.68	50.94
15	8	4.11	40.99	49.1	2717.56	815.13	2	1	3	165.01	19.22	12.92	3.69	50.87
16	1	5.68	38.85	50.33	2486.78	820.22	3	1	1	165.12	19.13	12.80	3.71	50.91
17	9	4	46.49	49.7	2476	828.69	3	1	3	164.96	19.22	12.94	3.71	50.87

Table 5.11 4 months ambient specimens tested in random order with testing results and measurements with respect to position, layout, and axis.

Order of Testing	Specimen	Tensile strain at Break	Tensile stress at Break	Ultimate Tensile Stress	E-Modulus	E-Modulus (1-3% Strain)	Position	Layout	Axis	Average Measurements (mm)				
		(%)	(MPa)	(MPa)	(MPa)	(MPa)				L	Wo	W	T	G
1	3	8.69	34.35	51.38	2601.71	819.8	1	1	1	166.10	19.27	12.89	3.76	51.41
2	4	7.74	32.62	49.6	2431.48	794.19	3	1	2	166.50	19.36	12.97	3.78	51.55
3	14	4.78	45.93	54.84	2709.67	920.86	2	2	2	166.42	19.37	12.93	3.51	51.46
4	17	4.71	48.28	55.46	2707.15	926.62	2	2	3	166.18	19.38	12.93	3.46	51.40
5	10	4.12	54.27	55.9	2753.46	944.68	3	2	1	166.08	19.30	12.90	3.41	51.34
6	11	5.12	44.19	55.49	2799.09	932.42	2	2	1	166.05	19.34	12.89	3.40	51.34
7	7	6.86	31.73	49.81	2455.59	821.59	1	1	3	166.32	19.31	12.91	3.73	51.48
8	5	5.69	36.96	50.66	2435.66	812.89	2	1	2	166.43	19.35	12.97	3.77	51.60
9	8	14.82	32.43	50.34	2479.24	829.68	2	1	3	166.25	19.32	12.93	3.77	51.53
10	6	5.84	36.51	49.82	2390.9	830.44	1	1	2	166.48	19.37	12.99	3.75	51.60
11	16	4.92	44.2	54.51	2725.91	922.02	1	2	3	166.27	19.38	12.87	3.47	51.40
12	15	4.25	51.81	55.27	2797.93	938.89	1	2	2	166.42	19.35	12.85	3.48	51.46
13	18	4.94	41.54	54.9	2761.97	921.44	3	2	3	166.23	19.37	12.91	3.47	51.40
14	2	7.05	34.17	51.42	2385.83	841.45	2	1	1	166.08	19.27	12.87	3.73	51.43
15	1	5.1	34.62	50.62	2766.86	815.48	3	1	1	166.07	19.27	12.88	3.72	51.38
16	12	5.55	43.47	55.34	2789.13	921.98	1	2	1	166.08	19.38	12.89	3.40	51.32
17	9	5.91	36.69	48.99	2645.53	809.05	3	1	3	166.23	68.32	12.94	3.79	51.51

Table 5.12 4 months desiccant specimens tested in random order with testing results and measurements with respect to position, layout, and axis.

Order of Testing	Specimen	Tensile strain at Break	Tensile stress at Break	Ultimate Tensile Stress	E-Modulus	E-Modulus (1-3% Strain)	Position	Layout	Axis	Average Measurements (mm)				
		(%)	(MPa)	(MPa)	(MPa)	(MPa)				L	Wo	W	T	G
1	11	6.9	36.3	53.2	2665.8	904.4	2	2	1	166.09	19.28	12.95	3.40	51.36
2	1	11.4	32.1	49.6	2515.4	825.9	3	1	1	166.08	19.23	12.87	3.72	51.40
3	3	11.8	29.4	47.0	2482.9	797.7	1	1	1	166.14	19.25	12.84	3.78	51.44
4	18	8.1	36.4	53.3	2656.0	909.8	3	2	3	166.22	19.37	13.03	3.48	51.39
5	12	5.4	43.8	54.4	2760.2	915.9	1	2	1	166.09	19.27	12.93	3.39	51.34
6	8	10.3	32.6	49.1	2512.7	820.1	2	1	3	166.32	19.28	12.89	3.72	51.51
7	6	5.6	36.9	49.1	2404.6	822.4	1	1	2	166.44	19.32	12.93	3.73	51.60
8	4	6.5	34.3	50.3	2690.5	839.8	3	1	2	166.45	19.30	12.93	3.68	51.55
9	5	5.6	35.3	48.4	2501.6	814.5	2	1	2	166.48	19.31	12.94	3.78	51.62
10	10	6.7	37.7	54.3	2741.2	914.9	3	2	1	166.09	19.37	12.94	3.39	51.35
11	9	7.0	31.7	48.7	2382.5	812.8	3	1	3	166.27	19.28	12.90	3.77	51.49
12	7	8.6	33.1	48.7	2449.2	823.8	1	1	3	166.27	19.27	12.88	3.74	51.43
13	2	6.3	36.3	49.1	2575.7	802.5	2	1	1	166.10	19.24	12.84	3.75	51.42
14	15	4.2	48.9	53.9	2758.8	915.9	1	2	2	166.43	19.34	12.95	3.48	51.47
15	17	5.0	41.3	53.5	2668.9	901.2	2	2	3	166.26	19.34	13.05	3.47	51.41
16	13	5.3	41.7	54.3	2688.7	917.0	3	2	2	166.46	19.36	12.95	3.49	51.49
17	14	4.0	53.5	54.3	2745.9	923.4	2	2	2	166.43	19.37	12.95	3.49	51.49
18	16	4.4	52.1	54.8	2699.8	928.7	1	2	3	166.23	19.37	12.99	3.45	51.41

Table 5.13 4 months desiccant and 2 days conditioned at 23° and 50% relative humidity. Specimens tested in random order with testing results and measurements with respect to position, layout, and axis.

Order of Testing	Specimen	Tensile strain at Break	Tensile stress at Break	Ultimate Tensile Stress	E-Modulus	E-Modulus (1-3% Strain)	Position	Layout	Axis	Average Measurements (mm)				
		(%)	(MPa)	(MPa)	(MPa)	(MPa)				L	Wo	W	T	G
1	3	5.76	38.51	47.3	2379.28	803.95	1	1	1	166.13	19.30	12.91	3.76	51.41
2	14	4.99	43.29	51.66	2776.42	888.3	2	2	2	166.44	19.39	13.03	3.51	51.49
3	17	7.27	33.62	50.06	2686.86	865.37	2	2	3	166.16	19.48	13.06	3.53	51.41
4	10	5.33	36.41	51.37	2703.17	882.78	3	2	1	166.10	19.45	12.97	3.44	51.31
5	11	11.62	36.09	51.96	2660.51	894.57	2	2	1	166.09	19.40	13.05	3.43	51.37
6	7	12.03	30.15	46.07	2441.09	784.96	1	1	3	166.21	19.33	12.94	3.80	51.42
7	5	9.87	31.44	45.88	2375.41	779.09	2	1	2	166.46	19.39	13.00	3.82	51.59
8	8	20.34	31.01	45.02	2392.21	790.32	2	1	3	166.33	19.35	12.95	3.81	51.50
9	6	14.49	29.86	46.74	2333.97	811.97	1	1	2	166.44	19.38	12.97	3.74	51.61
10	17	18.4	34.29	50.85	2648.99	866.85	1	2	3	166.19	19.46	12.99	3.51	51.44
11	15	5.33	40.42	50.46	2615.39	864.46	1	2	2	166.45	19.48	13.02	3.50	51.49
12	18	14.53	33.38	49.36	2696.79	860.59	3	2	3	166.16	19.42	13.01	3.51	51.40
13	2	16.22	31.21	45.49	2348.45	777.24	2	1	1	166.07	19.30	12.92	3.80	51.42
14	1	14.91	29.6	45.32	2356.24	764.73	3	1	1	166.07	19.31	12.92	3.78	51.39
15	12	17.9	35.85	50.89	2574.72	879.86	1	2	1	166.07	19.35	12.95	3.44	51.34
16	9	9	31.34	46.54	2463.31	790.46	3	1	3	166.22	19.35	12.95	3.79	51.50
17	13	5.52	39.34	49.45	2531.08	849.53	3	2	2	166.46	19.38	13.01	3.54	51.51

Table 5. 14 Measurements of the three analysts.

		1			2			3			4			5			6			7			8		
Specimen		1			4			7			10			13			16			19			22		
Analyst		I	II	III	I	II	III	I	II	III	I	II	III	I	II	III	I	II	III	I	II	III	I	II	III
Flat	Lo	165.3	165.36	165.38	165.44	165.47	165.48	165.35	165.44	165.44	165.36	165.44	165.38	165.39	165.41	165.4	165.4	165.5	165.49	165.44	165.49	165.47	165.37	165.44	165.37
		165.36	165.38	165.4	165.43	165.52	165.48	165.42	165.44	165.45	165.42	165.4	165.43	165.34	165.44	165.45	165.42	165.43	165.47	165.43	165.48	165.51	165.35	165.44	165.38
		165.37	165.37	165.37	165.4	165.5	165.5	165.42	165.44	165.49	165.38	165.41	165.45	165.43	165.4	165.41	165.4	165.46	165.47	165.38	165.46	165.48	165.34	165.42	165.37
	Wo	19.15	19.21	19.19	19.15	19.2	19.18	19.16	19.19	19.17	19.13	19.19	19.17	19.15	19.19	19.18	19.09	19.19	19.17	19.16	19.21	19.23	19.2	19.22	19.19
		19.16	19.21	19.17	19.24	19.2	19.17	19.12	19.2	19.17	19.12	19.18	19.16	19.15	19.18	19.16	19.12	19.2	19.18	19.27	19.19	19.22	19.2	19.21	19.19
		19.15	19.21	19.18	19.17	19.19	19.17	19.16	19.2	19.17	19.14	19.2	19.15	19.14	19.2	19.25	19.18	19.2	19.21	19.17	19.19	19.24	19.18	19.22	19.21
	Wc	12.77	12.85	12.85	12.8	12.95	12.82	12.81	12.82	12.82	12.79	12.97	12.83	12.81	12.85	12.82	12.77	12.86	12.83	12.79	12.83	12.82	12.8	12.86	12.83
		12.8	12.94	12.87	12.81	12.82	12.83	12.85	12.82	12.82	12.8	12.82	12.83	12.79	12.82	12.82	12.79	12.82	12.83	12.8	12.9	12.82	12.77	12.86	12.84
		12.81	12.85	12.87	12.77	12.82	12.82	12.82	12.82	12.83	12.81	13.02	12.83	12.78	12.86	12.82	12.86	12.87	12.84	12.73	12.83	12.82	12.82	12.83	12.87
	T	3.42	3.49	3.49	3.45	3.56	3.53	3.44	3.51	3.51	3.52	3.6	3.56	3.4	3.65	3.57	3.41	3.59	3.58	3.45	3.5	3.37	3.42	3.54	3.51
		3.45	3.52	3.52	3.46	3.53	3.51	3.45	3.52	3.55	3.39	3.57	3.58	3.51	3.58	3.57	3.42	3.58	3.58	3.47	3.57	3.53	3.38	3.52	3.5
		3.45	3.52	3.53	3.43	3.5	3.51	3.53	3.49	3.52	3.42	3.57	3.55	3.43	3.58	3.58	3.45	3.6	3.58	3.49	3.58	3.51	3.51	3.55	3.51
	G	51.05	51.07	51.11	51.05	51.1	51.1	51.13	51.12	51.1	51.09	51.07	51.12	51.1	51.12	51.11	51.02	51.1	51.13	51.09	51.09	51.16	51.06	51.08	51.1
		51.05	51.09	51.08	51.01	51.08	51.1	51.1	51.08	51.12	51.1	51.1	51.14	51.12	51.06	51.11	51.12	51.08	51.13	51.12	51.09	51.16	51.05	51.07	51.12
		51.05	51.07	51.1	51.05	51.08	51.11	51.08	51.12	51.11	51.04	51.1	51.12	51.08	51.07	51.12	51.1	51.12	51.12	51.06	51.13	51.14	51.06	51.06	51.1
Specimen		2			5			8			11			14			17			20			23		
On an Edge	Lo	165.44	165.45	165.47	165.48	165.48	165.46	165.49	165.49	165.48	165.48	165.44	165.48	165.5	165.45	165.47	165.48	165.48	165.49	165.46	165.52	165.46	165.43	165.46	165.45
		165.49	165.48	165.46	165.51	165.49	165.5	165.51	165.48	165.48	165.46	165.52	165.46	165.5	165.47	165.47	165.5	165.49	165.47	165.46	165.49	165.46	165.5	165.47	165.46
		165.49	165.46	165.47	165.45	165.48	165.47	165.44	165.54	165.49	165.48	165.47	165.47	165.48	165.5	165.45	165.46	165.54	165.49	165.44	165.47	165.47	165.43	165.44	165.45
	Wo	19.2	19.38	19.29	19.2	19.32	19.22	19.23	19.33	19.29	19.19	19.32	19.23	19.22	19.38	19.43	19.16	19.44	19.27	19.19	19.29	19.24	19.18	19.32	19.25
		19.26	19.39	19.32	19.18	19.36	19.21	19.19	19.28	19.29	19.18	19.32	19.26	19.21	19.32	19.26	19.16	19.37	19.24	19.19	19.33	19.22	19.23	19.27	19.26
		19.16	19.32	19.33	19.18	19.36	19.26	19.17	19.3	19.3	19.16	19.36	19.26	19.19	19.4	19.32	19.18	19.44	19.27	19.18	19.34	19.22	19.21	19.31	19.25
	Wc	12.84	12.91	12.89	12.92	13.08	12.88	12.86	12.9	12.89	12.86	12.93	12.89	12.9	13.08	12.88	12.86	12.89	12.96	12.85	13.21	12.92	12.88	13.02	12.95
		12.91	12.9	12.93	12.83	12.89	13.1	12.86	12.92	12.88	12.84	13.05	12.92	12.82	12.94	12.88	12.84	12.91	12.98	12.9	12.91	12.9	12.9	12.95	12.94
		12.83	12.9	12.89	12.87	12.89	12.88	12.83	12.94	12.88	12.87	12.95	12.9	12.87	12.99	12.89	12.85	12.92	12.99	12.83	13.16	12.91	12.86	12.98	13.02
	T	3.42	3.47	3.46	3.44	3.55	3.45	3.51	3.46	3.45	3.4	3.44	3.43	3.41	3.43	3.45	3.4	3.57	3.45	3.4	3.45	3.46	3.42	3.46	3.45
		3.43	3.45	3.46	3.4	3.45	3.45	3.4	3.44	3.45	3.35	3.44	3.44	3.39	3.51	3.45	3.4	3.49	3.45	3.48	3.47	3.45	3.44	3.43	3.45
		3.39	3.45	3.46	3.42	3.45	3.45	3.37	3.43	3.45	3.38	3.44	3.45	3.5	3.45	3.44	3.49	3.51	3.45	3.4	3.45	3.46	3.42	3.46	3.45
	G	51.01	51.02	51.03	51.03	51.04	51.02	50.95	50.99	51.04	51	51.01	51.02	50.98	51	51.03	51	51.01	51.03	51	51.02	51	50.97	51	50.99
		51	51.02	51.01	51.02	51.03	51.03	51.01	51.05	51.03	50.99	51.03	51.01	50.98	51.04	51.04	50.98	51.02	51.01	50.99	51	51.01	50.96	51	51
		50.95	50.98	51.02	50.99	51.03	51.03	51.01	51.03	51.03	50.99	51.02	51.02	51	51.03	51.03	50.97	51.02	51	50.94	51.01	51.01	50.95	51	50.98
Specimen		3			6			9			12			15			18			21			24		
Vertical	Lo	164.94	164.96	164.97	164.91	164.98	164.99	164.91	165.07	165.07	165.03	165.22	165.17	165.07	165.17	165.14	165.14	165.23	165.16	164.91	165.15	164.99	165.1	165.2	165.1
		164.92	165.08	164.96	164.9	165.13	165	164.99	165.05	165.08	165	165.11	165.08	165.09	165.09	165.25	165.06	165.11	165.13	165.02	165.11	164.98	164.98	165.09	165.08
		164.94	164.99	165.06	164.91	165.01	165.21	164.99	165.07	165.08	165.01	165.09	165.18	165.03	165.16	165.15	165.04	165.1	165.1	164.95	165.01	165.09	164.94	165.08	165.25
	Wo	19.1	19.19	19.19	19.17	19.19	19.19	19.26	19.18	19.17	19.15	19.19	19.18	19.14	19.18	19.18	19.15	19.18	19.17	19.12	19.18	19.16	19.12	19.15	19.14
		19.14	19.19	19.18	19.3	19.18	19.18	19.17	19.19	19.19	19.17	19.17	19.17	19.14	19.15	19.2	19.22	19.16	19.19	19.13	19.18	19.17	19.09	19.15	19.2
		19.16	19.18	19.18	19.13	19.18	19.19	19.16	19.15	19.18	19.17	19.19	19.21	19.14	19.18	19.2	19.15	19.18	19.18	19.13	19.17	19.15	19.07	19.17	19.16
	Wc	12.79	12.97	12.86	12.86	12.88	12.87	12.82	12.98	12.86	12.82	12.87	12.85	12.81	12.84	12.86	12.82	12.84	12.84	12.83	12.85	12.84	12.83	12.96	12.84
		12.83	12.91	12.91	12.86	12.87	12.87	12.84	12.9	12.85	12.78	12.85	12.85	12.85	12.84	12.85	12.98	12.85	12.85	12.83	12.85	12.85	12.8	12.84	12.84
		12.82	12.85	12.86	12.87	12.9	12.87	12.84	12.86	12.85	12.81	12.85	12.85	12.83	12.91	12.85	12.83	12.84	12.84	12.8	12.85	12.83	12.81	12.84	12.85
	T	3.42	3.45	3.44	3.41	3.42	3.43	3.36	3.44	3.43	3.38	3.43	3.41	3.38	3.51	3.43	3.4	3.44	3.44	3.42	3.45	3.43	3.49	3.49	3.48
		3.43	3.45	3.45	3.41	3.44	3.42	3.42	3.47	3.44	3.37	3.42	3.42	3.38	3.45	3.44	3.38	3.43	3.43	3.43	3.5	3.43	3.45	3.6	3.49
		3.43	3.45	3.45	3.41	3.48	3.42	3.42	3.45	3.44	3.38	3.43	3.42	3.41	3.52	3.43	3.42	3.45	3.45	3.42	3.45	3.43	3.46	3.59	3.5
	G	50.96	50.97	50.96	50.87	50.92	50.93	50.83	50.85	50.84	50.88	50.87	50.88	50.87	50.87	50.95	50.86	50.88	50.89	50.87	50.91	50.93	50.94	50.95	50.94
		50.97	50.96	50.97	50.79	50.93	50.93	50.82	50.83	50.85	50.85	50.88	50.87	50.9	50.94	50.96	50.85	50.9	50.9	50.92	50.93	50.94	50.92	50.93	50.96
		50.94	50.99	50.98	50.81	50.91	50.93	50.83	50.83	50.83	50.85	50.88	50.87	50.88	50.97	50.95	50.88	50.89	50.9	50.92	50.94	50.94	50.87	50.93	50.95

5.3 ANALYSIS

The following analysis was done on the effects of the build orientation for the first build setup in Figure 3.1 in regards to the mechanical properties and the effects of the environmental and aging conditions for the 18 Type I specimens. The effects of the build orientation on the mechanical properties for the 24 Type I specimens, shown in Figure 3.2. An analysis was developed to determine the ability of the RP technology to build consistent 3D parts. This is to find out the variability on the specimens, the different analyst, and the instrument that was used for measuring. Three analyst measured the 24 specimens, built on the Viper Si^2, three times at a selective region (gage length, width of the narrow section, thickness, overall width, and overall length) giving a total of 1,080 measurements. Before making the measurements, the caliper used was examined for accuracy by measuring two gage blocks of 50 and 25 mm for every 50 specimen measurements. Other than the analysts, there was another person that read the randomized order, as shown in Tables 5.1 to 5.13, of the specimens to be measured and gathered the data from the analyst. The randomization was done using Microsoft® Excel. The analysis was carried out with 5% level of significance using Statgraphics® software.

5.3.1 Effects of Build Orientation of First Build Setup on Mechanical Properties

The results gathered from the tensile testing in Table 5.1 were analyzed for the effects of the build orientation factors (axis, position and layout) on the ultimate tensile stress and E-Modulus (1-3% strain). Table 5.15 and Table 5.17 demonstrate the mean of the ultimate tensile stress and E-Modulus (1-3% strain) respectively for each of the factors. It demonstrates the standard error

of every respective mean that was evaluated from its sampling variability. The 95.0% confidence interval for each of the factor means is demonstrated on the lower and upper limit columns.

Multifactor ANOVA was employed for the ultimate tensile stress and E-Modulus (1-3% strain) variables through the levels of position, layout and axis. Tables 5.16 and 5.18 show the variability of the ultimate tensile stress and E-Modulus (1-3% Strain) composed in contribution to the factors (position, layout and axis). The F-ration are established by the residual mean square error.

Table 5.15 Least squares means for ultimate tensile stress with 95.0 percent confidence intervals.

Level	Count	Mean	Stnd. Error	Lower Limit	Upper Limit
Position					
1	6	48.4356	0.2045	47.99	48.8811
2	6	48.2699	0.2045	47.8243	48.7155
3	6	48.2487	0.2045	47.8031	48.6942
Layout					
1	9	48.0306	0.166973	47.6668	48.3944
2	9	48.6055	0.166973	48.2417	48.9693
Axis					
1	6	48.2884	0.2045	47.8428	48.7339
2	6	48.32328	0.2045	47.8772	48.7684
3	6	48.343	0.2045	47.8974	48.7885
Grand Mean	18	48.318			

Table 5.16 Analysis of variance for Ultimate Tensile Stress – Type III sums of squares.

Source	Sum of Squares	Df	Mean Square	F-Ratio	P-Value
Position	0.125652	2	0.0628258	0.25	0.7825
Layout	1.48715	1	1.48715	5.93	0.0315
Axis	0.0091516	2	0.0045758	0.02	0.982
Residual	3.01105	12			
Total (corrected)	4.633	17			

Table 5.17 Least squares means for E-Modulus (1-3% Strain) with 95.0 percent confidence intervals.

Level	Count	Mean	Stnd. Error	Lower Limit	Upper Limit
Position					
1	6	847.512	4.38702	837.954	857.071
2	6	842.329	4.38702	832.77	851.887
3	6	842.149	4.38702	832.591	851.708
Layout					
1	9	837.281	3.58198	829.477	845.086
2	9	850.712	3.58198	842.908	858.517
Axis					
1	6	844.441	4.38702	834.882	853.999
2	6	842.51	4.38702	832.951	852.068
3	6	845.04	4.38702	835.482	854.599
Grand Mean	18	843.997			

Table 5.18 Analysis of variance for E-Modulus (1-3% Strain) – Type III sums of squares.

Source	Sum of Squares	Df	Mean Square	F-Ratio	P-Value
Position	111.332	2	55.666	0.48	0.629
Layout	811.744	1	811.744	7.03	0.0211
Axis	20.981	2	10.4905	0.09	0.9138
Residual	1385.71	12	115.475		
Total (corrected)	2329.76	17			

To determine what means are significantly different from which means, a multiple range test was done. Tables 5.19 through 5.24 give a comparison to find out the difference in means on position, axis, and layout on ultimate tensile stress and E-Modulus (1-3% strain). The tables demonstrate the difference between each of the means. The homogeneous groups containing an X developed a group of means in such a way that there was no statistically significant difference. The multiple ranges were employed to discriminate the Fisher's least significant difference (LSD). This test can prove that there is a 5.0% risk of identifying each pair of means significantly different when the actual difference equals 0.

To show what factor has a statistically significant effect on the variable (ultimate tensile stress and E-Modulus (1-3% strain)), Figures 5.1 and 5.2 demonstrate the means and 95.0% confidence ultimate tensile stress and E-Modulus (1-3% strain) by position, respectively. This is shown because the blue lines that include the least significant difference overlap. Figure 5.3 and 5.4 show the means 95.0% confidence ultimate tensile stress and E-Modulus (1-3% strain) by axis respectively. The graphs demonstrate that there are no statistically significant differences between the mean values of ultimate tensile stress and E-Modulus (1-3% strain) from either position or axis to another at a level of confidence of 95.0%. On the other hand, Figures 5.5 and 5.6 and Table 5.23 and 5.24 demonstrate that there is a statically significant difference between the mean values on both the ultimate tensile stress and E-Modulus (1-3% strain) from one level of layout to another at a level of confidence of 95.0%. The differences in means are shown in Tables 5.23and 5.24 and are clearly illustrated in Figure 5.3.

Table 5.19 Multiple Range test for ultimate tensile stress by position.

Position	Count	LS Mean	LS Sigma	Homogeneous Groups
3	6	48.2487	0.2045	X
2	6	48.2699	0.2045	X
1	6	48.4356	0.2045	X
Contrast			**Difference**	**−/+ Limits**
1−2			0.165662	0.674575
1−3			1.186898	0.674575
2−3			0.0212359	0.674575

Table 5.20 Multiple range test for E-Modulus (1-3% Strain) by position.

Position	Count	LS Mean	LS Sigma	Homogeneous Groups
3	6	842.149	4.38702	X
2	6	842.329	4.38702	X
1	6	847.512	4.38702	X
Contrast			**Difference**	**−/+ Limits**
1−2			5.18379	13.5178
1−3			5.36304	13.5178
2−3			0.179243	13.5178

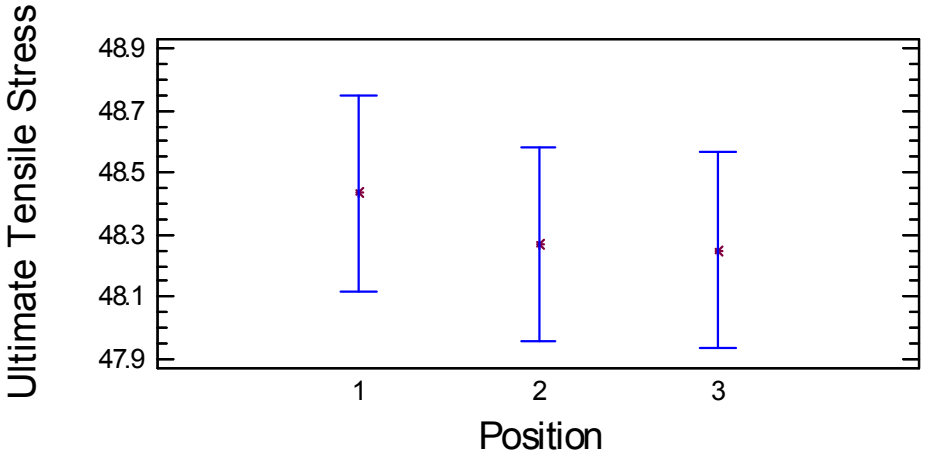

Figure 5.1 Means and 95% confidence ultimate tensile stress by position intervals.

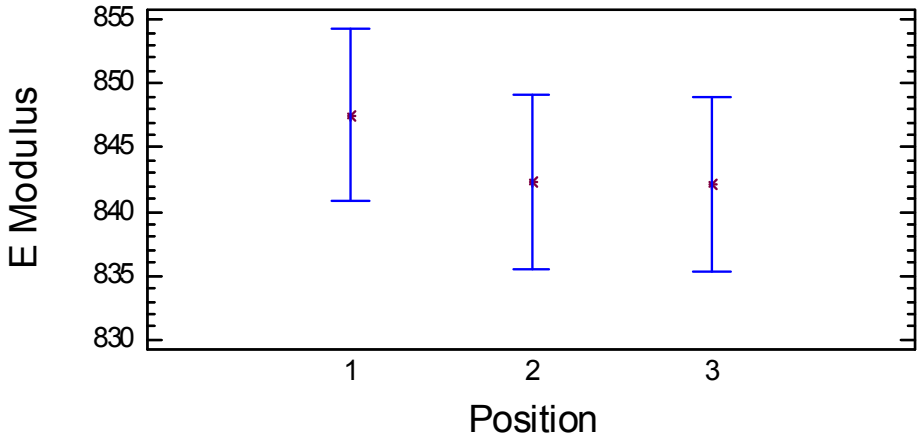

Figure 5.2 Means and 95% confidence E-Modulus (1-3% Strain).

Table 5.21 Multiple range test for ultimate tensile stress by axis.

Axis	Count	LS Mean	LS Sigma	Homogeneous Groups
1	6	48.2884	0.226663	X
2	6	48.3228	0.226663	X
3	6	48.343	0.226663	X
Contrast			**Difference**	**−/+ Limits**
1−2			-0.0344467	0.683237
1−3			-0.0546127	0.683237
2−3			-0.020166	0.683237

Table 5.22 Multiple range test for E-Modulus (1-3% Strain) by axis.

Axis	Count	LS Mean	LS Sigma	Homogeneous Groups
1	6	844.441	5.06489	X
2	6	842.51	5.06489	X
3	6	845.04	5.06489	X
Contrast			**Difference**	**−/+ Limits**
1−2			1.93086	15.2673
1−3			-0.599529	15.2673
2−3			-2.53039	15.2673

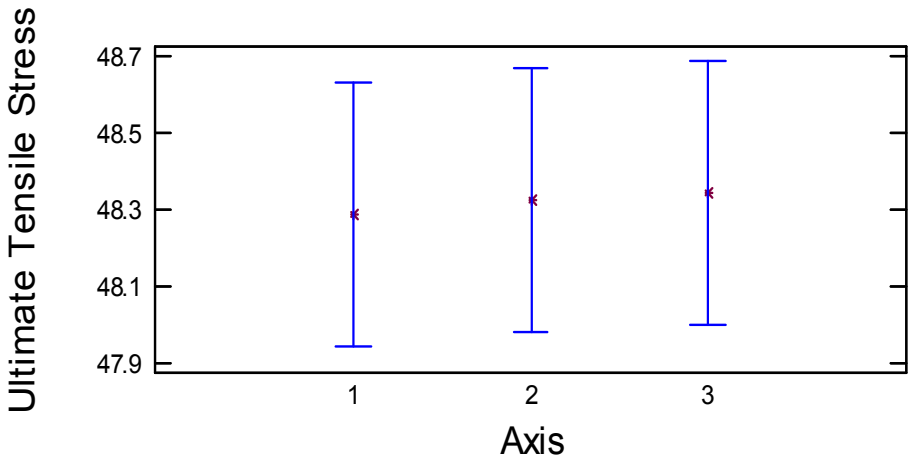

Figure 5.3 Means and 95% confidence ultimate tensile stress by axis intervals.

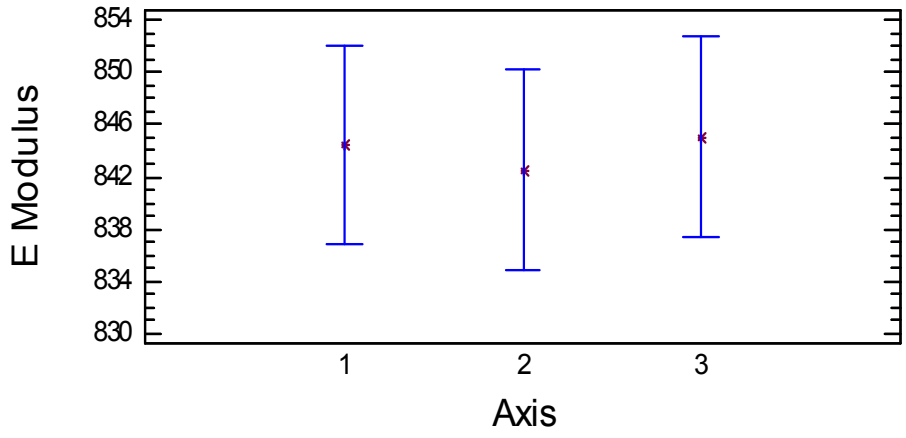

Figure 5.4 Means and 95% confidence E-Modulus (1-3% Strain) by axis intervals.

Table 5.23 Multiple range test for ultimate tensile test by layout.

Layout	Count	LS Mean	LS Sigma	Homogeneous Groups
1	9	48.0306	0.147805	X
2	9	48.6055	0.147805	X
Contrast			**Difference**	**−/+ Limits**
1−2			*-0.574872	0.443119

Table 5.24 Multiple range test for E-Modulus (1-3% Strain) by layout.

Layout	Count	LS Mean	LS Sigma	Homogeneous Groups
1	9	837.281	3.24681	X
2	9	850.712	3.24681	X
Contrast			**Difference**	**−/+ Limits**
1−2			*-13.4308	9.73396

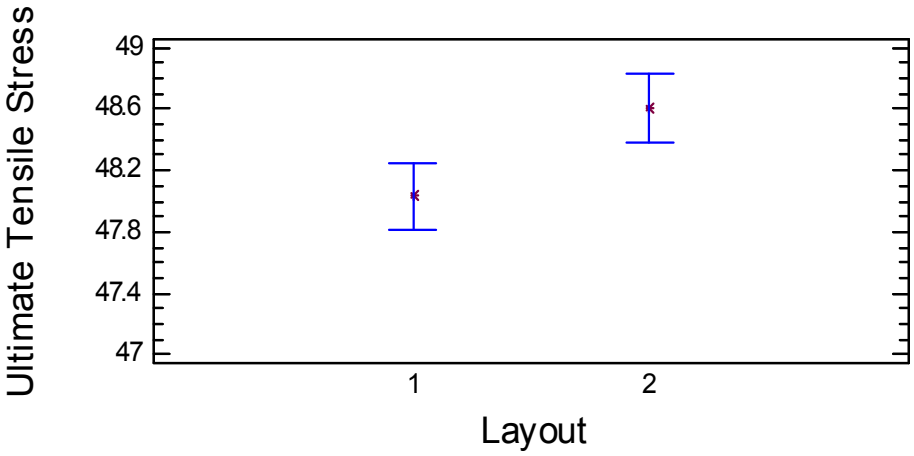

Figure 5.5 Means and 95% confidence ultimate tensile stress by layout intervals.

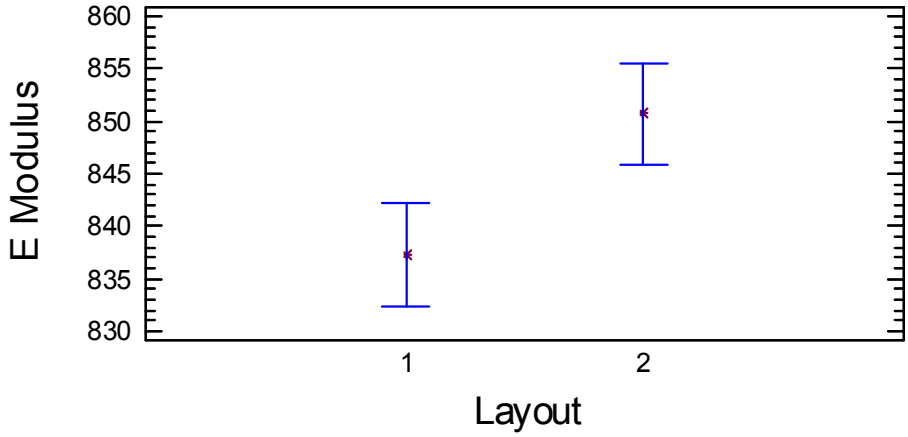

Figure 5.6 Means and 95% confidence E-Modulus (1-3% Strain) by layout intervals.

The null hypothesis is tested by the Chochran's, Bartlett's, Hartley's, and Levene's statistics on Tables 5.25 and 5.26 to demonstrate that the variables E-Modulus (1-3% Strain) and ultimate tensile stress within each of the levels of each of the factors are the same (Montgomery, 2001). Given that the minimum value of the P-Value is greater than or equal to 0.05, there is not a statistically significant difference among the standard deviations at the 95.0% confidence levels (Quintana *et al.*, 2007).

Table 5.25 Variance check on E-Modulus (1-3% Strain) by factor.

Variable	Position		Layout		Axis	
Test	Result	P-Value	Result	P-Value	Result	P-Value
Cochran's C	0.792199	0.0102567	0.581576	0.652453	0.644052	0.118842
Bartlett's	1.64263	0.0327656	1.01358	0.652199	1.22144	0.252139
Hartley's	8.98335	-	1.38992	-	3.85366	-
Levene's	4.1458	0.0368713	0.492572	0.492866	0.633125	0.544538

Table 5.26 Variance check on E-Modulus (1-3% Strain) by factor.

Variable	Position		Layout		Axis	
Test	Result	P-Value	Result	P-Value	Result	P-Value
Cochran's C	0.42136	0.858304	0.691264	0.275288	0.473777	0.601257
Bartlett's	1.06735	0.638287	1.08232	0.275082	1.05905	0.673552
Hartley's	2.30937	-	2.23902	-	2.31481	-
Levene's	0.703578	0.510428	1.20908	0.287784	0.868366	0.439698

5.3.2 Effects on Mechanical Properties Based on Aging

The mechanical properties of the build setup of 18 Type I tensile specimens were mechanically tested under different aging conditions (4 days, 1 month and 4 months) based on the different environmental conditions (ambient, desiccant, and desiccant and 23±3°C and 50±5% RH). Table 5.27 shows that there is a statistically significant difference between the mean values of the E-Modulus for four days to a month as compared to the other two time periods at a 95% confidence level. For the ultimate tensile stress, all are statistically significantly different from one another. These results are graphically supported in Figures 5.7 and 5.8.

Table 5.27 Multiple range test for E-Modulus (1-3 % strain) and ultimate tensile stress by aging in ambient condition.

Age	Count	*E Modulus (1-3% strain)*			*UTS*		
		LS Mean	LS Sigma	Homogeneous Groups	LS Mean	LS Sigma	Homogeneous Groups
4	17	785.978	10.9469	X	45.7165	0.500894	X
30	17	870.793	10.9459	X	52.6088	0.500894	X
120	17	873.112	10.9469	X	54.2359	0.500894	X
Contrast			**Difference**	**−/+ Limits**		**Difference**	**−/+ Limits**
4−30			*-87.1341	31.1272		*-8.51941	
4−120			*-84.8153	31.1272		*-6.89235	
30−120			2.31882	31.1272		*1.62706	

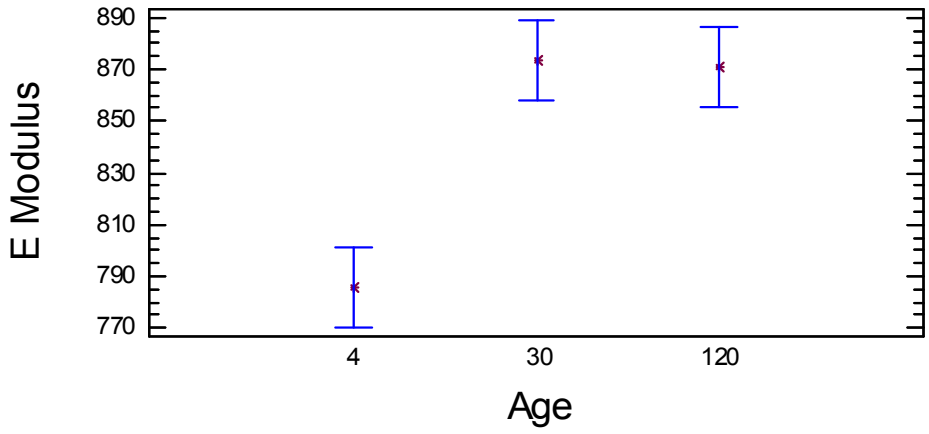

Figure 5.7 Means and 95% confidence for ambient E-Modulus (1-3% Strain) by aging in 4 days, 30 days, and 120 days intervals.

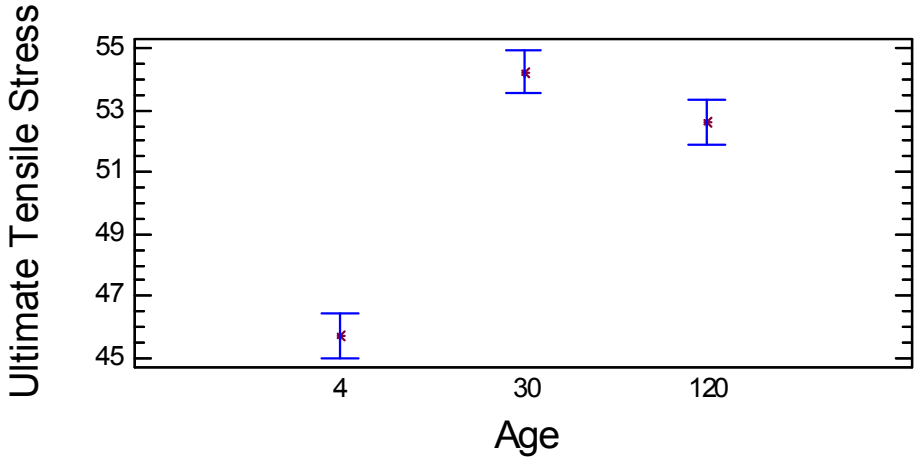

Figure 5.8 Means and 95% confidence for ambient ultimate tensile stress by aging in 4 days, 30 days, and 120 days intervals.

The study of the 18 specimens under the desiccant condition were analyzed and showed that four days was statistically significant different to one month and four months under both the E-Modulus (1-3% strain) and ultimate tensile strength as can be seen in Table 5.28. This conclusion is also illustrated graphically in Figure 5.9 for E-Modulus and 5.10 for ultimate tensile stress.

Table 5.28 Multiple range test for E-Modulus (1-3 % Strain) and ultimate tensile stress by aging in desiccant condition.

Age	Count	*E Modulus (1-3% strain)*			*UTS*		
		LS Mean	**LS Sigma**	**Homogeneous Groups**	**LS Mean**	**LS Sigma**	**Homogeneous Groups**
4	18	794.523	9.90934	X	44.6806	0.4778	X
30	18	839.244	9.90934	X	52.09	0.4778	X
120	18	866.15	9.90934	X	51.4444	0.4778	X
Contrast			**Difference**	**−/+ Limits**		**Difference**	**−/+ Limits**
4−30			*-44.7206	28.1342		*-7.40944	1.35655
4−120			*-71.6267	28.1342		*-6.76389	1.35655
30−120			-26.9061	28.1342		0.645556	1.35655

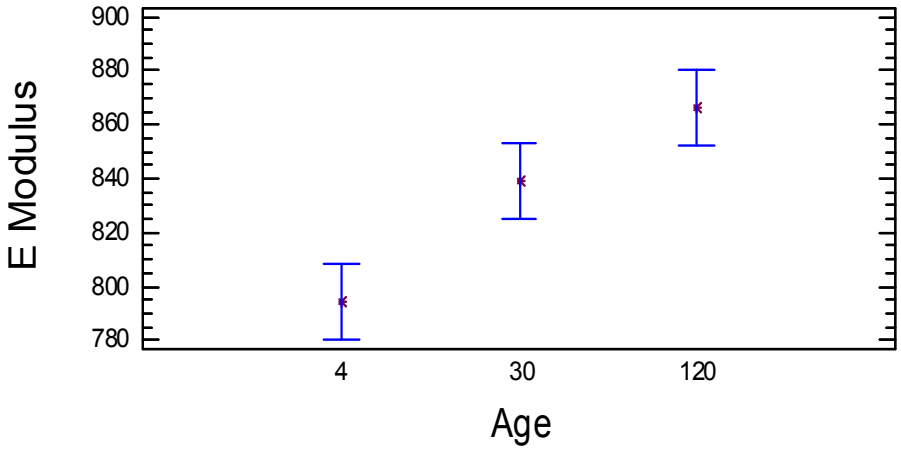

Figure 5.9 Means and 95% confidence for desiccant, E-Modulus (1-3% Strain) by aging in 4 days, 30 days, and 120 days intervals.

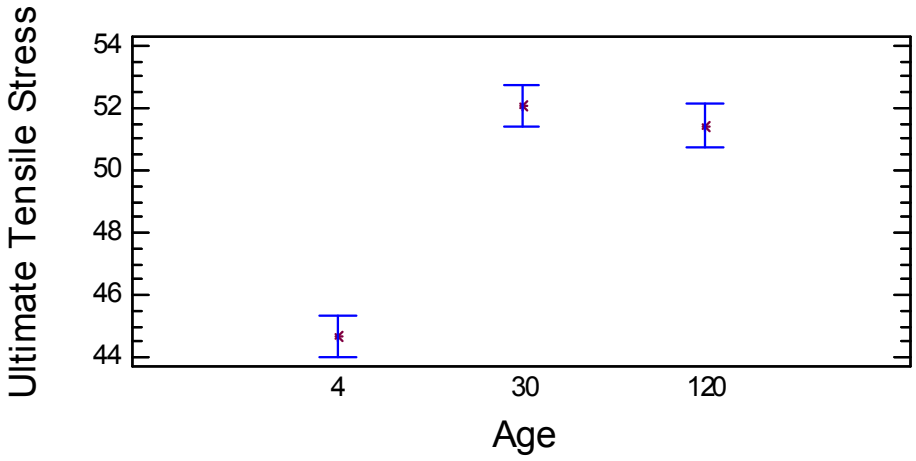

Figure 5.10 Means and 95% confidence for desiccant, ultimate tensile stress by aging in 4 days, 30 days, and 120 days intervals.

The build setup of the 18 specimens was also studied under the condition of desiccant for every aging condition and 23±3°C and 50±5% relative humidity for two full days. The ultimate tensile strength showed that all of the aging conditions are statistically significantly different and for the E-Modulus four days is statistically significantly different to one month and four months as shown in Table 5.29. Figure 5.11 graphically supports the results from the table for E-Modulus and so does Figure 5.12 for ultimate tensile stress.

Table 5.29 Multiple range test for E-Modulus (1-3 % Strain) and ultimate tensile stress by aging in a temperature of 23 ± 2° and 50 ± 5% RH condition.

Age	Count	*E Modulus (1-3% strain)*			*UTS*		
		LS Mean	LS Sigma	Homogeneous Groups	LS Mean	LS Sigma	Homogeneous Groups
4	17	787.815	9.65656	X	45.9394	0.519129	X
30	17	857.472	9.65656	XX	51.3165	0.519129	X
120	17	832.649	9.65656	X	48.4953	0.519129	X
Contrast			**Difference**	**–/+ Limits**		**Difference**	**–/+ Limits**
4−30			*-69.6565	27.4582		*-5.37706	1.47613
4−120			*-44.8335	27.4582		*-2.55588	1.47613
30−120			24.8229	27.4582		*2.82118	1.47613

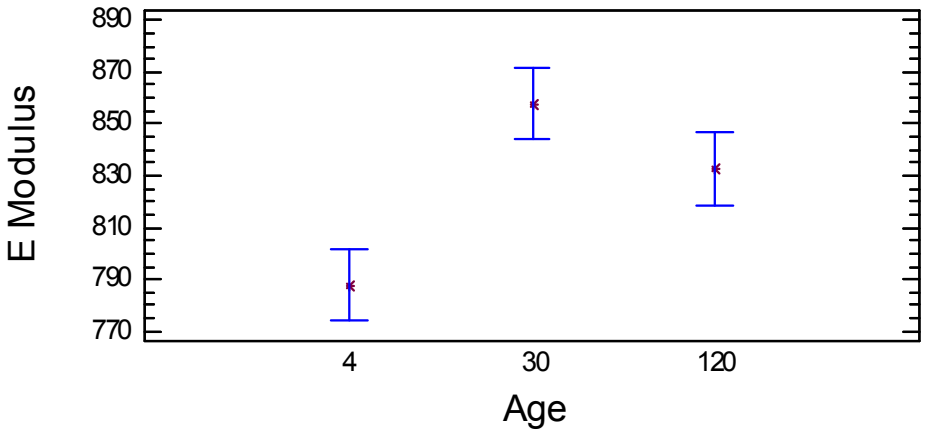

Figure 5.11 Means and 95% confidence for a condition at a temperature of 23 ± 2° and 50±5% RH, E-Modulus (1-3% Strain) by aging in 4 days, 30 days, and 120 days intervals.

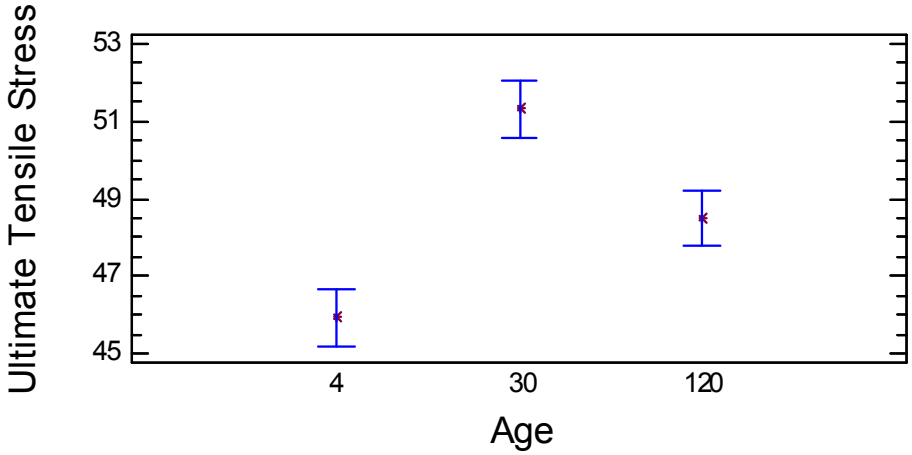

Figure 5.12 Means and 95% confidence for a condition at a temperature of 23 ± 2° and 50±5% RH, ultimate tensile stress by aging in 4 days, 30 days, and 120 days intervals.

The null hypothesis of the medians for the ultimate tensile stress and E-Modulus with respect to the aging levels, states that there is a statistically significant difference since the P-Value is less than 0.05 in all the cases as can be seen in Table 5.30 and Table 5.31.

Table 5.30 Kruskal Wallis test for ultimate tensile stress by aging.

Age	*Ambient*		*Desiccant*		*23°C and 50%*	
	Sample Size	**Average Rank**	**Sample Size**	**Average Rank**	**Sample Size**	**Average Rank**
4	17	9	18	9.55556	17	13.3824
30	17	37.9412	18	38	17	38.9412
120	17	31.0588	18	34.9444	17	25.6765
Test Statistic	35.1695		35.482		25.1383	
P-Value	2.30691E-08		1.97325E-08		3.47758E-06	

Table 5.31 Kruskal Wallis test for E-Modulus (1-3% Strain) by aging.

Age	*Ambient*		*Desiccant*		*23° and 50%*	
	Sample Size	**Average Rank**	**Sample Size**	**Average Rank**	**Sample Size**	**Average Rank**
4	17	12.2353	18	16	17	14.6471
30	17	33.7647	18	29.8889	17	36.0588
120	17	32	18	36.6111	17	27.2941
Test Statistic	21.9814		16.0711		17.8265	
P-Value	0.000016858		0.000323747		0.000135	

For the variance check in Tables 5.32 and 5.33, ambient and desiccant plus two days conditioned (23°C and 50% RH) are statistically significantly different based on the four statistics because the P-Value is greater than 0.05.

Table 5.32 Variance check ultimate tensile stress by aging.

Factor	*Ambient*		*Desiccant*		*23°C and 50%*	
Test	**Result**	**P-Value**	**Result**	**P-Value**	**Result**	**P-Value**
Cochran's C	0.53353	0.0679466	0.603726	0.008321	0.462817	0.279025
Bartlett's	1.0888	0.137148	1.16051	0.024741	1.04493	0.358324
Hartley's	2.56028	–	3.09068	–	2.06752	–
Levene's	3.77072	0.0301286	13.007	2.726E-05	1.54935	0.222819

Table 5.33 Variance check E-Modulus (1-3% Strain) by aging.

Factor	*Ambient*		*Desiccant*		*23° and 50%*	
Test	**Result**	**P-Value**	**Result**	**P-Value**	**Result**	**P-Value**
Cochran's C	0.538126	0.0610829	0.48914	0.157390	0.442101	0.391937
Bartlett's	1.08973	0.134438	1.0686	0.192263	1.03819	0.41681
Hartley's	2.45909	–	2.45892	–	1.96779	–
Levene's	3.53337	0.030702	5.83744	0.0052138	1.50334	0.23267

5.3.3 Effects on Mechanical Properties Based on Conditioning

For this study, the effect of mechanical properties on different conditions, 1) being ambient 2) desiccant 3) desiccant and two days at 23±3°C and 50±5% RH, is analyzed with a build setup of 18 tensile specimens. Desiccant is statistically significantly different to desiccant plus two days 23±3°C and 50±5% relative humidity condition only for the ultimate tensile stress which is shown in Table 5.34 and illustrated in Figure 5.13. However, there was no significance in the E-Modulus as shown in Figure 5.14.

Table 5.34 Multiple range test for ultimate tensile stress and E-Modulus (1-3 % Strain) by condition (ambient, desiccant, and a temperature of 23° and 50% RH) in 4 days.

Condition	Count	*Ultimate Tensile Stress*			*E Modulus (1-3% strain)*		
		LS Mean	LS Sigma	Homogeneous Groups	LS Mean	LS Sigma	Homogeneous Groups
1	17	45.7165	0.42952	XX	785.978	8.97197	X
2	18	44.6806	0.417418	X	794.523	8.71919	X
3	17	45.9394	0.42952	X	787.815	8.97197	X
Contrast			**Difference**	**–/+ Limits**		**Difference**	**–/+ Limits**
1–2			1.03592	1.20361		-8.54569	25.1415
1–3			-0.222941	1.22068		-1.83765	25.4981
2–3			*-1.25886	1.20361		6.70804	25.1415

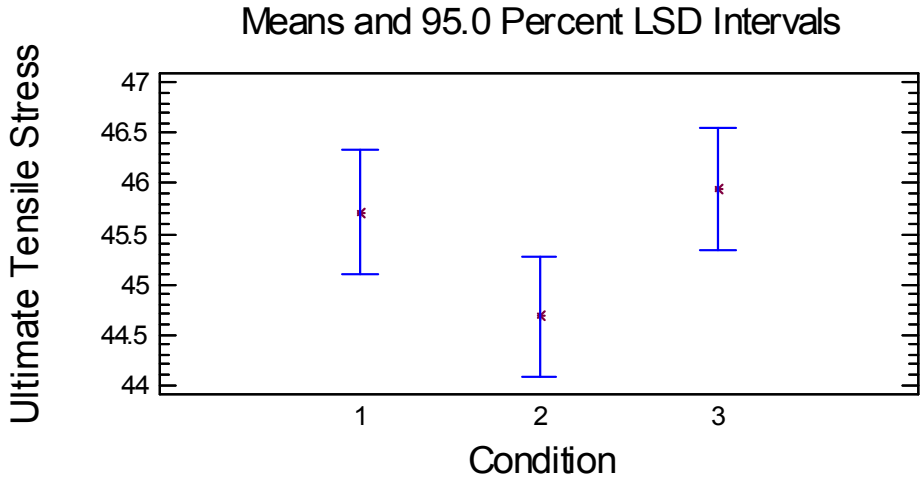

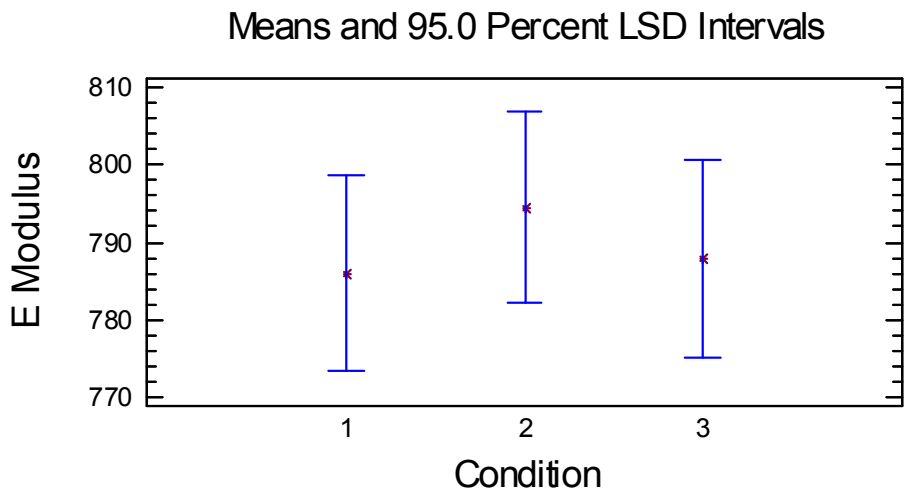

Figure 5.14 Means and 95% confidence for 4 days, E-Modulus (1-3% Strain) by condition intervals.

A similar study was performed for one month and showed that ambient is statistically significantly different to desiccant and desiccant plus two days at 23±3°C and 50±5% relative humidity condition for the ultimate tensile strength. On the E-Modulus, ambient is statistically significantly different to desiccant and this is displayed in both Table 5.35 and Figure 5.15 for ultimate tensile stress and Figure 5.16 for E-Modulus.

Table 5.35 Multiple range test for ultimate tensile stress and E-Modulus (1-3 % Strain) by condition (ambient, desiccant, and a temperature of 23° and 50% relative humidity) in 1 month.

Condition	Count	*Ultimate Tensile Stress*			*E Modulus (1-3% strain)*		
		LS Mean	LS Sigma	Homogeneous Groups	LS Mean	LS Sigma	Homogeneous Groups
1	17	54.2359	0.414331	X	873.112	8.94243	X
2	18	52.09	0.402657	X	839.244	8.69048	X
3	17	51.3165	0.414331	X	857.472	8.94243	XX
Contrast			**Difference**	**–/+ Limits**		**Difference**	**–/+ Limits**
1–2			*2.14588	1.16105		*33.8679	25.0587
1–3			*2.91941	1.17752		15.64	25.4141
2–3			0.773529	1.16105		-18.2279	25.0587

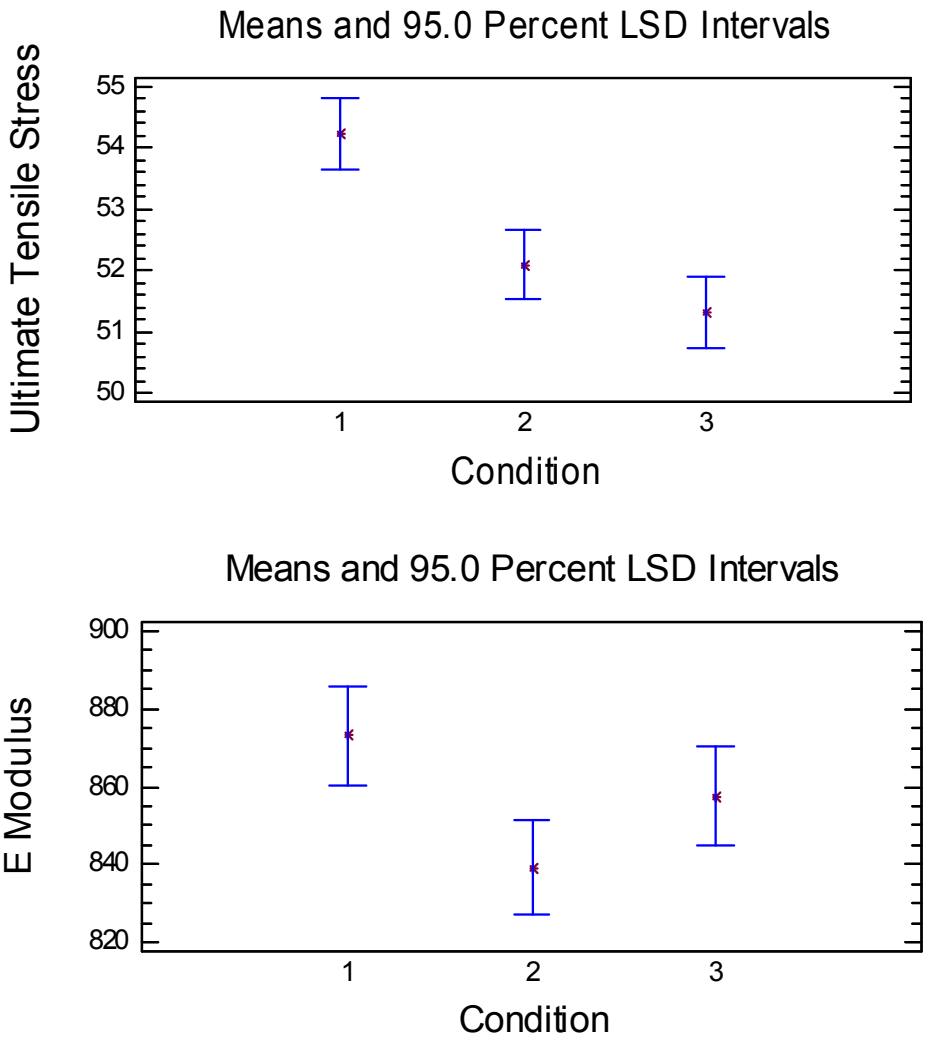

Figure 5.16 Means and 95% confidence for 1 month, E-Modulus (1-3% Strain) by condition intervals.

Table 5.36 demonstrates the analysis of 4 months in the different environmental conditions, showing that desiccant plus two days at 23±3°C and 50±5% RH is statically significantly different to ambient and desiccant on the ultimate tensile stress. For E-Modulus ambient is statically significantly different to desiccant and two days at 23±3°C and 50±5% RH. This is also supported by Figure 5.17 and 5.18 for ultimate tensile stress and E-Modulus, respectively.

Table 5.36 Multiple range test for ultimate tensile stress and E-Modulus (1-3 % Strain) by condition (ambient, desiccant, and a temperature of 23° and 50% RH) in 4 months.

Condition	Count	*Ultimate Tensile Stress*			*E Modulus (1-3% strain)*		
		LS Mean	LS Sigma	Homogeneous Groups	LS Mean	LS Sigma	Homogeneous Groups
1	17	52.6088	0.636553	X	870.793	12.5095	X
2	18	51.4444	0.618618	X	866.15	12.157	XX
3	17	48.4953	0.636553	X	832.649	12.5095	X
Contrast			**Difference**	**−/+ Limits**		**Difference**	**−/+ Limits**
1−2			1.16438	1.78376		4.64294	35.0543
1−3			*4.11353	1.80907		*38.1441	35.5516
2−3			*2.94915	1.78376		33.5012	35.0543

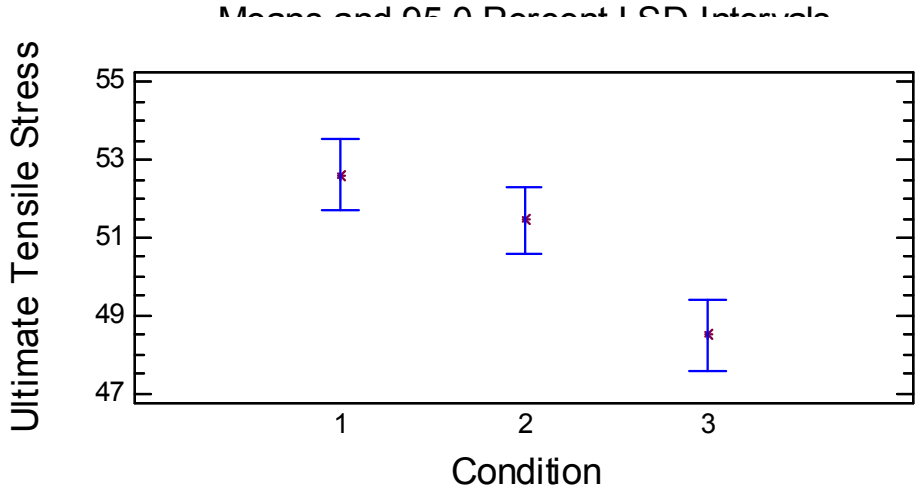

Figure 5.17 Means and 95% confidence for 4 months, ultimate tensile stress by condition intervals.

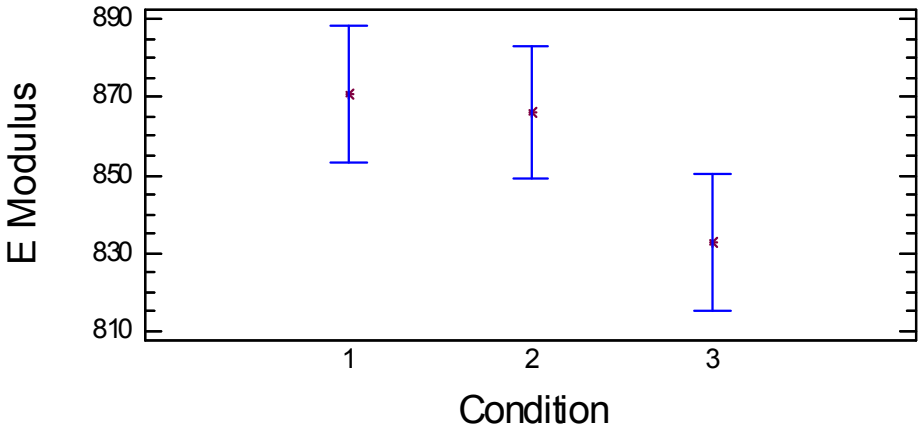

Figure 5.18 Means and 95% confidence for 4 months, E-Modulus (1-3% Strain) by condition intervals.

The Kruskal Wallis test results concludes that 1 month and 4 months are statistically significantly different for ultimate tensile stress and E-Modulus by the different conditions as shown in Table 5.37 and 5.38.

Table 5.37 Kruskal Wallis test for ultimate tensile stress by condition.

Condition	*4 Days*		*1 Month*		*4 Months*	
	Sample Size	**Average Rank**	**Sample Size**	**Average Rank**	**Sample Size**	**Average Rank**
1	17	29.1176	17	38.2353	17	35.7353
2	18	20.1389	18	23.1667	18	27.25
3	17	30.6176	17	18.2941	17	16.4706
Test Statistic	4.93395		16.0531		13.8089	
P-Value	0.084841		0.000326677		0.00100333	

Table 5.38 Kruskal Wallis test for E-Modulus (1-3% Strain) by condition.

Condition	*4Days*		*1 Month*		*4 Months*	
	Sample Size	**Average Rank**	**Sample Size**	**Average Rank**	**Sample Size**	**Average Rank**
1	17	25	17	34.3529	17	31.5294
2	18	28.5556	18	19.5	18	28.8889
3	17	25.8235	17	26.0588	17	18.9412
Test Statistic	0.531575		8.41949		6.5491	
P-Value	0.766602		0.014850100		0.037834	

5.3.4 Effect of Build Orientations of Second Build Setup on Mechanical Properties

A study was done with a build setup of the 24 tensile test specimens which were treated four days ambient and 23±2°C and 50±5% RH. For this study, the desire was to determine the effect of build orientation on the mechanical properties. Table 5.39 shows that the E-Modulus (1-3% Strain) is statistically significantly different to all layout orientations as shown in Figure 5.19 as compared to E-Modulus and ultimate tensile stress. Layout 1 (flat) is statistically significantly different to Layout 2 (on an edge) and 3 (vertical). This is also shown in Figure 5.20 for E-Modulus (1-3% strain) and Figure 5.21 for ultimate tensile stress. Figures 5.22 through 5.24 shows that there is no statistically significant difference on the different positions of the specimen when built on the platform. The null hypothesis of the Kruskal Wallis test states that since all of the P-Values are less than 0.05, all the mechanical properties are statistically significantly different among the 95% confidence level of the mechanical properties as shown in Table 5.40.

Table 5.39 Multiple range tests for E-Modulus, E-Modulus (1-3% Strain), and ultimate tensile stress by layout.

	E Modulus				*E Modulus (1-3% Strain)*			
Layout	**Count**	**LS Mean**	**LS Sigma**	**Homogeneous Groups**	**Count**	**LS Mean**	**LS Sigma**	**Homogeneous Groups**
1	8	2498.8	32.0102	X	8	851.153	2.66808	X
2	8	2733.08	32.0102	X	8	903.48	2.66808	X
3	8	2735.53	32.0102	X	8	919.394	2.66808	X
Contrast			**Difference**	**–/+ Limits**			**Difference**	**–/+ Limits**
1–2			*-234.281	94.1426			*-52.3275	7.84688
1–3			*-236.73	94.1426			*-68.2412	7.84688
2–3			-2.44875	94.1426			*-15.9137	7.84688

	Ultimate Tensile Stress			
Layout	**Count**	**LS Mean**	**LS Sigma**	**Homogeneous Groups**
1	8	48.5275	0.206333	X
2	8	51.1662	0.206333	X
3	8	51.5325	0.206333	X
Contrast			**Difference**	**–/+ Limits**
1–2			*-2.63875	0.606829
1–3			*-3.005	0.606829
2–3			-0.36625	0.606829

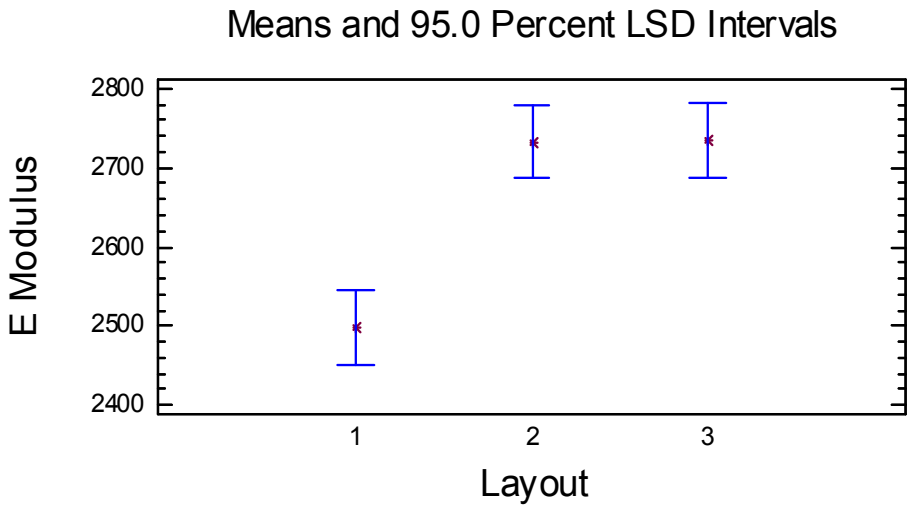

Figure 5.19 Means and 95% confidence, E-Modulus by layout intervals.

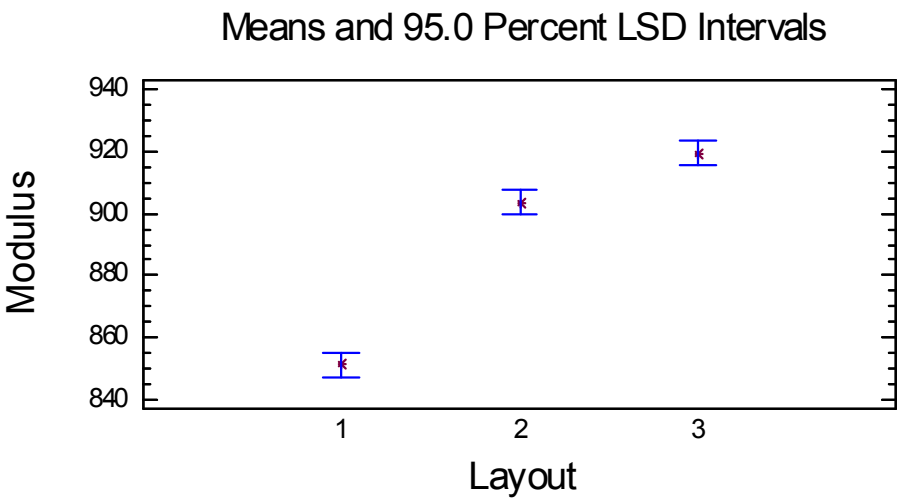

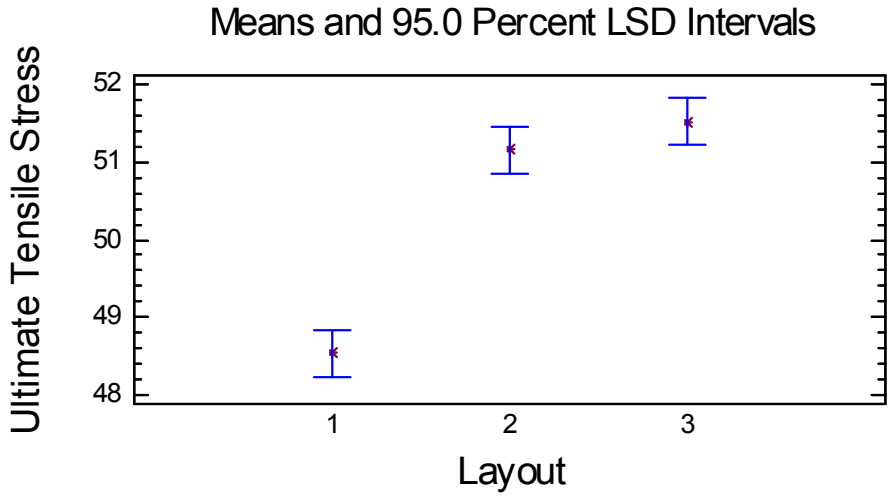

Figure 5.21 Means and 95% confidence, ultimate tensile stress by layout intervals.

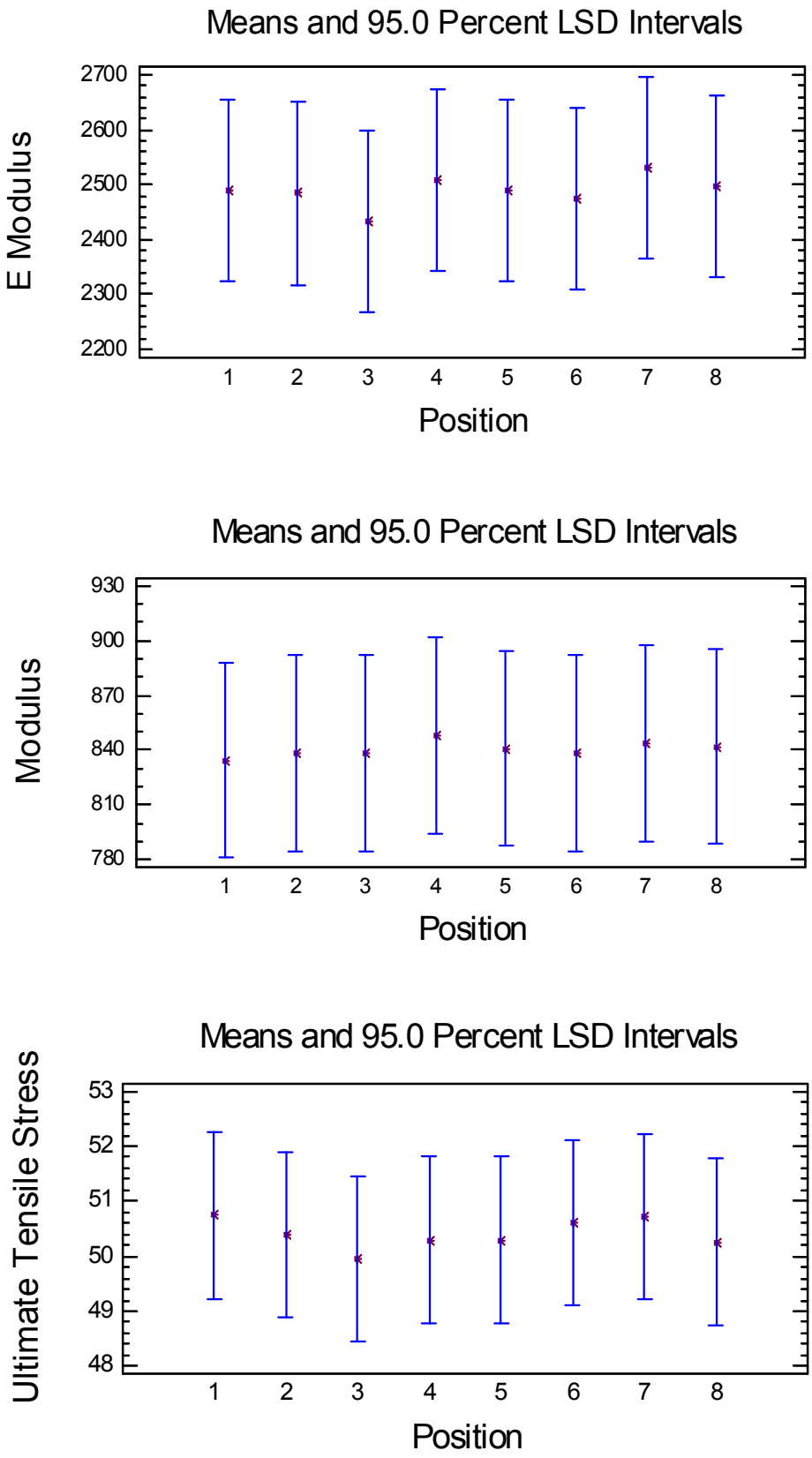

Figure 5.24 Means and 95% confidence ultimate tensile stress by position intervals.

Table 5.40 Kruskal Wallis test for E-Modulus, E-Modulus (1-3% Strain), ultimate tensile stress, tensile strain at break, and tensile stress at break by layout.

	E Modulus		*E Modulus (1-3%)*		*UTS*	
Layout	**Sample Size**	**Average Rank**	**Sample Size**	**Average Rank**	**Sample Size**	**Average Rank**
1	8	4.875	8	4.5	8	4.5
2	8	16.25	8	12.75	8	14.875
3	8	16.375	8	20.25	8	18.125
Test Statistic	13.955		19.86		16.212	
P-Value	0.000932632		0.000048692		0.000301716	
	Tensile Strain at Break		***Tensile Stress at Break***			
Layout	**Sample Size**	**Average Rank**	**Sample Size**	**Average Rank**		
1	7	18.7143	8	4.85714		
2	7	10.2857	8	15.4286		
3	10	9.7	8	15.8		
Test Statistic	7.66086		11.5566			
P-Value	0.0217003		0.003094010			

5.3.5 Analysis on Second Build Setup Specimens

An analysis was performed for three analyst measuring 24 test specimens. The measurements were taken on the gage length, width of the narrow section, thickness, overall width, and overall length. Each specimen was measured three times. The gage length for analyst 1 is statistically significant to the measurement taken by analyst 3 shown in Table 5.41. This can be seen in Figure 5.25 by means and 95% confidence intervals. Figures 5.26 and 5.27 shows the spread of the measurements of the analysts on the gage length. On the analysis of the width of the narrow section, analyst 1 is statistically significantly different to the measurements taken by analyst 2 and 3 which is stated on Table 5.42. Figure 5.28 supports the conclusions drawn. Figures 5.29 and 5.30 show the spread of the measurements taken by the analyst on the width of the narrow section of the specimens. The measurements taken by the analysts on the

thickness of the specimens are statistically significantly different from all the analysts as stated on Table 5.43 and Figure 5.31. Figures 5.32 and 5.33 demonstrates the spread of measurements on the thickness of the specimens. Table 5.44 demonstrates that the measurements by analyst 1 are statistically significantly different to the measurements taken by the other two analysts. This is supported by Figure 5.34. Figures 5.35 and 5.36 demonstrate the scattering of the measurements of the overall width. On the overall length of the specimen there was no statistically significantly difference as shown in Table 5.45 on the measurements taken by the three analysts which is also illustrated on Figures 5.37 through 5.49. The Kruskal Wallis test results on Table 5.46 present that the P-Values are less than 0.05 for the gage length, width of the narrow section, thickness and width overall. This proves that the mentioned factor levels are statistically significantly different except the overall length of the specimen. The statistics test exhibited in Table 5.47 that width, thickness, and width overall have small P-Values less than 0.05.

Table 5.41 Multiple range test for gage length by analyst.

	Gage Length			
Analyst	**Count**	**LS Mean**	**LS Sigma**	**Homogeneous Groups**
1	72	50.9766	0.0998596	X
3	72	51.0027	0.0998596	XX
2	72	51.0148	0.0998596	X
Contrast			**Difference**	**−/+ Limits**
1−2			-0.0261111	0.0278374
1−3			*-0.0381944	0.0278374
2−3			-0.0120833	0.0278374

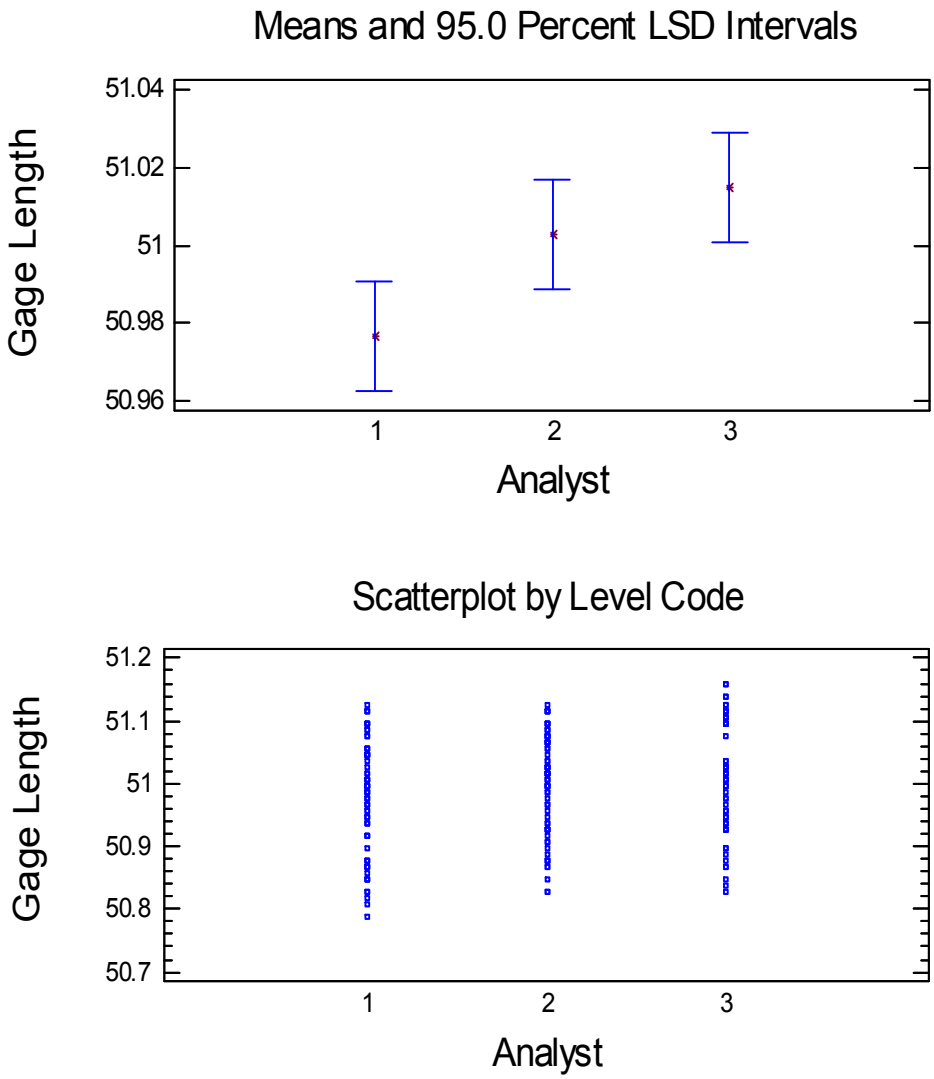

Figure 5.26 Gage length versus analyst scatter plot by analyst.

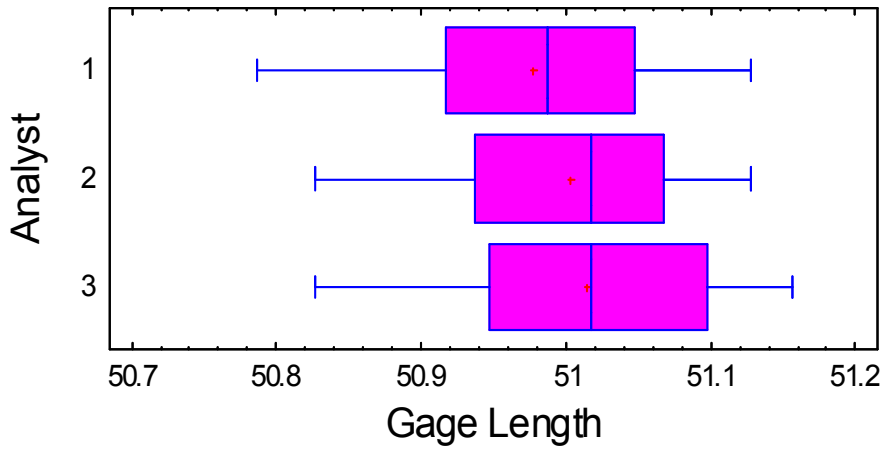

Figure 5.27 Box and Whisker plot, gage length by analyst.

Table 5.42 Multiple range test for width of narrow section by analyst.

	Width of Narrow Section			
Analyst	**Count**	**LS Mean**	**LS Sigma**	**Homogeneous Groups**
1	72	12.8304	0.00702951	X
3	72	12.8697	0.00702951	X
2	72	12.9015	0.00702951	X
Contrast			**Difference**	**−/+ Limits**
1−2			*-0.0711111	0.0195958
1−3			*-0.0393056	0.0195958
2−3			0.0318056	0.0195958

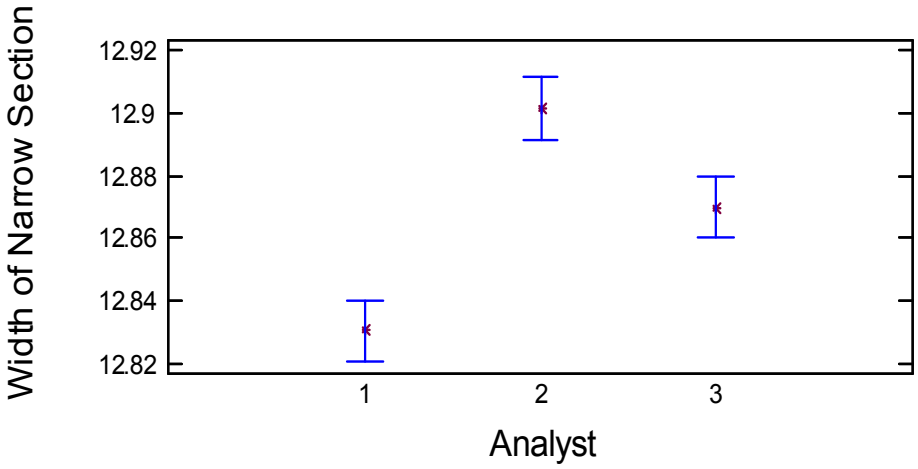

Figure 5.28 Means and 95% confidence intervals for the analyst.

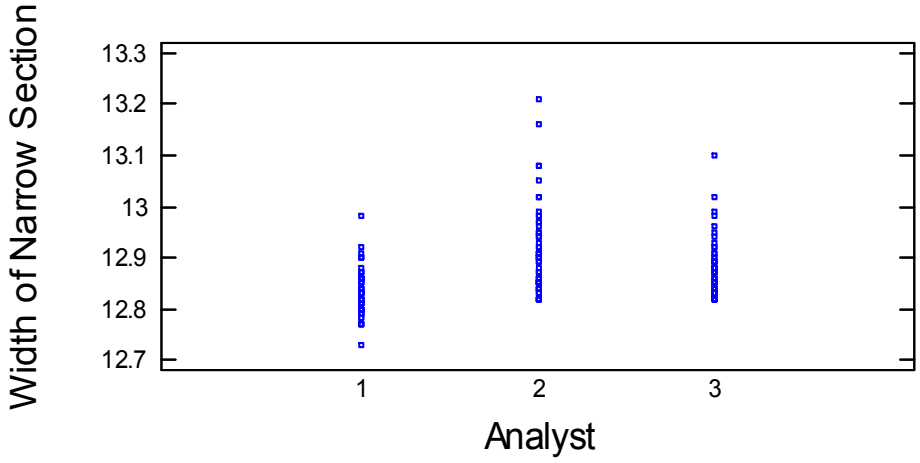

Figure 5.29 Width of the narrow section versus analyst scatter plot.

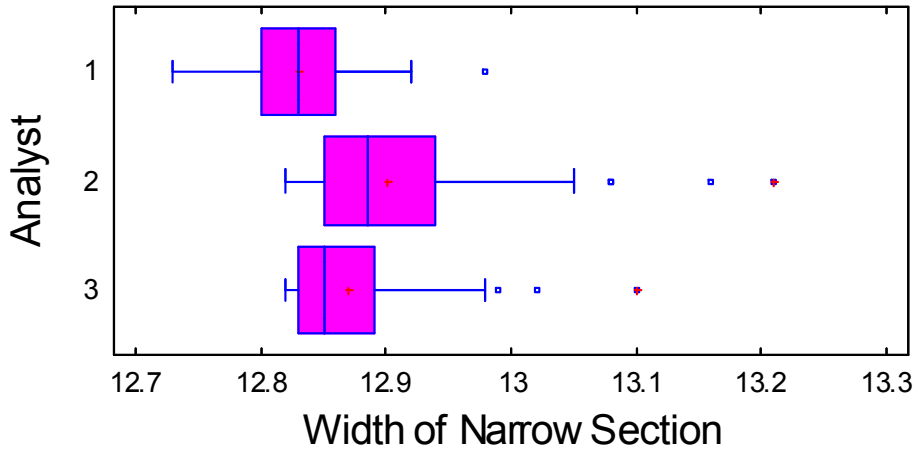

Figure 5.30 Box and Whisker plot, width of the narrow section by analyst.

Table 5.43 Multiple range test for thickness by analyst.

	Thickness			
Analyst	**Count**	**LS Mean**	**LS Sigma**	**Homogeneous Groups**
1	72	3.42625	0.0058938	X
3	72	3.47375	0.0058938	X
2	72	3.49417	0.0058938	X
Contrast			**Difference**	**−/+ Limits**
1−2			*-0.0679167	0.0164299
1−3			*-0.0475	0.0164299
2−3			*0.0204167	0.0164299

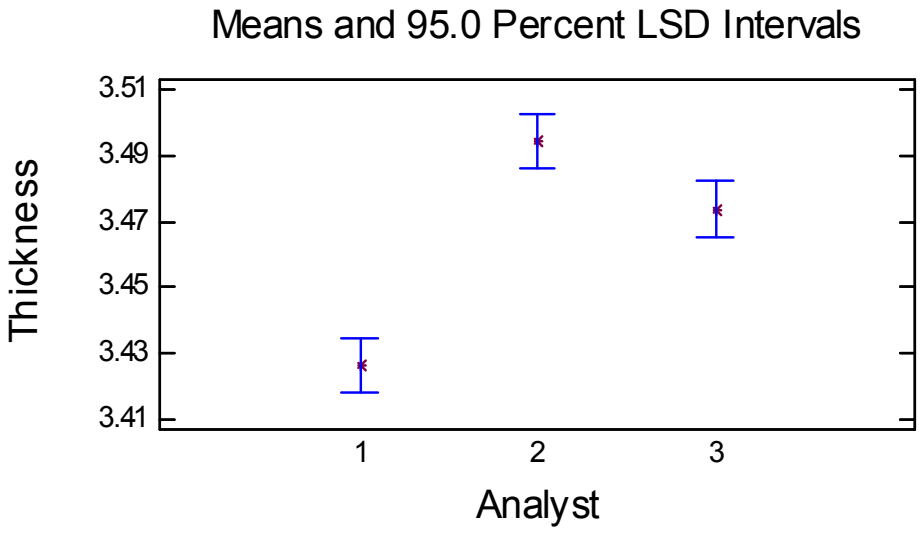

Figure 5.31 Means and 95% confidence intervals for the analyst.

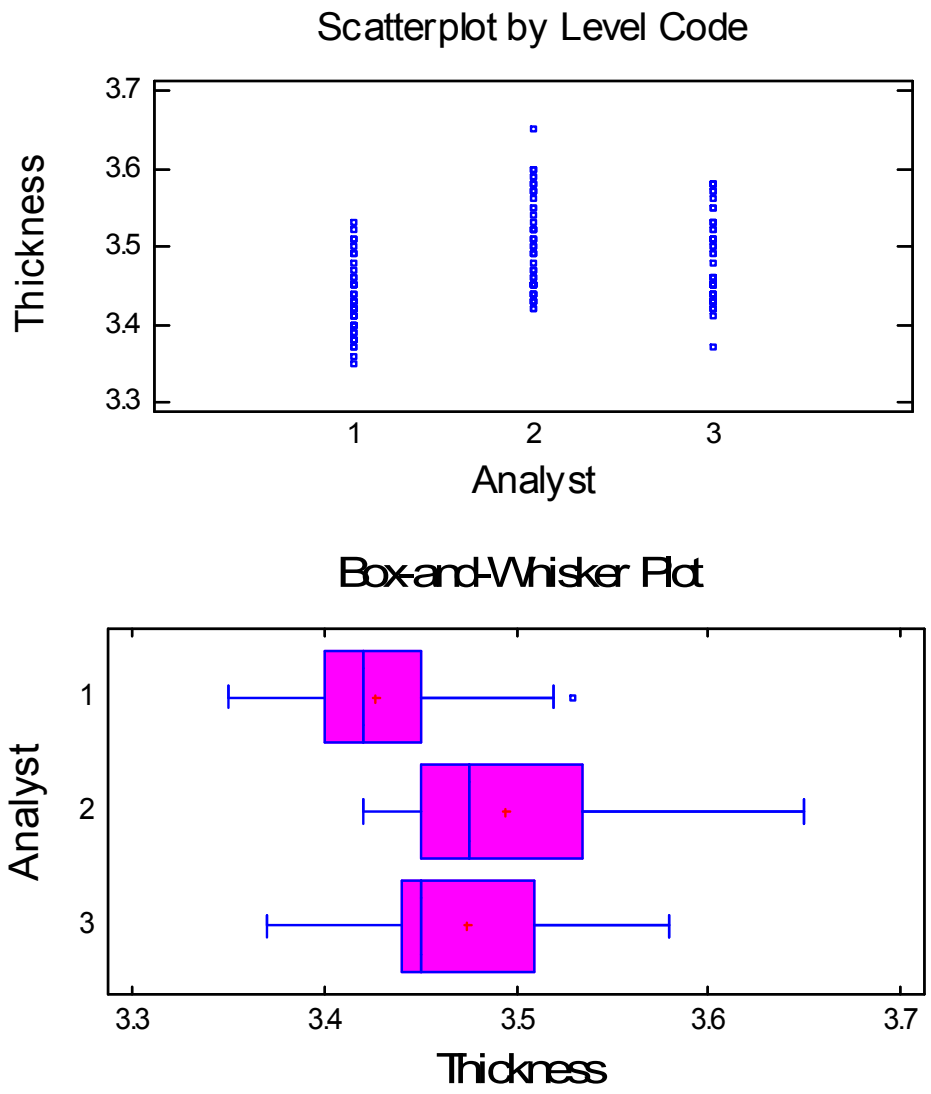

Figure 5.33 Box and Whisker plot, thickness by analyst.

Table 5.44 Multiple range test for width overall by analyst.

	Width Overall			
Analyst	**Count**	**LS Mean**	**LS Sigma**	**Homogeneous Groups**
1	72	19.1686	0.00874107	X
3	72	19.2219	0.00874107	X
2	72	19.2394	0.00874107	X
Contrast			**Difference**	**−/+ Limits**
1−2			*-0.0708333	0.0243671
1−3			*-0.0533333	0.0243671
2−3			0.0175	0.0243671

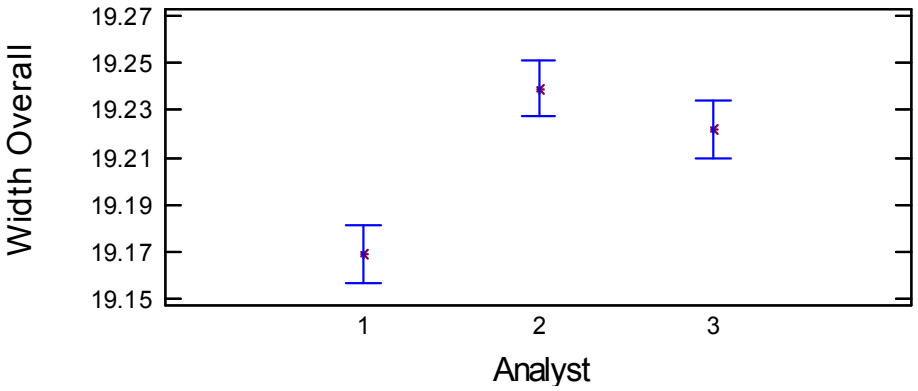

Figure 5.34 Means and 95% confidence intervals for the analyst.

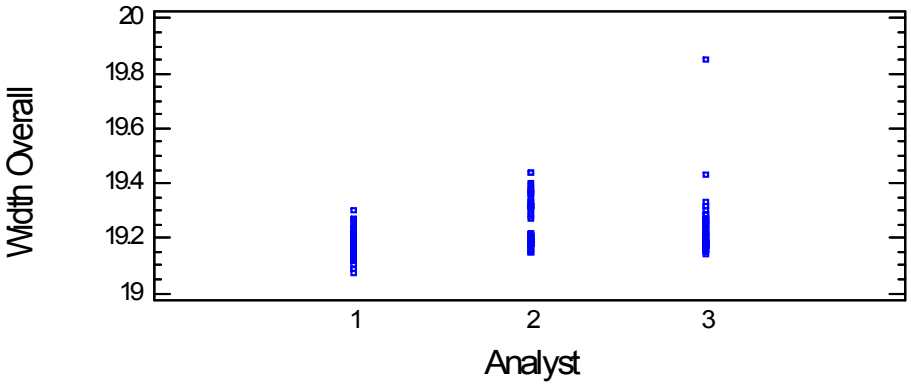

Figure 5.35 Width overall versus analyst scatter plot.

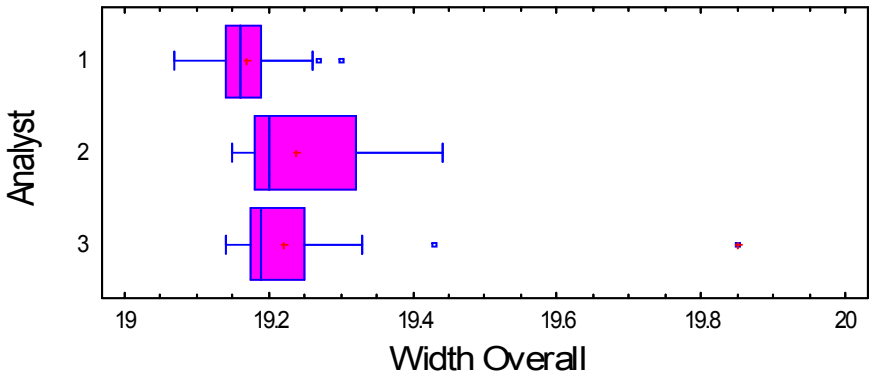

Figure 5.36 Box and Whisker plot, width overall by analyst.

Table 5.45 Multiple range test for length overall by analyst.

	Length Overall			
Analyst	**Count**	**LS Mean**	**LS Sigma**	**Homogeneous Groups**
1	72	165.284	0.022831	X
3	72	165.334	0.022831	X
2	72	165.338	0.022831	X
Contrast			**Difference**	**−/+ Limits**
1−2			-0.0538889	0.0636448
1−3			-0.0498611	0.0636448
2−3			0.00402778	0.0636448

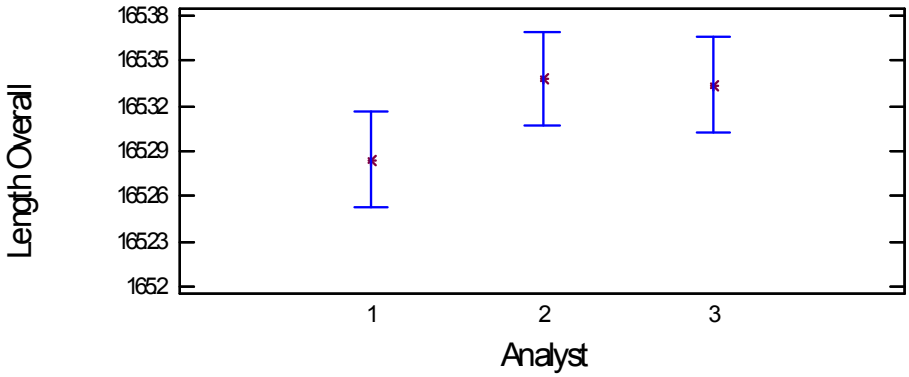

Figure 5.37 Means and 95% confidence intervals for the analyst.

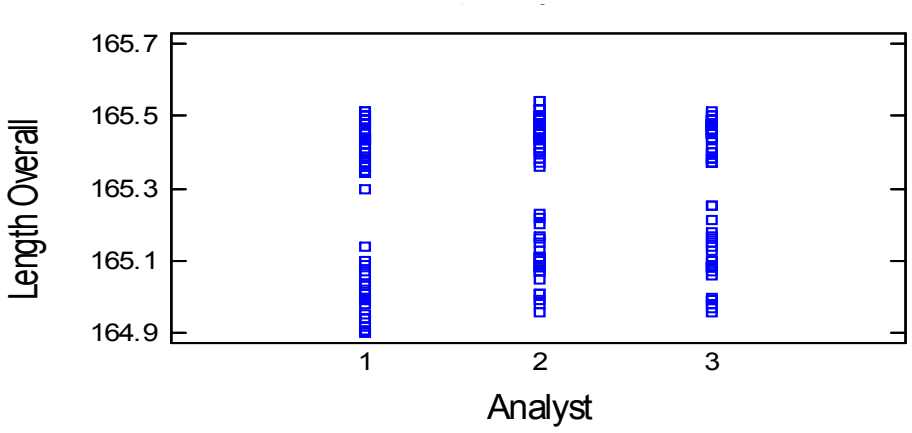

Figure 5.38 Length overall versus analyst scatter plot.

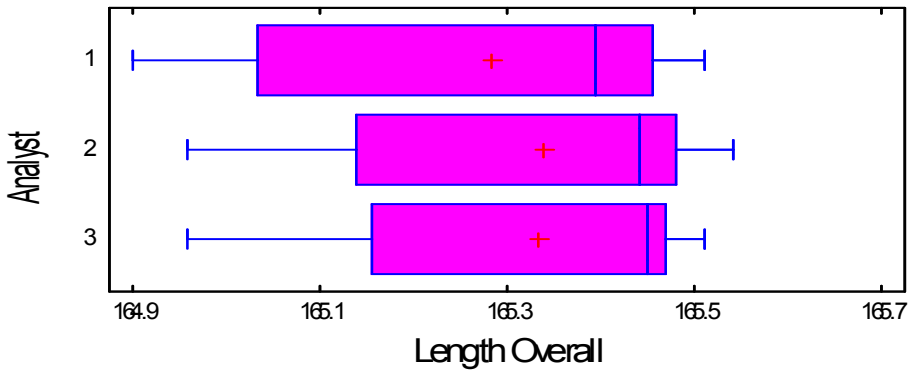

Figure 5.39 Box and Whisker plot, length overall by analyst.

Table 5.46 Kruskal Wallis test for gage length, width of narrow section, thickness, width overall and length overall by analyst.

	Gage Length		*Width*		*Thickness*		*Width Overall*		*Length Overall*	
Analyst	**Sample Size**	**Average Rank**	**Sample Size**	**Average Rank**	**Sample Size**	**Average Rank**	**Sample Size**	**Average Rank**	**Sample Size**	**Average Rank**
1	72	93.4653	72	68.4444	72	62.1875	72	67.5694	72	94.1736
2	72	111.618	72	139.84	72	141.16	72	136.125	72	117.118
3	72	120.417	72	117.215	72	122.153	72	121.806	72	114.208h
Test Statistic	6.9762		49.3692		63.251		48.5508		-5.76492	
P-Value	0.0305588		1.90E-11		0		2.87E-11		-0.0559968	

Table 5.47 Varience check – Analyst by gage length, width of narrow section, thickness, width overall, and length overall.

Factor	*Gage Length*		*Width*		*Thickness*		*Width Overall*		*Length Overall*	
Test	**Result**	**P-Value**	**Result**	**P-Value**	**Result**	**P-Value**	**Result**	**P-Value**	**Result**	**P-Value**
Cochran's C	0.360877	0.806101	0.596891	5.92E-08	0.447041	0.024079	0.506182	4.53E-04	0.418689	0.101765
Bartlett's	1.00395	0.658813	1.17285	4.69E-08	1.04566	0.008865	1.20803	2.06E-09	1.01549	0.196557
Hartley's	1.23089	–	3.85004	–	2.09478	–	4.71256	–	1.45422	–
Levene's	0.464513	0.629076	7.91719	0.000482	5.21861	0.006129	3.39507	0.035363	0.946144	0.389861

5.4 RESULTS SUMMARY

The different build orientations (flat, on an edge, and vertical) showed to have statistically different mechanical properties as determined by using measurements of ultimate tensile stress and E-Modulus. Statistical differences in mechanical properties were also found as a result of aging the time between sample production and mechanical testing (4 days, 1 month, and 4 months) and pre-conditioning the storage conditions of the tensile specimens (ambient, desiccant, and desiccant and 23°C and 50±5% RH).

The percent difference between ultimate tensile stress and E-Modulus by Layout 1 (flat) and Layout 2 (on an edge) tested on 4 days ambient, demonstrated on Table 5.48, shows the statistically different mechanical properties. Additional investigations were studied at different aging (4 days, 1 month, and 4 months) and pre-conditions (ambient, desiccant, and desiccant and 23°C and 50±5% RH). Tables 5.49 and 5.50 show the percent difference in the mechanical properties based on different conditions on ultimate tensile stress and E-Modulus, respectively.

Table 5.48 Percent difference between ultimate tensile stress and E-Modulus by layout.

% Difference	Ultimate Tensile Stress	E-Modulus
	3.539	4.596

Table 5.49 Percent difference on ultimate tensile stress by layout on aging and preconditioning illustrated by 18 specimens.

% Difference	Ultimate Tensile Stress		
	Ambient	Desiccant	Environmental Chamber
4 Days	6.3	5.2	7.8
1 Month	5.2	4.0	5.9
4 Months	8.9	9.4	9.3

Table 5.50 Percent difference on E-Modulus by layout on aging and pre-conditioning illustrated by 18 samples.

% Difference	E-Modulus		
	Ambient	Desiccant	Environmental Chamber
4 Days	8.4	6.8	8.7
1 Month	7.4	5.2	6.8
4 Months	11.8	10.6	9.7

Another layout was included in the study for the setup of 24 specimens. Layout 3 (vertical) showed to have a high percent difference on Layout 1 (flat) as demonstrated on Table 5.51. The research concluded that the building orientation, aging, and pre-conditioning are factors which affect the mechanical properties of the tensile test specimens. The supported analysis shows evidence that the different conditions impact the performance of the material.

Table 5.51 Percent difference between ultimate tensile stress and E-Modulus by layout on aging and pre-conditions illustrated by 24 samples.

% Difference	Ultimate Tensile Stress	E-Modulus
Layout 2 - 1	8.9	9.3
Layout 3 - 1	10.1	10.8
Layout 3 - 2	1.4	1.7

CHAPTER 6 CONCLUSIONS AND RECOMMENDATIONS

6.1 CONCLUSIONS

A study was developed to better understand the behavior of the commercially available resin, WaterShed™ 11120 (DSM Somos®, Elgin, IL), under different circumstances such as build orientation, aging and environmental conditions. Two different build setups that hold 18 and 24 specimens were designed to investigate these effects. Viper Si^2 stereolithography RP technology (Viper Si^2, 3D Systems, Valencia, CA) was used to manufacture the Type I tensile specimens with the recommended settings from DSM Somos® Product Data Sheet using a solid state laser with a wavelength of 350 nm. Three experiments were performed using these two different build setups.

On the first setup of 18 specimens (first experiment) the mechanical properties of the different build orientations were studied. These samples were mechanically tested and results showed that only Layout had a statistical significance on Ultimate Tensile Strength (UTS) and E-Modulus (E). The difference between average UTS and E for each of the samples built flat and on an edge were ~3.53% (43.2 vs. 44.8 MPa) and ~4.59% (763.9 vs. 800.7 MPa), respectively. Using the same build setup of 18 specimens a second experiment was conducted. This experiment investigated the effects of different aging (4, 30, and 120 days) and conditioning (ambient, desiccant, and desiccant plus two days ASTM pre-conditioning) on the mechanical properties. The specimens treated at Ambient conditions at the different time frames (4, 30, and 120 days) had the highest mechanical values of UTS and E (UTS: 45.7±1.6, 54.2±1.8, and 52.6±2.6 MPa, E: 777.3±38.5, 873.1±36.6, and 870.8±57.3 MPa, for 4, 30, and 120 days,

respectively) compared to the specimens treated at Desiccant (UTS: 44.7±1.6, 52.1±1.5, and 51.4±2.7 MPa, E: 794.5±32.5, 839.1±39.1, and 866.1±50.0 MPa, for 4, 30, and 120 days, respectively) and Desiccant plus two days ASTM pre-conditioning (UTS: 45.9±2.1, 51.3±1.8, and 48.5±2.5 MPa, E: 787.8±39.8, 857.5±32.7, and 832.6±45.9 MPa, for 4, 30, and 120 days, respectively). As a result, the % difference of the Aging and Pre-conditions for UTS and E at Ambient (UTS: 6.3, 5.2, and 8.9 %, E: 8.4, 7.4, and 11.8%, for 4, 30, and 120 days, respectively), Desiccant (UTS: 5.2, 4.0, and 9.4 %, E: 6.8, 5.2, and 10.6 %, for 4, 30, and 120 days, respectively), and Desiccant plus two days ASTM pre-conditioning (UTS: 7.8, 5.9, and 9.3 %, E: 8.7, 6.8, and 9.7 %, for 4, 30, and 120 days, respectively). These two experiments done with a build setup of 18 specimens concluded that the building orientation (Layout), aging, and pre-conditioning are factors that affect the mechanical properties of the tensile test specimens.

The final experiment using build setup 2 of 24 tensile specimens was done to investigate an additional build orientation (vertical). Results demonstrated that samples built flat (Layout 1) had a low value of UTS and E (UTS: 45.2±0.8 and E: 791.5 ±9.4 MPa) compared to the specimens fabricated on an edge (Layout 2) (UTS: 49.6±0.7 and E: 872.5±6.9 MPa) and vertical (Layout 3) (UTS: 50.3±0.6 and E: 887.1±12.5 MPa). Results showed that Layout 3 had the highest UTS and E compared to Layouts 1 and 2. Thus, the % difference of the built orientation between the UTS and E by Layout (vertical and flat) was 10.10 and 10.80, respectively, (vertical and on an edge) was 1.40 and 1.70, respectively, and (on an edge and flat) was 8.90 and 9.30, respectively. The results can conclude that the orientation of the layers of the specimens produced statistically different mechanical properties.

The researched work demonstrates the effects of build orientation, aging and conditioning on the mechanical properties. Consequently, identifying the affects on the mechanical properties of the commercially available resin can help improve the production process for end use products.

6.2 RECOMMENDATIONS FOR FUTURE RESEARCH WORK

This investigation demonstrates the potential that RP technology of SL has when manufacturing repeatable and reproducible 3D parts. The research also showed the effects of build layout (flat, on an edge and vertical) among the effects of aging (4 days, 1 month, and 4 months) and environmental conditions (ambient, desiccant and desiccant and 23±2°C and 50±5% RH) on the commercially available SL resin WaterShed® 11120. Even though the build procedure and the environmental conditions were well controlled and monitored, there were limitations. Several restrictions resulted when it came to test the Type I specimens. The specimens were in a controlled environment (23±2°C and 50±5% RH) and about to be tested in the tensile machine but there was a need for a bigger building envelope to build additional specimens for each of the levels of importance in order to obtain wider results for analysis. Investigations for different types of SLA technology with bigger building envelopes for the same type of research should be looked into. In addition there should be a focus on reducing and removing the effects of layout by the addition of CNTs in the resin. Future research should efficiently focus on the manufactured specimens and test them in a controlled environment lab (23±2°C and 50±5% RH).

To conduct the conditioning and testing of the Type I tensile specimens correctly based on the ASTM D638, the specimens should be built and tested in a controlled environment of 23±2°C and 50±5% RH. Having the Viper Si^2 and INSTRON® 5866 in a lab room with the

stated restriction the results obtained, can help achieve more accurate results if followed by the specifications of the ASTM D638. After building, specimens should be cleaned and be kept in the lab. Specimens kept under these conditions will not be exposed to any draw backs of temperature and humidity or even both. If the lab room is controlled by a temperature and humidity sensor, this may allow for adequate conditions where test specimens may remain in the lab for further research.

The RP technology used for the present research is SL. A suggestion would be to use another SL machine besides Viper Si^2 which may have a larger building envelope to build additional specimens for each of the levels of importance to obtain wider results for analysis. 3D system SLA 500 has a building envelope of 508 mm x 508 mm x 610 mm which requires 254 L of polymer and due to the large chamber, it can manufacture large 3D prototypes. Type I tensile specimens can be manufactured with this SL technology in different orientations within the vat with various replicates to improve and understand the effects of the different orientation of the specimen within the vat.

There has been research of the dispersion of CNTs in polymer resin. Research has shown that the addition and dispersion has improved the mechanical properties of the commercially available resin as the percentage concentration is increased. The future research should investigate the dispersion of the CNTs to reinforce the material and remove the effects of layout on the mechanical properties of the commercially available resin. Along with that, an investigation should be done to determine the behavior which CNTs will have on the elasticity of the nanocomposite specimens. Therefore another DOE can be performed with the design controlled experimental conditions stated in this study.

REFERENCES

1. American Society for Testing and Materials, Standard 638, 2005, *Standard Test Method for Tensile Properties of Plastic*, Annual Book of ASTM Standards, vol. 8.01, PA, USA.
2. Ahn, S., Montero, M., Odell, D., Roundy, S., Wright, P.K., 2002, "Anisotropic Material Properties of Fused Deposition Modeling ABS," *Rapid Prototyping Journal*, vol.8, no. 4, pp. 248-257.
3. Allcock, H.R., Lampe F.W., Mark, J.E., 2003, *Contemporary Polymer Chemistry*, Third Edition, Pearson Education, NJ, USA.
4. Ang, K.C., Leong, K.F., Chua, C.K., 2006, "Investigation of the Mechanical Properties and Porosity Relationships in Fused Deposition Modeling-Fabricated Porous Structures," *Rapid Prototyping Journal*, vol.12, no. 2, pp. 100-105.
5. Arcaute-Cantu, K., 2004, Complex Silicone Cardiovascular Models Manufactured Using a Dip-Spin Coating Technique and Water-Soluble Molds, M.S. edition, University of Texas at El Paso, El Paso, Texas, USA.
6. Augsburg, M., Storch, S., Nissen, F., Witt, G., 2004, "Rapid Prototyping with Ceramic-Filled Epoxy Resin by Optoforming," *Rapid Prototyping Journal*, vol. 10, no. 4, pp.225-231.
7. Bellini, A., Güçeri, S., 2003, "Mechanical Characterization of Parts Fabricated Using Fused Deposition Modeling," *Rapid Prototyping Journal*, vol. 9, no.4, pp. 252-264.
8. Bellini, A., Shor, L., Guceri, S.I., 2005, "New Developments in Fused Deposition Modeling of Ceramics," *Rapid Prototyping Journal*, vol.11, no. 4, pp. 214-220.

9. Bens, A., Seitz, H., Bermes, G., Emons, M., Pansky, A., Roitzheim, B., Tobiasch, E., Tille, C., 2007, "Non-Toxic Flexible Photopolymers for Medical Stereolithography Technology," *Rapid Prototyping Journal*, vol. 13, no. 1, pp. 38-47.

10. Bertsch, A., Bernhard, P., Vogt, C., Renaud, P., 2000, "Rapid Prototyping of Small Size Objects," *Rapid Prototyping Journal*, vol. 6, no. 4, pp. 259-266.

11. Campanelli, S.L., Cardano, G., Giannoccaro, R., Ludocico, A.D., Bohez, E.L.J., 2007, "Statistical Analysis of the Stereolithographic Procesws to Improve the Accuracy," *Computer-Aided Design*, vol. 39, pp. 80-86.

12. Cheah, C.M., Nee, A.Y.C., Fuh, J.Y.H., Lu, L., Choo, Y.S., Miyazawa, T., 1997, "Characteristics of Photopolymeric Material used in Rapid Prototypes Part I. Mechanical Properties in the Green State," *Journal of Materials Processing Technology*, vol. 67, pp. 41-45.

13. Cheah, C.M., Fuh, J.Y.H., Nee, A.Y.C., Lu, L., 1999, "Mechanical Characteristics of Fiber-Filled Photo-Polymer used in Stereolithography," *Rapid Prototyping Journal*, vol. 5, no. 3, pp. 112-119.

14. Cheng, W., Fuh, J.Y.H., Nee, A.Y.C., Wong, Y.S., Loh, H.T., Miyazawa, T., 1995, "Multi-Objective Optimization of Part-Building Orientation in Stereolithography," *Rapid Prototyping Journal*, vol. 1, no. 4, pp. 12-23.

15. Chockalingam, K., Jawahar, N., Chandrasekhar, U., 2006, "Influence of Layer Thickness on Mechanical Properties in Stereolithography," *Rapid Prototyping Journal*, vol. 12, no. 2, pp. 106-113.

16. Chockalingam, K., Jawahar, N., Chandrasekhar, U., Ramanathan, K.N., 2008, "Establishment of Process Model for Part Strength in Stereolithography," *Journal of Materials Processing Technology*, in press.

17. Chua, C.K., Chou, S.M., Wong, T.S., 1998, "A Study of the State-of-the-Art Rapid Prototyping Technologies," *International Journal of Advanced Manufacturing Technology*, vol. 14, pp. 146-152.

18. Chuk, R.N., Thomson, V.J., 1998, "A Comparison of Rapid Prototyping Techniques used for Wind Tunnel Model Fabrication," *Rapid Prototyping Journal*, vol. 4, no. 4, pp. 185-196.

19. Curtis, J.D., Hanna, S.D., Patterson, E.A., Taroni, M., 2003, "On the Use of Stereolithography for the Manufacture of Photoelastic Models," *Society for Experimental Mechanics*, vol.43, no. 2, pp.148-162.

20. Danby®, 2009. *Simplicity® Product Manual SHCC6026* [Online]. Available: HTTP://WWW.DANBY.COM/PRODUCT/SHCC6026/12 [03-12-09]

21. Danby®, 2009. *Simplicity® Product Specs SHCC6026* [Online]. Available: HTTP://WWW.DANBY.COM/PRODUCT/SHCC6026/12 [03-12-09]

22. Davis, J.R. (ed) 2004, *Tensile Testing*, Second Edition, ASM International, USA.

23. De Laurentis, K.F., Mavroidis, C., 2004, "Rapid Fabrication of Non-Assembly Robotic Hand with Embedded Components," Assembly Automation, vol. 24, no. 4, pp. 394-405.

24. Dimitrov, D., Van Wijck, W., Schreve, K., De Beer, N., 2006, "Investigating the Achievable Accuracy of Three Dimensional Printing," *Rapid Prototyping Journal*, Vol. 12, no. 1, pp.42-52.

25. DSM Somos®, 2008. *WaterShed™ 11120 – Product Data Sheet* [Online]. Available: HTTP://WWW.DSM.COM/EN_US/HTML/DSMS/PD_PRODUCT_DATA_SHEETS.HTM [2/21/2008]

26. Dulieu-Barton, J.M., Fulton, M.C., 2000, "Mechanical Properties of a Typical Stereolithography Resin," *Strain*, vol. 36, no. 2, pp. 81-87.

27. Evans, M.A., Ian Campbell, R., 2003, "A Comparative Evaluation of Industrial Design Models Produced Using Rapid Prototyping and Workshop-Based Fabrication Techniques," *Rapid Prototyping Journal*, vol. 9, no. 5, pp. 344-351.

28. Fuh, J.Y.H., Lu, L., Tan, C.C., Shen, Z.X., Chew, S., 1999, "Curing Characteristics of Acrylic Photopolymer used in Stereolithography Process," *Rapid Prototyping Journal*, vol. 5, no. 1, pp. 27-34.

29. Gibson, I., Shi, D., 1997, "Material Properties and Fabrication Parameters in Selective Laser Sintering Process," *Rapid Prototyping Journal*, vol. 3, no. 4, pp. 129-136.

30. Gray IV, R.W., Baird, D.G., Bøhn, J.H., 1998, "Effects of Processing Conditions on Short TLCP Fiber Reinforced FDM Parts," *Rapid Prototyping Journal*, vol.4, no. 1, pp.14-25.

31. Hague, R., Mansour, S., Saleh, N., 2003, "Design Opportunities with Rapid Manufacturing," *Assembly Automation*, vol. 23, no. 4, pp. 346-356.

32. Hague, R., Mansour, S., Saleh, R., Harris, R., 2004, "Materials Analysis of Stereolithography Resins for use in Rapid Manufacturing," *Journal of Materials Science*, vol. 39, pp. 2457-2464.

33. Hanumaiah, N., Ravi, B., 2007, "Rapid Tooling form Accuracy Estimation Using Region Elimination Adaptive Search Based Sampling Technique," *Rapid Prototyping Journal*, vol. 13, no. 3, pp 182-190.

34. Hull, C., Feygin, M., Baron, Y., Sanders, R., Sachs, E., Lightman, A., Wohlers, T., 1995, "Rapid Prototyping: Current Technology and Future Potential," *Rapid Prototyping Journal*, vol. 1, no. 1, pp. 11-19.

35. INSTRON® 2004, *Accessories for Materials Testing*, First Edition, INSTRON Corporation, Norwood, MA.

36. INSTRON® 2006, *Universal Materials Testing Machines* [Online]. Available: HTTP://WWW.INSTRON.US/WA/PRODUCTS/UNIVERSAL_MATERIAL/DEFAULT.ASPX [2/21/08]

37. Karalekas, D., 2003, "Study of the Mechanical Properties of Nonwoven Fibre Mat Reinforced Photopolymers used in Rapid Prototyping," *Materials and Design*, vol. 24, pp. 665-670.

38. Karalekas, D.E., Aggelopoulos, A., 2004, "On the use of Stereolithography Built Photoelastic models for Stress Analysis Investigations," *Materials and Design*, vol.27, pp. 100-106.

39. Karalekas, D., Antoniou, K., 2004, "Composite Rapid Prototyping: Overcoming the Drawback of Poor Mechanical Properties," *Journal of Materials Processing Technology*, vol. 153-154, pp. 526-530.

40. Karalekas, D., Rapti, D., 2002, "Investigation of the Processing Dependence of SL Solidification Residual Stresses," *Rapid Prototyping Journal*, vol. 8, no. 4, pp. 243-247.

41. Kruskal, W.H., and Wallis, W.A., 1952, "Use of Ranks of One Criterion Variance Analysis," *Journal of the American Statistical Association,* vol. 47, pp. 583-621.

42. Kruth, J.P., Levy, G., Klocke, F., Childs, T.H.C., 2007, "Consolidation Phenomena in Laser and Powder-Bed Based Layered Manufacturing," *CIRP Annals - Manufacturing Technology*, vol. 56, no. 2, pp. 730-759.

43. Kulkarni, P., Marsan, A., Dutta, D., 2000, "A Review of Process Planning Techniques in Layered Manufacturing," *Rapid Prototyping Journal*, vol. 6, no. 1, pp. 18-35.

44. Levy, G.N., Schindel, R., Kruth, J.P., 2003, "Rapid Manufacturing and Rapid Tooling with a Layer Manufacturing (LM) Technologies, State of The Art and Future Perspectives," *CIRP Annals – Manufacturing Technology*, vol. 52, no. 2, pp. 589-609.

45. Levy, G.N., Schindel, R., Schleiss, P., Micari, F., Fratini, L., 2003, "On the Use of SLS Tools in Sheet Metal Stamping," *CIRP Annals – Manufacturing Technology*, vol. 52, no. 1, pp. 249-252.

46. Levy, G.N., Boehler, P., Martinoni, R., Schindel, R., Schleiss, P., 2005, "Controlled Local Properties in the same part with Sintaflex a new Elastomer Powder Material for the SLS Process," *Proceedings of the 16th Annual Solid Freeform Fabrication Symposium*, University of Texas at Austin, TX, August 3-5, pp. 197-207.

47. Levy, G.N., Schindel, R., Schleiss, P., Spierings, A., 2007, "Quality Management Representation and Application for Rapid Manufacturing with SLS (Selective Laser Sintering)," *15th International Symposium on Electromachining (ISEM XV),*

48. Levy, G.N., Schindel, R., Schleiss, P., 2007, "Quality Management for Rapid Manufacturing with SLS (Selective Laser Sintering) is Essential," *Proceedings of the*

16th Annual Solid Freeform Fabrication Symposium, University of Texas at Austin, TX, August 6-8, pp.

49. McClurkin, J.E., Rosen, D.W., 1998, "Computer-Aided Build Style Decision Support for Stereolithography," *Rapid Prototyping Journal*, vol. 4, no. 1, pp. 4-13.
50. Montgomery, D.C., 2001, *Design and Analysis of Experiments*, fifth edition, Wiley, New York, pp. 856.
51. Munguia, J., De Ciurana, J., Riba, C., 2008, "Pursuing Successful Rapid Manufacturing: a Users' Best-Practice Approach," *Rapid Prototyping Journal*, vol. 14, no. 3, pp. 173-179.
52. Noorani, R., 2006, *Rapid Prototyping Principles and Applications*, John Wiley & Sons, NJ, USA.
53. Onuh, S.O., Hon, K.K.B., 1998, "Optimising Build Parameters for Improved Surface Finish in Stereolithography," *Internaltional Journal of Machine Tools and Manufacture*, vol. 38, no. 4, pp. 329-342.
54. Ottomer, X., Colton, F.S., 2002, "Effects of Aging on Epoxy-Based Rapid Tooling Materials," *Rapid Prototyping Journal*, vol. 8, no. 4, pp. 215-223.
55. Palmer, J.A., Jokiel, B., Nordquiest, C.D., Kast, B.A., Awood, C.J., Grant, E., Livingston, F.J., Medina, F., Wicker, R.B., 2006, "Mesoscale RF Relay Enabled by Integraded Rapid Manufacturing," *Rapid Prototyping Journal*, vol. 12, no. 3, pp. 148-155.
56. Quintana, R., Puebla, K., Wicker, R.B., 2007, "Effects of Build Orientation on Tensile Strength for Stereolithography Manufactured ASTM D-638 Type I Specimens of

DSM SOMOS® 11120 Resin," *Journal of Advanced Manufacturing Technology*, to appear.

57. Quintana, R., Puebla, K., Wicker, R.B., 2007, "Design of Experiments Approach for Statistical Classification of Stereolithogrpahy Manufacturing Build Parameters: Effects of Build Orientation on Mechanical Properties for ASTM D-638 Type I Tensile Test Specimens of DSM SOMOS® 11120 Resin," *Proceedings of the 18th Annual Solid Freeform Fabrication Symposium*, University of Texas at Austin, TX, August 6-8, pp. 340-357.
58. Renap, K., Kruth, J.P., 1995, "Recoating Issues in Stereolithography," *Rapid Prototyping Journal*, vol. 1, no. 3, pp. 4-16.
59. Rochus, P., Plesseria, J.Y., Van Elsen, M., Kruth, J.P., Carrus, R., Dormal, T., 2007, "New Applications of Rapid Prototyping and Rapid Manufacturing (RP/RM) Technologies for Space Instrumentation," *Acta Astronautica*, vol. 61, pp. 352-359.
60. Rodriguez, J.F., Thomas, J.P., Renaud, J.E., 2001, "Mechanical Behavior of Acrylonitrile Butadiene Styrene (ABS) Fused Deposition Materials, Experimental Investigation," *Rapid Prototyping Journal*, vol. 7, no. 3, pp. 148-158.
61. Saleh, N., Hopkinson, N., Hague, R.F.M., Wise, S., 2004, "Effects of Electroplating on the Mechanical Properties of Stereolithography and Laser Sintered Parts," *Rapid Prototyping Journal*, vol. 10, no. 5, pp. 305-315.
62. Salmoria, G.V., Ahrens, C.H., Fredel, M., Soldi, V., Pires, A.T.N., 2005, "Stereolithography Somos 7110 Resin: Mechanical Behavior and Fractography of Parts Post-Cured by Different Methods," *Polymer Testing*, vol. 24, pp. 157-162.

63. Sandoval, J.H., Ochoa, L., Hernandez, A., Lozoya, O., Soto, K.F., Murr, L.E., Wicker, R.B., 2005, "Nanotailoring Stereolithography Resins for unique Applications using Carbon Nanotubes," *Proceedings of the 16th Annual Solid Freeform Fabrication Symposium*, University of Texas at Austin, TX, August 3-5, pp. 513-524.

64. Sandoval, J.H., Soto, K.F., Murr, L.E., Wicker, R.B., 2007, "Nanotailoring Photocrosslinkable Epoxy Resins with Multi-Walled Carbon Nanotubes for Stereolithography Layered Manufacturing," *Journal of Materials Science*, vol. 42, pp. 156-165.

65. Sandoval, J.H., Wicker, R.B., 2006, "Functionalizing Stereolithography Resins: Effects of Dispersed Multi-Walled Carbon Nanotubes on Physical Properties," *Rapid prototyping Journal*, vol. 12, no. 5, pp. 292-303.

66. Sandoval, J.H., 2006, *Functionalizing Epoxy-Based Stereolithography Resins using Multi-Walled Carbon Nanotubes*, M.S. edition, University of Texas at El Paso, El Paso, Texas, USA.

67. Scheirs, J., 2000, Compositional and Failure Analysis of Polymers a Practical Approach, John Wiley & Sons, London, UK.

68. Upcraft, S., Fletcher, R., 2003, "The Rapid Prototyping Technologies," *Assembly Automation*, vol. 23, no. 4, pp. 318-330.

69. Wicker, R.B., Medina, F., Elkins, C.J., 2004, "Multiple Material Micro-Fabrication: Extending Stereolithography to Tissue Engineering and Other Novel Applications," *Proceedings of the 15th Annual Solid Freeform Fabrication Symposium*, University of Texas at Austin, TX, August 3-5, pp. 154-164.

70. Wiedemann, B., Dusel, K.-H., Eschl, J., 1995, "Investigation into the Influence of Material and Process on Part Distortion," *Rapid Prototyping Journal,* vol. 1, no. 3, pp. 17-22.

71. Yang Liu, X., Fiang, F., 2003, "Environmental Effects on the Dimensional of SL5195 Resin," *Rapid Prototyping Journal*, vol. 9, no. 2, pp. 88-94.

APPENDIX A

The following tables are from the effects of the mechanical properties based on aging, conditioning, and the dimensional analysis.

Table A.1 Least squares means for ultimate tensile stress for the different aging (ambient, desiccant and 23° and 50% RH) with 95 percent confidence intervals.

	Ambient				
Level / ***Age***	**Count**	**Mean**	**Stnd. Error**	**Lower Limit**	**Upper Limit**
4	17	45.7165	0.500894	44.7094	46.7236
30	17	54.2359	0.500894	53.2288	55.243
120	17	52.6088	0.500894	51.6017	53.6159
Grand Mean	51	50.8537			
	Desiccant				
Level / ***Age***	**Count**	**Mean**	**Stnd. Error**	**Lower Limit**	**Upper Limit**
4	18	44.6806	0.4778	43.7213	45.6398
30	18	52.09	0.4778	51.1308	53.0492
120	18	51.4444	0.4778	50.4852	52.4037
Grand Mean	54	49.405			
	23°C and 50%				
Level / ***Age***	**Count**	**Mean**	**Stnd. Error**	**Lower Limit**	**Upper Limit**
4	17	45.9394	0.519129	44.8956	46.9832
30	17	51.3165	0.519129	50.2727	52.3603
120	17	48.4953	0.519129	47.4515	49.5391
Grand Mean	51	48.5837			

Table A.2 Least squares means for E-Modulus (1-3% Strain) for the different aging (ambient, desiccant and 23° and 50% RH) with 95 percent confidence intervals.

	Ambient				
Level / ***Age***	**Count**	**Mean**	**Stnd. Error**	**Lower Limit**	**Upper Limit**
4	17	785.978	10.9469	763.967	807.988
30	17	873.112	10.9464	851.102	895.122
120	17	870.793	10.9469	848.783	892.803
Grand Mean	51	843.294			
	Desiccant				
Level / ***Age***	**Count**	**Mean**	**Stnd. Error**	**Lower Limit**	**Upper Limit**
4	18	794.523	9.90934	774.629	814.417
30	18	839.244	9.90934	819.35	859.138
120	18	866.15	9.90934	846.256	886.044
Grand Mean	54	833.3.6			
	23° and 50%				
Level / ***Age***	**Count**	**Mean**	**Stnd. Error**	**Lower Limit**	**Upper Limit**
4	17	787.815	9.65656	768.399	807.231
30	17	857.472	9.65656	838.056	876.888
120	17	832.649	9.65656	813.233	852.065
Grand Mean	51	825.979			

Table A.3 Analysis of variance ultimate tensile stress for different aging at different conditions (ambient, desiccant and 23° and 50% RH) – Type III sums of squares.

	Ambient				
Source	**Sum of Squares**	**Df**	**Mean Square**	**F-Ratio**	**P-Value**
Age	695.483	2	347.741	81.53	0.0000
Residual	204.73	48	4.26521		
Total (corrected)	900.213	50			
	Desiccant				
Source	**Sum of Squares**	**Df**	**Mean Square**	**F-Ratio**	**P-Value**
Age	606.401	2	303.2	73.78	0.0000
Residual	209.573	51	4.10927		
Total (corrected)	815.974	53			
	23°C and 50%				
Source	**Sum of Squares**	**Df**	**Mean Square**	**F-Ratio**	**P-Value**
Age	245.958	2	122.979	26.84	0.0000
Residual	219.908	48	4.58141		
Total (corrected)	465.865	50			

Table A.4 Analysis of variance E-Modulus (1-3% Strain) for different aging at different conditions (ambient, desiccant and 23° and 50% RH) – Type III sums of squares.

	Ambient				
Source	**Sum of Squares**	**Df**	**Mean Square**	**F-Ratio**	**P-Value**
Age	83817.7	2	41908.9	20.57	0.0000
Residual	97784.8	48	2037.18		
Total (corrected)	181603	50			
	Desiccant				
Source	**Sum of Squares**	**Df**	**Mean Square**	**F-Ratio**	**P-Value**
Age	47125.5	2	23562.7	13.33	0.0000
Residual	90143	51	1767.51		
Total (corrected)	137269	53			
	23° and 50%				
Source	**Sum of Squares**	**Df**	**Mean Square**	**F-Ratio**	**P-Value**
Age	42376.7	2	21188.4	13.37	0.0000
Residual	76091.3	48	1585.24		
Total (corrected)	118468	50			

Table A.5 Summary statistics for ultimate tensile stress by aging at different conditions.

	Ambient								
Age	**Count**	**Mean**	**Variance**	**Standard Deviation**	**Minimum**	**Maximum**	**Range**	**Standard Skewness**	**Standard Kurtosis**
4	17	45.7165	2.66645	1.63293	43.25	48.25	5.0	0.106968	-1.27912
30	17	54.2359	3.30233	1.81723	51.96	57.13	5.17	0.412157	-1.35170
120	17	52.6088	6.82685	2.61282	48.99	55.9	6.91	0.0216693	-1.66412
Total	51	50.8537	18.0043	4.24314	43.25	57.13	13.88	-0.852908	-1.7964
	Desiccant								
Age	**Count**	**Mean**	**Variance**	**Standard Deviation**	**Minimum**	**Maximum**	**Range**	**Standard Skewness**	**Standard Kurtosis**
4	18	44.6806	2.47711	1.57388	42.35	48.03	5.68	0.71632	-0.531688
30	18	52.09	2.40808	1.5518	50.21	55.09	4.88	1.3202	-0.491884
120	18	51.4444	7.44261	2.72812	47	54.8	7.8	-0.197792	-1.59311
Total	54	49.405	15.3957	3.92374	42.35	55.09	12.74	-0.834515	-1.81117
	23°C and 50%								
Age	**Count**	**Mean**	**Variance**	**Standard Deviation**	**Minimum**	**Maximum**	**Range**	**Standard Skewness**	**Standard Kurtosis**
4	17	45.9394	4.30649	2.07521	42.62	49.46	6.84	-0.22628	-0.9898878
30	17	51.3165	3.07666	1.75404	48.93	53.97	5.04	0.350681	-1.35393
120	17	48.4953	6.36106	2.52211	45.02	51.96	6.94	-0.0825915	-1.49577
Total	51	48.5837	9.31731	3.05243	42.62	53.97	11.35	-0.319344	-1.31956

Table A.6 Summary statistics for E-Modulus (1-3% Strain) by aging at different conditions.

	Ambient								
Age	**Count**	**Mean**	**Variance**	**Standard Deviation**	**Minimum**	**Maximum**	**Range**	**Standard Skewness**	**Standard Kurtosis**
4	17	785.978	1485.37	38.5405	727.68	842.62	114.94	0.0556638	-1.3028
30	17	873.112	1337.4	36.5704	820.56	919.42	98..86	0.0022027	-1.59469
120	17	870.793	3288.78	57.3479	794.19	944.68	150.49	0.120579	-1.72797
Total	51	843.294	3632.05	60.2665	727.68	944.68	217	-0.0027263	-1.36113
	Desiccant								
Age	**Count**	**Mean**	**Variance**	**Standard Deviation**	**Minimum**	**Maximum**	**Range**	**Standard Skewness**	**Standard Kurtosis**
4	18	794.523	1054.8	32.4778	738.98	842.81	103.83	-0.336749	-1.15089
30	18	839.244	1654.04	40.6699	759	898.3	139.3	-0.0409835	-0.617006
120	18	866.15	2593.68	50.9282	797.7	928.7	131	-0.0875573	-1.76902
Total	54	833.306	2589.97	50.8918	738.98	928.7	189.72	0.947719	-1.13952
	23° and 50%								
Age	**Count**	**Mean**	**Variance**	**Standard Deviation**	**Minimum**	**Maximum**	**Range**	**Standard Skewness**	**Standard Kurtosis**
4	17	787.815	1584.74	39.8088	707.36	834.62	127.26	-0.733649	-0.908664
30	17	857.472	1068.46	32.6873	815.13	907.45	92.32	0.201679	-1.50891
120	17	832.649	2102.51	45.8531	764.73	894.57	129.84	-0.190556	-1.49746
Total	51	825.979	2369.36	48.6761	707.36	907.45	200.09	-0.792862	-0.939986

Table A.7 Least squares means for ultimate tensile stress for the different conditions (ambient, desiccant and 23° and 50% RH) at different time points (4 days, 1 month, and 4 months) with 95 percent confidence intervals.

	4 Days				
Level *Condition*	**Count**	**Mean**	**Stnd. Error**	**Lower Limit**	**Upper Limit**
1	17	45.7165	0.42952	44.8533	46.5796
2	18	44.6806	0.417418	43.8417	45.5194
3	17	45.9394	0.42952	45.0763	46.8026
Grand Mean	52	45.4455			
	1 Month				
Level *Condition*	**Count**	**Mean**	**Stnd. Error**	**Lower Limit**	**Upper Limit**
1	17	54.2359	0.414331	53.4033	55.0685
2	18	52.09	0.402657	51.2808	52.8992
3	17	51.3165	0.414331	50.4838	52.1491
Grand Mean	52	52.5475			
	4 Months				
Level *Condition*	**Count**	**Mean**	**Stnd. Error**	**Lower Limit**	**Upper Limit**
1	17	52.6088	0.636553	51.3296	53.888
2	18	51.4444	0.618618	50.2013	52.6876
3	17	48.4953	0.636553	47.2161	49.7745
Grand Mean	52	50.8495			

Table A.8 Least squares means for E-Modulus (1-3% Strain) for the different conditions (ambient, desiccant and 23° and 50% RH) at different time points (4 days, 1 month, and 4 months) with 95 percent confidence intervals.

	4 Days				
Level *Condition*	**Count**	**Mean**	**Stnd. Error**	**Lower Limit**	**Upper Limit**
1	17	785.978	8.97197	767.948	804.008
2	18	794.523	8.71919	777.001	812.045
3	17	787.815	8.97197	769.785	805.845
Grand Mean	52	2655.8			
	1 Month				
Level *Condition*	**Count**	**Mean**	**Stnd. Error**	**Lower Limit**	**Upper Limit**
1	17	873.112	8.94243	855.141	891.082
2	18	839.244	8.69048	821.78	856.708
3	17	857.472	8.94243	839.501	875.442
Grand Mean	52	856.609			
	4 Months				
Level *Condition*	**Count**	**Mean**	**Stnd. Error**	**Lower Limit**	**Upper Limit**
1	17	870.793	12.5095	845.654	895.932
2	18	866.15	12.157	841.72	890.58
3	17	832.649	12.5095	807.51	857.788
Grand Mean	52	856.531			

Table A.9 Analysis of variance ultimate tensile stress for different conditions at different time points (4 days, 1 month and 4 months) – Type III sums of squares.

	4 Days				
Source	**Sum of Squares**	**Df**	**Mean Square**	**F-Ratio**	**P-Value**
Condition	15.9166	2	7.9583	2.54	0.0894
Residual	153.678	49	3.13629		
Total (corrected)	169.595	51			
	1 Month				
Source	**Sum of Squares**	**Df**	**Mean Square**	**F-Ratio**	**P-Value**
Condition	77.9866	2	38.9933	13.36	0.0000
Residual	143.001	49	2.91839		
Total (corrected)	220.988	51			
	4 Months				
Source	**Sum of Squares**	**Df**	**Mean Square**	**F-Ratio**	**P-Value**
Condition	153.202	2	76.601	11.12	0.0001
Residual	337.531	49	6.88839		
Total (corrected)	490.733	51			

Table A.10 Analysis of variance E-Modulus (1-3% Strain) for different conditions at different time points (4 days, 1 month and 4 months) – Type III sums of squares.

	4 Days				
Source	**Sum of Squares**	**Df**	**Mean Square**	**F-Ratio**	**P-Value**
Condition	713.309	2	356.654	0.26	0.7716
Residual	67053.4	49	1368.44		
Total (corrected)	67766.7	51			
	1 Month				
Source	**Sum of Squares**	**Df**	**Mean Square**	**F-Ratio**	**P-Value**
Condition	10064.5	2	5032.25	3.7	0.0318
Residual	66612.5	49	1359.44		
Total (corrected)	76677	51			
	4 Months				
Source	**Sum of Squares**	**Df**	**Mean Square**	**F-Ratio**	**P-Value**
Condition	14817.6	2	7408.81	2.78	0.0715
Residual	130353	49	2660.27		
Total (corrected)	145171	51			

Table A.11 Summary statistics for ultimate tensile stress by condition at different time points (4 days, 1 month, and 4 months).

	4 Days								
Condition	**Count**	**Mean**	**Variance**	**Standard Deviation**	**Minimum**	**Maximum**	**Range**	**Standard Skewness**	**Standard Kurtosis**
1	17	45.7165	2.66645	1.63293	43.25	48.25	5	0.106968	-1.27912
2	18	44.6806	2.47711	1.57388	42.35	48.03	5.68	0.71632	-0.531688
3	17	45.9394	4.30649	2.07521	42.62	49.46	6.84	-0.22628	-0.989878
Total	52	45.4308	3.32538	1.82356	42.35	49.46	7.11	0.527424	-1.55989
	1 Month								
Condition	**Count**	**Mean**	**Variance**	**Standard Deviation**	**Minimum**	**Maximum**	**Range**	**Standard Skewness**	**Standard Kurtosis**
1	17	54.2359	3.30233	1.81723	51.96	57.13	5.17	0.412157	-1.35178
2	18	52.09	2.40808	1.5518	50.21	55.09	4.88	1.3202	-0.491884
3	17	51.3165	3.07666	1.75404	48.93	53.97	5.04	0.350681	-1.35393
Total	52	52.5387	4.33309	2.08161	48.93	57.13	8.2	1.08853	-0.816929
	4 Months								
Condition	**Count**	**Mean**	**Variance**	**Standard Deviation**	**Minimum**	**Maximum**	**Range**	**Standard Skewness**	**Standard Kurtosis**
1	17	52.6088	6.82685	2.61282	48.99	55.9	6.91	0.0216693	-1.66412
2	18	51.4444	7.44261	2.72812	47	54.8	7.8	-0.197792	-1.59311
3	17	48.4953	6.36106	2.52211	45.02	51.96	6.94	-0.0825915	-1.49577
Total	52	50.861	9.62222	3.10197	45.02	55.9	10.88	-0.204561	-1.43253

Table A.12 Summary statistics for ultimate tensile stress by condition at different time points (4 days, 1 month, and 4 months).

	4 Days								
Condition	**Count**	**Mean**	**Variance**	**Standard Deviation**	**Minimum**	**Maximum**	**Range**	**Standard Skewness**	**Standard Kurtosis**
1	17	785.978	1485.37	38.5405	727.68	842.62	114.94	0.0556638	-1.3028
2	18	794.523	1054.8	32.4778	738.98	842.81	103.83	-0.336749	-1.15089
3	17	787.815	1584.74	39.8088	707.36	834.62	127.26	-0.733649	-0.908664
Total	52	789.537	1328.76	36.4521	707.36	842.81	135.45	-0.715313	-1.78788
	1 Month								
Condition	**Count**	**Mean**	**Variance**	**Standard Deviation**	**Minimum**	**Maximum**	**Range**	**Standard Skewness**	**Standard Kurtosis**
1	17	873.112	1337.4	36.5704	820.56	919.42	98.86	0.0022027	-1.59469
2	18	839.244	1654.04	40.6699	759	898.3	139.3	-0.0409835	-0.617006
3	17	857.472	1068.46	32.6873	815.13	907.45	92.32	0.201679	-1.50891
Total	52	856.275	1503.47	38.7746	759	919.42	160.42	-0.27427	-1.19813
	4 Months								
Condition	**Count**	**Mean**	**Variance**	**Standard Deviation**	**Minimum**	**Maximum**	**Range**	**Standard Skewness**	**Standard Kurtosis**
1	17	870.793	3288.78	57.3479	794.19	944.68	150.49	0.120579	-1.72797
2	18	866.15	2593.68	50.9282	797.7	928.7	131	-0.0875573	-1.76902
3	17	832.649	2102.51	45.8531	764.73	894.57	129.84	-0.190556	-1.49746
Total	52	856.716	2846.49	53.3525	764.73	944.68	179.95	0.317323	-2.12781

Table A.13 Least squares means for E-Modulus, E-Modulus (1-3% Strain), ultimate tensile stress, tensile strain at break, and tensile stress at break with 95.0 percent confidence intervals.

	E Modulus				
Level *Layout*	**Count**	**Mean**	**Stnd. Error**	**Lower Limit**	**Upper Limit**
1	8	2498.8	32.0102	2432.23	2565.37
2	8	2733.08	32.0102	2666.51	2799.65
3	8	2735.53	32.0102	2668.96	2802.1
Grand Mean	24	2655.8			
	E Modulus (1-3% Strain)				
Level *Layout*	**Count**	**Mean**	**Stnd. Error**	**Lower Limit**	**Upper Limit**
1	8	851.153	2.66808	845.604	856.701
2	8	903.48	2.66808	897.931	909.029
3	8	919.394	2.66808	913.845	924.942
Grand Mean	24	891.342			
	Ultimate Tensile Stress				
Level *Layout*	**Count**	**Mean**	**Stnd. Error**	**Lower Limit**	**Upper Limit**
1	8	48.5275	0.206333	48.0984	48.9566
2	8	51.1662	0.206333	50.7372	51.5953
3	8	51.5325	0.206333	51.1034	51.9616
Grand Mean	24	50.4087			
	Tensile Strain at Break				
Level *Layout*	**Count**	**Mean**	**Stnd. Error**	**Lower Limit**	**Upper Limit**
1	7	12.63	1.59196	9.31933	15.9407
2	7	8.79143	1.59196	5.48076	12.1021
3	10	9.275	1.59196	6.5051	12.0449
Grand Mean	24	10.2321			
	Tensile Stress at Break				
Level *Layout*	**Count**	**Mean**	**Stnd. Error**	**Lower Limit**	**Upper Limit**
1	7	25.2671	2.76724	19.5123	31.0219
2	7	35.8786	2.76724	30.1238	41.6334
3	10	35.332	2.76724	30.5172	40.1468
Grand Mean	24	32.1592			

Table A.14 Analysis of variance for E-Modulus, E-Modulus (1-3% Strain), ultimate tensile stress, tensile strain at break, and tensile stress at break – Type III sums of squares.

Source	Sum of Squares	Df	Mean Square	F-Ratio	P-Value
	E Modulus				
Layout	295826	2	147913	18.04	
Residual	467967	21	8197.2		
Total (corrected)	467967	23			
	E Modulus (1-3% Strain)				
Layout	20395.4	2	10197.7	179.07	
Residual	1195.93	21	56.9491		
Total (corrected)	21591.4	23			
	Ultimate Tensile Stress				
Layout	43.0058	2	21.5029	63.14	
Residual	7.15229	21	0.340585		
Total (corrected)	50.1581	23			
	Tensile Strain at Break				
Layout	63.5953	2	31.7977	1.79	0.1911
Residual	372.548	21	17.7404		
Total (corrected)	436.143	23			
	Tensile Stress at Break				
Layout	526.23	2	263.115	4.91	0.0178
Residual	1125.67	21	53.6033		
Total (corrected)	1651.9	23			

Table A.15 Summary statistics for E-Modulus, E-Modulus (1-3% Strain), ultimate tensile stress, tensile strain at break, and tensile stress at break by analyst.

	E Modulus								
Analyst	**Count**	**Mean**	**Variance**	**Standard Deviation**	**Minimum**	**Maximum**	**Range**	**Standard Skewness**	**Standard Kurtosis**
1	8	2498.8	7560.06	86.9486	2394.18	2643.03	248.85	0.263688	-0.444589
2	8	2733.08	9227.86	96.0618	2591.42	2866.41	274.99	-0.0017458	-0.5566
3	8	2735.53	7803.67	88.3384	2638.32	2875.73	237.41	0.655792	-0.790679
Total	24	2655.8	20346.4	142.641	2394.18	2875.73	481.55	-0.564304	-0.687226
	E Modulus (1-3% Strain)								
Analyst	**Count**	**Mean**	**Variance**	**Standard Deviation**	**Minimum**	**Maximum**	**Range**	**Standard Skewness**	**Standard Kurtosis**
1	8	851.153	88.2391	9.39357	830.5	862.03	31.53	-1.86534	2.24493
2	8	903.48	41.7349	6.46025	895.63	914.84	19.21	0.594254	-0.121368
3	8	919.394	40.8734	6.39323	911.37	929.08	17.71	0.478922	-0.532732
Total	24	891.342	938.754	30.6391	830.5	929.08	98.58	-1.23318	-1.1883
	Ultimate Tensile Stress								
Analyst	**Count**	**Mean**	**Variance**	**Standard Deviation**	**Minimum**	**Maximum**	**Range**	**Standard Skewness**	**Standard Kurtosis**
1	8	48.5275	0.42465	0.651652	47.03	49.09	2.06	-2.40634	2.88804
2	8	51.1662	0.461484	0.679326	50.28	52.41	2.13	0.661666	0.202399
3	8	51.5325	0.135621	0.368268	51.09	52.05	0.96	0.122246	-1.01912
Total	24	50.4087	2.18079	1.47675	47.03	52.41	5.38	-1.37632	-0.687306
	Tensile Strain at Break								
Analyst	**Count**	**Mean**	**Variance**	**Standard Deviation**	**Minimum**	**Maximum**	**Range**	**Standard Skewness**	**Standard Kurtosis**
1	7	12.63	3.00837	1.73446	9.54	14.63	5.09	-0.90516	0.297786
2	7	8.79143	9.30148	3.04983	3.7	11.36	7.66	-1.18288	-0.255178
3	10	9.275	33.1876	5.76087	4.53	23.92	19.39	2.77012	3.24099
Total	24	10.1125	18.9627	4.35462	3.7	23.92	20.22	2.36214	3.11622
	Tensile Stress at Break								
Analyst	**Count**	**Mean**	**Variance**	**Standard Deviation**	**Minimum**	**Maximum**	**Range**	**Standard Skewness**	**Standard Kurtosis**
1	7	25.2671	124.377	11.1524	0.05	31.06	31.01	-2.82214	3.71064
2	7	35.8786	38.0071	6.16499	31.89	48.36	16.47	1.95583	1.48311
3	10	35.332	16.8186	4.10104	27.61	41.94	14.33	-0.387699	0.209404
Total	24	32.5558	71.8217	8.47477	0.05	48.36	48.31	4.50201	9.64098

Table A.16 Least squares means for gage length, width of narrow section, thickness, width overall, and length overall with 95.0 percent confidence intervals

	Gage Length				
Level *Analyst*	**Count**	**Mean**	**Stnd. Error**	**Lower Limit**	**Upper Limit**
1	72	50.9766	0.00998596	50.9569	50.9963
2	72	51.0027	0.00998596	50.983	51.0224
3	72	51.0148	0.00998596	50.9951	51.0345
Grand Mean	216	50.998			
	Width of Narrow Section				
Level *Analyst*	**Count**	**Mean**	**Stnd. Error**	**Lower Limit**	**Upper Limit**
1	72	12.8304	0.00702951	12.8166	12.8443
2	72	12.9015	0.00702951	12.8877	12.9154
3	72	12.8697	0.00702951	12.8559	12.8836
Grand Mean	216	12.8672			
	Thickness				
Level *Analyst*	**Count**	**Mean**	**Stnd. Error**	**Lower Limit**	**Upper Limit**
1	72	3.42625	0.0058938	3.41463	3.43787
2	72	3.49417	0.0058938	3.48255	3.50578
3	72	3.47375	0.0058938	3.46213	3.48537
Grand Mean	216	3.46472			
	Width Overall				
Level *Analyst*	**Count**	**Mean**	**Stnd. Error**	**Lower Limit**	**Upper Limit**
1	72	19.1686	0.00874107	19.1514	19.1858
2	72	19.2394	0.00874107	19.2222	19.2567
3	72	19.2219	0.00874107	19.2047	19.2392
Grand Mean	216	19.21			
	Length Overall				
Level *Analyst*	**Count**	**Mean**	**Stnd. Error**	**Lower Limit**	**Upper Limit**
1	72	165.284	0.022831	165.239	165.329
2	72	165.338	0.022831	165.293	165.383
3	72	165.334	0.022831	165.289	165.379
Grand Mean	216	165.319			

Table A.17 Analysis of variance for gage length, width of narrow section, thickness, width overall and length overall – Type III sums of squares.

	Gage Length				
Source	**Sum of Squares**	**Df**	**Mean Square**	**F-Ratio**	**P-Value**
Analyst	0.0548787	2	0.0274394	3.82	0.0234
Residual	1.5293	213	0.0071798		
Total (corrected)	1.58418	215			
	Width of Narrow Section				
Source	**Sum of Squares**	**Df**	**Mean Square**	**F-Ratio**	**P-Value**
Analyst	0.182719	2	0.0913597	25.68	
Residual	0.757814	213	0.0035578		
Total (corrected)	0.940533	215			
	Thickness				
Source	**Sum of Squares**	**Df**	**Mean Square**	**F-Ratio**	**P-Value**
Analyst	0.174858	2	0.0874292	34.96	
Residual	0.532725	213	0.0025011		
Total (corrected)	0.707583	215			
	Width Overall				
Source	**Sum of Squares**	**Df**	**Mean Square**	**F-Ratio**	**P-Value**
Analyst	0.196033	2	0.0980167	17.82	
Residual	1.17177	213	0.0055013		
Total (corrected)	1.3678	215			
	Length Overall				
Source	**Sum of Squares**	**Df**	**Mean Square**	**F-Ratio**	**P-Value**
Analyst	0.129753	2	0.0648764	1.73	0.18
Residual	7.99394	213	0.0375302		
Total (corrected)	8.1237	215			

Table A.18 Summary statistics for gage length, width of narrow section, thickness, width overall, and length overall by analyst.

	Gage Length								
Analyst	**Count**	**Mean**	**Variance**	**Standard Deviation**	**Minimum**	**Maximum**	**Range**	**Standard Skewness**	**Standard Kurtosis**
1	72	50.9766	0.0077731	0.088165	50.787	51.127	0.34	-0.924663	-1.42442
2	72	51.0027	0.006315	0.079467	50.827	51.127	0.3	-1.63681	1.2389
3	72	51.0148	0.0074513	0.0863211	50.827	51.157	0.33	-0.865905	-1.43423
Total	216	50.998	0.0073683	0.0858386	50.787	51.157	0.37	-1.91755	-2.18817
	Width of Narrow Section								
Analyst	**Count**	**Mean**	**Variance**	**Standard Deviation**	**Minimum**	**Maximum**	**Range**	**Standard Skewness**	**Standard Kurtosis**
1	72	12.8304	0.0016548	0.0406787	12.73	12.98	0.25	2.56324	3.17447
2	72	12.9015	0.0063709	0.0798177	12.82	13.21	0.39	5.82023	5.85941
3	72	12.8697	0.0026478	0.0514569	12.82	13.1	0.28	6.97199	9.48058
Total	216	12.8672	0.0043746	0.0661406	12.73	13.21	0.48	11.2589	16.543
	Thickness								
Analyst	**Count**	**Mean**	**Variance**	**Standard Deviation**	**Minimum**	**Maximum**	**Range**	**Standard Skewness**	**Standard Kurtosis**
1	72	3.42625	0.0016012	0.0400154	3.35	3.53	0.18	2.49204	0.290003
2	72	3.49417	0.0033542	0.0579157	3.42	3.65	0.23	2.39782	-1.13906
3	72	3.47375	0.0025477	0.0504749	3.37	3.58	0.21	2.76461	-0.529652
Total	216	3.46472	0.0032911	0.057368	3.35	3.65	0.3	4.49859	0.109718
	Width Overall								
Analyst	**Count**	**Mean**	**Variance**	**Standard Deviation**	**Minimum**	**Maximum**	**Range**	**Standard Skewness**	**Standard Kurtosis**
1	72	19.1686	0.0017727	0.0421033	19.07	19.3	0.23	2.02025	1.81996
2	72	19.2394	0.0063772	0.0798571	19.15	19.44	0.29	3.35664	-0.675524
3	72	19.2219	0.0083539	0.0913997	19.14	19.85	0.71	16.9065	54.7452
Total	216	19.21	0.0063619	0.0797613	19.07	19.85	0.78	18.6946	57.0018
	Length Overall								
Analyst	**Count**	**Mean**	**Variance**	**Standard Deviation**	**Minimum**	**Maximum**	**Range**	**Standard Skewness**	**Standard Kurtosis**
1	72	165.284	0.0471405	0.217119	164.9	165.51	0.61	-2.42522	-2.17591
2	72	165.338	0.0330338	0.181752	164.96	165.54	0.58	-2.69298	-1.84424
3	72	165.334	0.0324164	0.180046	164.96	165.51	0.55	-2.95777	-1.58218
Total	216	165.319	0.0377846	0.194383	164.9	165.54	0.64	-4.86649	-2.83448

APPENDIX B

Information for every batch manufactured with the Viper Si^2 was monitored for properties such as duration of built, temperature, relative humidity, and specifications obtained from machine.

Table B.1 Batch data for initial and final stage of the build.

Aging	Batch	Date	Start Time	Viper Temp (ºC)	*Initial*			End Time	*Finish*		
					RH (%)	Temp (ºC)	Atmospheric Pressure		RH (%)	Temp (ºC)	Atmospheric Pressure
4 Days (18 Specimens)	1	7/1/07	12:32 a.m.	28.3	26	27	26.05	9:36 a.m.	29	27	26.1
4 Months (18 specimens)	2	8/29/07	11:11 p.m.	26.9	32	25	26.22	9:58 a.m.	40	25	26.31
	3	9/3/07	1:29 a.m.	23.3	40	21	26.22	1:45 p.m.	33	21	26.19
	4	9/3/07	11:46 p.m.	23.4	37	21	26.16	12:46 p.m.	40	23	26.1
1 Month (18 specimens)	5	12/22/07	1:37 a.m.	26.7	28	24	26.05	10:25 a.m.	21	26	26.34
	6	12/23/07	12:02 a.m.	26.8	21	25	26.37	8:53 a.m.	21	25	26.34
	7	12/24/07	12:21 a.m.	26.8	21	25	26.28	9:13 a.m.	21	25	26.37
4 Days (18 specimens)	8	1/2/08	11:08 p.m.	24.1	22	22	26.28	7:56 a.m.	22	22	26.28
	9	1/3/08	11:14 p.m.	24.2	22	22	26.25	8:05 a.m.	22	22	26.28
	10	1/4/08	11:30 p.m.	24.3	23	22	26.22	8:22 a.m.	23	22	26.16
4 Days (24 specimens)	11	3/28/08	2:38 p.m.	24.9	23	22	25.96	3:31 p.m.	19	29	25.93
	12	6/9/08	7:46 a.m.	25.3	24	22	26.05	8:37 a.m.	25	24	26.02
	13	7/1/08	8:41 p.m	26.6	44	23	26.22	9:37 a.m.	40	22	26.1

Table B.2 Data gathered for each of the batches from the Viper Si^2.

Aging	Batch	Border Speed	Hatch Speed	Fill Speed	Pre Dip	Z Wait	Sweeps	*Beam Characteristics*			*Build Initialization*		*Start Layer*	*Resin Leveling*	*High Resolution Spot*	
								Maximum Laser Power (mW)	Peak Sum Ratio	Beam Width	Build Start Overhead	Leveler Calibration	Average Time	Average Time	Peak Sum Ratio	Beam Width
4 Days (18 Specimens)	1	18.6	82.9	28.2	10	10	1	46	0.165	9.93	77.123	35.175	5.211	0.45	0.25	3
4 Months (18 specimens)	2	13.3	62.8	21.4	10	10	1	34	0.1549	10.83	86.639	35.175	5.228	0.598	0.25	3
	3	10.8	50.8	17.3	10	10	1	28	0.156	10.98	91.177	35.175	5.202	0.623	0.25	3
	4	11.3	52.8	18	10	10	1	29	0.1574	10.87	90.379	35.175	5.205	0.538	0.25	3
1 Month (18 specimens)	5	19.1	91.6	31.2	10	10	1	50	0.1527	9.83	24.628	35.175	5.207	0.457	0.25	3
	6	18.9	91.6	31.2	10	10	1	50	0.1516	9.86	25.346	35.175	5.209	0.344	0.25	3
	7	19	91.6	31.2	10	10	1	50	1.1522	9.9	25.817	35.175	5.215	0.468	0.25	3
4 Days (18 specimens)	8	18.7	91.6	31.2	10	10	1	50	0.1503	10.02	27.779	35.175	5.23	0.347	0.25	3
	9	18.7	91.6	31.2	10	10	1	50	0.1497	10.06	28.227	35.175	5.212	0.327	0.25	3
	10	18.9	91.6	31.2	10	10	1	50	0.1516	10.03	28.788	35.175	5.217	0.353	0.25	3
4 Days (24 specimens)	11	20	91.6	31.2	10	10	1	50	0.1602	9.43	30.945	35.175	5.203	0.169	0.25	3
	12	19.7	91.6	31.2	10	10	1	50	0.1576	9.76	50.983	35.175	5.211	0.089	0.25	3
	13	18.9	89.7	30.5	10	10	1	49	0.1549	10.27	49.256	35.175	5.224	0.072	0.25	3

Table B.3 Time for each batch to be tensile tested.

Aging	Batch	*Pre-conditioning*			*Tensile Testing*	
		Date In	**Date Out**	**Time**	**Date**	**Time**
4 Days (18 Specimens)	1	N/A			7/2/07	11:41 a.m.
4 Months (18 specimens)	2	*1/1/08*	*1/3/08*	*12:10p.m*	1/3/08	12:10 p.m.
	3	*Ambient*			1/6/08	2:50 p.m.
	4	*Desiccant*			1/5/08	3:54 p.m.
1 Month (18 specimens)	5	*Desiccant*			1/22/08	12:45 p.m.
	6	*1/23/08*	*1/25/08*	*11:25 a.m.*	1/25/08	11:25 a.m.
	7	*Ambient*			1/24/08	12:20 p.m.
4 Days (18 specimens)	8	*Desiccant*			1/7/08	10:06 a.m.
	9	*1/8/08*	*1/10/08*	*10:20 a.m.*	1/10/08	10:20 a.m.
	10	*Ambient*			1/9/08	10:50 a.m.
4 Days (24 specimens)	11	*3/4/08*	*3/6/08*	*5:31 p.m*	*3/6/08*	*5:31 p.m*
	12	*6/14/08*	*6/16/08*	*10:56 a.m.*	6/16/08	10:56 a.m.
	13	*7/6/08*	*7/8/08*	*11:53 a.m.*	7/8/08	11:53 a.m.

CURRICULUM VITAE

Karina Puebla was born on March 5, 1983 in Cd. Juarez, Chihuahua, Mexico. She is the fourth daughter of six children of Lino Puebla Ojeda and Ignacia Campa Ortega. She completed her high school education at Stephen F. Austin High School in El Paso, Texas in May 2001. Thereafter, she enrolled at the University of Texas at El Paso (UTEP) in August of 2001 and was awarded a Bachelor of Science in Mechanical Engineering in May 2006. Soon after, she entered the graduate program at UTEP in August 2006 working towards a Master of Science in Metallurgical and Materials Engineering. During her graduate studies she worked at the W.M. Keck Center for 3D Innovation as a research assistant and was a co-author of a publication with Dr. Ryan B. Wicker. While continuing her graduate studies, Karina was awarded the Louis Stokes Alliance for Minority Participation (LSAMP) Bridge to the Doctorate.

Permanent Address: 10077 Imperial St
El Paso, TX 79924

This thesis was typed by Karina Puebla.